8-24-2016

Osmoregulatory Physiology and its Evolution in the Threespine Stickleback (Gasterosteus aculeatus)

Jeffrey N. Divino
University of Connecticut - Storrs, jeffrey.divino@uconn.edu

Osmoregulatory Physiology and its Evolution in the Threespine Stickleback (*Gasterosteus aculeatus*)

Jeffrey Nicholas Divino, PhD

University of Connecticut, 2016

Maintaining ion balance in environments of changing salinity is one of the greatest physiological challenges facing aquatic organisms and by comparing populations inhabiting different salinity regimes, we can learn how physiological plasticity evolves in response to local osmotic stress. I characterized the evolution of osmoregulatory responses in representative marine, anadromous, and freshwater (FW) populations of Threespine Stickleback (*Gasterosteus aculeatus*) by comparing survival and physiological measures in F_1-generation fish following salinity challenge. Juveniles from a population landlocked for ~10,000 years displayed ontogenetically-delayed seawater (SW) tolerance, a lower maximum salinity threshold, and did not upregulate the Na^+/K^+-ATPase (NKA) ion transporter as much as marine counterparts (Chapter 1). Stickleback also responded to salinity stress by remodeling their gill epithelium: I observed a higher density of ionoregulatory cells when juveniles were subjected to both low and high salinities, and the latter treatment induced strong upregulation of ion secretory cells (Chapter 2). Finally, I examined the speed at which osmoregulatory plasticity evolves by comparing halotolerance between an anadromous population and descendants that had been FW-restricted for only two generations (Chapter 3). The lake-introduced group had improved survival in FW, but also retained SW tolerance and had similar increases in gill NKA activity, gill $Na^+/K^+/2Cl^-$ cotransporter abundance, and organic osmolytes in SW. Overall, the differentiated responses to salinity I observed among stickleback populations indicate that osmoregulation has evolved in a manner consistent with local adaptation and following FW invasions, positive selection on FW tolerance acts more rapidly than relaxed selection on SW tolerance.

Osmoregulatory Physiology and its Evolution in the Threespine Stickleback (*Gasterosteus aculeatus*)

Jeffrey Nicholas Divino

B.S., Gordon College, 2002

M.S., University of Alberta, 2005

A Dissertation

Submitted in Partial Fulfillment of the

Requirements for the Degree of

Doctor of Philosophy

at the

University of Connecticut

2016

APPROVAL PAGE

Doctor of Philosophy Dissertation

Osmoregulatory Physiology and its Evolution in the Threespine Stickleback (*Gasterosteus aculeatus*)

Presented by

Jeffrey Nicholas Divino, B.S., M.S.

Major Advisor _____
Eric T. Schultz

Associate Advisor _____
John A. Baker

Associate Advisor _____
Elizabeth L. Jockusch

Associate Advisor _____
Stephen D. McCormick

Associate Advisor _____
J. Larry Renfro

University of Connecticut

2016

Acknowledgements

To complete a dissertation, you cannot simply work on it; you must be married to it. This is highly problematic for graduate students who are *already* married! So I must first thank my patient and understanding wife, Tatyana, for putting up with my polygamy for six of our 13 years of marriage. Moreover, we had a child during the first and last years of this degree, and I would like Sofia and young Nathan to know that I cherish them and was thinking of them even while away from home. Though I strove to maximize my time spent with them when I was not conducting research, studying for classes, and teaching, it breaks my heart to think of the precious moments I missed of their early life stages now gone by. But I am pleased to have more family time now that I am no longer a Professional Student. I also look forward to the day my children will read this book and discover all that I was working on when I disappeared for long stretches of the day (or week!).

Quite certainly, this dissertation could not have been completed without the support of my immediate and extended family, primarily those who provided child care. I am indebted to my in-laws Valentina and Alex Krasnoshek, as well as the rest of the Krasnoshek Clan: Vickie, Lena, and now Aide. (Surely if you sat through the defense seminar rehearsal I gave from my living room television, you should be mentioned here by name.) I also express my gratitude to my parents, Mimmo and Karen Divino who have always prioritized my education and, especially nearing the end of my degree, insisted on repeatedly making the 2-h drive from their home to mine to help out with domestic needs…despite facing risks of highway breakdown in cars that were driven 0.25-0.5 million miles! I have been encouraged by many other well-wishing friends and family, including my sister Ariane and aunt Linda, who both traveled great distances to come to my defense.

Now to take an academic turn, I wish to express my appreciation for the three professors whose mentorship has most strongly influenced the direction of my professional life in ecology: Dorothy Boorse, my undergraduate advisor at Gordon College, William Tonn, my Master's advisor at the University of Alberta, and now Eric Schultz, who has been so much more than a PhD advisor at UConn. My relationship with Eric began when I joined his lab to research fecundity in river herring, and this side

project eventually blossomed into a publication and several conference presentations. Later, Eric was at the forefront of an exciting new collaboration with several researchers investigating the evolution of salinity tolerance in Threespine Stickleback and he brought me to one of their initial meetings. After recognizing that the potential for discovery in this largely unexplored area was limitless, I immediately made it the subject of my dissertation and began to carve out my own research niche under Eric's expert guidance. I appreciated his hands-off approach to overseeing student-driven research. However, he also provided more direct aid when my burgeoning PhD project left me buried in gill samples generated from large-scale experiments on more than 10,000 juvenile fish. After my personal realization (one faced by most graduate students) that multiple lifetimes would be required to pursue every burning question and perform all intriguing analyses, Eric helped me reassess my project goals and transform my mounting anxiety into a clear plan of action. Out of our constructive discussions emerged a research framework that optimized merit and achievability and culminated in these chapters.

Eric is deeply invested in both the professional and personal well-being of his students and he consistently demonstrated that he has my best interests in mind and, throughout my program, has always reserved (and sometimes made) time to meet with me to converse about all things related to my research, grad school life, career goals, and more. Eric also sets high standards for his students and his challenging and copious editorial suggestions have substantially improved my writing and my presentation skills. By addressing his insightful questions, I became a better scientist with the knowledge and confidence to stand behind the validity, interpretation, and significance of my findings, as well as critically evaluate and discuss the work of scientific peers.

I also thank the other members of my Graduate Advisory Committee, John Baker, Elizabeth Jockusch, Stephen McCormick, and Larry Renfro, whose unique areas of expertise improved my dissertation research in different ways. Thank you for being available particularly when urgencies arose, and I hope to remain in professional contact with each of you, having now – as was put during my defense examination – crossed over from student to colleague.

Science is not a solitary endeavor, especially when the study populations are 3,500 miles away! I am deeply thankful to John Baker (Clark University), Michael Bell (Stony Brook), and Frank von Hippel (University of Alaska Anchorage) who collected the parental generation of wild Threespine Stickleback from remote sites in Alaska. Under these principal investigators labored students and technicians led by Justin Golub, Miguel Reyes, Jennifer Rollins, Daniella Swenton, and Matthew Wund. These field crews shipped to our lab with more than 16,700 F_1-generation embryos over four summers of research, which my team and I reared and used in a multitude of experiments. And let me not overlook the study organism! I thank the many stickleback that made the ultimate sacrifice for the advancement of our scientific understanding. All stickleback entrusted to my care were treated with respect, and I gathered as much information as possible from them to generate the valuable data I report in this volume.

My own blood, sweat, and tears could only get me so far with this ambitious project. Researchers with differing specializations mutually benefit when they work together. I thank my major collaborators Steve McCormick (Conte Anadromous Fish Research Center), Michelle Monette (Western Connecticut State University), and Paul Yancey (Whitman College), in whose labs many of my samples were processed on the way to making important molecular discoveries that enriched this study and also formed lasting professional bonds and friendships. During my trips to Conte, I received expert training from Michael O'Dea (1962-2014) and Amy Regish. At the other institutions, Aiden Ford, Socheata Lim, Robert Toth, and Kyle Flannery provided more helping hands with extensive sample processing.

Closer to home, I thank the many Schultz Lab members who served as assistants with fish care, data collection, or provided advice over the years of this study. These include the comrades who languished with me for countless hours in the windowless confines of the Fish Room: my older lab brother Jonathan Velotta and five trusty sidekicks who, in addition to helping me, conducted independent stickleback-related projects between 2010 and 2015: Dante Paolino, David Fryxell, Silvana Luongo, Sammy Beynor, and Zachary Skelton. I am also grateful to graduate student lab mates Justin Davis, Michael Smircich, Kasey Pregler, Lauren Barbieri, Jacob Kasper, in addition to the many undergraduate students that advanced the osmoregulatory cause: Nicolle Murphy, Steven Ehrlich, Megan Cruz, Cody

Roberge, Emmanuel Seow Tzer Yeun, Nishita Patel, Grace Casselberry, Rebecca Colby, Emily Funk, and Marat Vasilenko. More broadly, I thank my fellow graduate students and the helpful administrative staff in UConn's Department of Ecology and Evolutionary Biology (EEB), as well as logistical support from Biology Central Services, and the Aquatics Facility.

The experiments I present here could not have been performed without financial support, which was used to purchase supplies ranging from fish nets to reagents for molecular assays. Generous funding came through a Multidisciplinary Environmental Research Award from UConn's Center for Environmental Sciences and Engineering, the John Rankin Scholarship Fund to EEB and the Connecticut State Museum of Natural History, a Grants-in-Aid of Research award from Sigma Xi, and MVAO.

Lastly, it is with humility that I recognize that not everyone gets to spend their time trying to understand the natural world. I consider myself privileged to have had both the academic ability and the opportunity to pursue scholarly goals and enjoy a fulfilling career in ecological education and research.

"*I do not feel obliged to believe that the same God who has endowed us with senses, reason, and intellect has intended us to forgo their use and by some other means to give us knowledge which we can attain by them.*" – Galileo Galilei, 1615

Contents

Statement of Author Contributions

Chapter 1: Osmoregulatory divergence in Threespine Stickleback ecotypes: effects of early ontogeny and salinity acclimation on halotolerance and gill Na^+/K^+-ATPase activity

Content in this dissertation chapter will be included in a manuscript with the following authors:

Jeffrey Divino, Stephen McCormick, and Eric Schultz

Author Contributions:

Study Conception & Design – JD, ES, SM

Funding Acquisition – JD, ES

Data Collection – JD, ES, SM

Analysis & Interpretation – JD, ES, SM

Writing of Original Draft – JD

Chapter 2: Characterizing population- and salinity-dependent divergence in gill ionocyte composition among Threespine Stickleback ecotypes using scanning electron microscopy

Content in this dissertation chapter will be included in a manuscript with the following authors:

Jeffrey Divino, Dante Paolino, Silvana Luongo, Zachary Skelton, and Eric Schultz

Author Contributions:

Study Conception & Design – JD, ES

Funding Acquisition – JD, ES, DP, SL

Data Collection – DP, SL, JD, ES

Analysis & Interpretation – JD, DP, ZS, SL, ES

Writing of Original Draft – JD

Chapter 3: Osmoregulatory physiology and rapid evolution of salinity tolerance in Threespine Stickleback recently introduced to fresh water

A manuscript version of this dissertation chapter has been published with the following citation:

Divino JN, Monette MY, McCormick SD, Yancey PH, Flannery KG, Bell MA, Rollins JL, von Hippel FA, Schultz ET (2016) Osmoregulatory physiology and rapid evolution of salinity tolerance in threespine stickleback recently introduced to fresh water. Evol Ecol Res 17:179-201

Author Contributions:

Study Conception & Design – JD, ES, SM, MB, FvH

Funding Acquisition – JD, ES, MM, MB, JR

Data Collection – JD, ES, MM, SM, PY, KF, *with fieldwork from* MB, JR, FvH

Analysis & Interpretation – JD, ES, MM, SM, PY, KF

Writing of Original Draft – JD

Critical Manuscript Revision – JD, ES, MM, SM, PY, MB, FvH

Final Manuscript Approval – JD, MM, SD, PY, KF, MB, JR, FvH, ES

Preface

Euryhalinity & osmoregulation in fishes.— Aquatic organisms must continually contend with water and ion imbalances imposed by an environmental osmotic pressure, which is often different than that of their tissues and may fluctuate across relatively short spatial and temporal scales. This physiological problem can be fatal if the internal-external osmotic gradient is great, but can be mitigated through the energy-consuming task of osmoregulation (reviewed by Marshall & Grosell 2006). Euryhalinity is the ability of an organism to detect changes in environmental osmolality and respond rapidly and appropriately to maintain ion homeostasis across a wide salinity spectrum. Euryhalinity is an important evolutionary innovation that facilitated range expansion by ancestrally marine or estuarine taxa into freshwater (FW) halohabitats (Lee & Bell 1999). For example, in fishes, the most diverse group of vertebrates, an estimated 3-5% of species are euryhaline, approximately a third of which are diadromous (Helfman et al. 2009; McCormick et al. 2013a). Colonization of FW habitats by euryhaline fishes has often yielded prolific radiations in geographically isolated and heterogeneous FW lakes and streams, such as by catfishes and cyprinids (Betancur-R 2010; Nakatani et al. 2011). In fact, the disproportionality of FW species is exceedingly large: 43% of all fish diversity (~12,000 species) is found exclusively in FW, which makes up <0.01% of the Earth's available water (Nelson 2006). The high potential for evolutionary divergence following the invasion of disconnected FW systems by founding euryhaline species dispersing across marine environments has made this subset of fishes important for cladogenesis (Schultz & McCormick 2013).

Selection on osmoregulation.— Comparisons of the characteristics of the osmoregulatory response across species or among salinity-divergent populations allow tests of fundamental predictions concerning the pace and outcome of evolution of halotolerance. When a population of marine or anadromous colonizers becomes geographically stranded in FW (i.e., landlocked), positive selection for enhanced performance in ion-poor conditions is intense, since survival is contingent on maintaining homeostasis. Consequently, FW tolerance is expected to improve rapidly as landlocked descendants adapt to local FW conditions.

Selection for SW tolerance, meanwhile, is no longer imposed on the landlocked population, and thus euryhalinity might erode through mutation accumulation in the gene networks associated with hypo-osmoregulation (Snell-Rood et al. 2010). However, the evolutionary effects of this relaxed selection are less clear because they depend on maintenance costs and degree of pleiotropy of the genes essential for hypo-osmoregulation (Lahti et al. 2009). If energetic costs to maintain a functional osmoregulatory response to high salinity are high, or the genes involved largely reside in a distinct regulatory module (or both), then loss of these traits should be more rapid than if costs are small and/or genes were highly integrated within networks necessary for the fish to function in FW.

Field sampling and salinity challenge experiments have provided empirical evidence for evolutionary differences in halotolerance indicative of local adaptation among populations evolving under divergent salinity regimes. For example, when Mummichog (*Fundulus heteroclitus*) occupying headwater reaches of the Potomac and James Rivers were exposed to SW, they had lower survival, greater osmotic stress, and a dampened transcriptomic response compared to estuarine counterparts in the Chesapeake Bay (Whitehead et al. 2011, 2012). In a related genus, expression profiles of osmoregulatory genes between two sister species of fundulids corresponded to their divergent halohabitats. The euryhaline Rainwater Killifish (*Lucania parva*) has a broad coastal range that includes the full FW-SW gradient, whereas the Bluefin Killifish (*L. goodei*) is restricted to FW lakes. Berdan and Fuller (2012) found that, compared to Rainwater Killifish, the species under relaxed selection for SW tolerance failed to upregulate a suite of hypoosmoregulatory genes when exposed to SW. Similar halohabitat transitions exist among populations of Clupeidae, which have also resulted in divergence in osmoregulatory capacity. Compared to ancestral anadromous Alewives (*Alosa pseudoharengus*), derived landlocked populations have lower survival and higher osmotic imbalance when challenged with SW (Velotta et al. 2014).

Halotolerance also differs along the axis of ontogeny, particularly in diadromous species, and early life stages are often the most vulnerable to perturbations in salinity regime. SW tolerance is generally positively correlated with size and age in most euryhaline fishes (Zydlewski & Wilkie 2013), and may be linked to entry into a new developmental stage, as most notably exhibited in the parr-smolt

transformation in juvenile salmonids (McCormick 2013). Since landlocked juveniles remain in FW beyond the natural timing of their outmigration to SW, comparative studies on evolution of the osmoregulatory system should include these young age-classes.

From performance to mechanism.— The precise physiological mechanisms by which euryhaline fishes adjust their osmoregulatory systems have been intensively studied in several groups of teleosts: eels, clupeids, salmonids, killifish, and tilapia (reviewed by Evans et al. 2005; McCormick et al. 2013a). To combat osmotic stress at the cellular level, cells regulate their internal osmolality and volume by adjusting electrolyte and osmolyte concentrations (Kültz 2012). At the organismal level, the gill, kidney, and gut epithelia work together to more efficiently restore and maintain ion homeostasis of the surrounding extracellular fluid, which buffers the cells against osmotic perturbations. For example, on the vascularized surface of the gill, specialized ion transporting cells called ionocytes secrete excess ions from circulating plasma (hypo-osmoregulation) or take up ions from the environment (hyper-osmoregulation) to compensate for diffusive ion gains in seawater (SW) or losses in FW. These cell types differ markedly in their morphology and euryhaline fishes can plastically switch from hypo- to hyper-osmoregulation by remodeling their ion-exchanging epithelia upon entering new halohabitats (McCormick 2001; Kaneko & Hiroi 2008). Osmoregulatory responses trigger cell signaling cascades that alter gene expression within hours of perception of a change in environmental osmolality (Kültz 2012, 2013; Whitehead et al. 2012), and gill epithelial remodeling may become evident after one day of exposure to a new salinity (Hiroi et al. 2005). However, full acclimation usually requires several weeks and involves transporter rearrangement and ionocyte recruitment (e.g., Evans 2010; Christensen et al. 2012).

A growing body of cellular physiological research has produced detailed models of branchial ionocyte function via identification and mapping of key membrane-bound transporters. The basolateral sodium-potassium ATPase pump (NKA) plays a critical role in both hypo- and hyper-osmoregulation because it establishes a negative membrane potential inside the ionocyte and establishes a strong sodium gradient that can drive the work of secondary co-transporters and exchangers. Current models of hypo-

osmoregulation appear to be highly similar across taxa, pairing basolateral sodium-potassium-chloride cotransporter (NKCC) and apical cystic fibrosis transmembrane conductance regulator (CFTR) for chloride secretion (reviewed by McCormick 2001; Edwards & Marshall 2013). The consequent build-up of apical chloride facilitates paracellular extrusion of sodium (Kaneko & Hiroi 2008).

In contrast, ion transport models of hyper-osmoregulation are more taxon-specific and involve combinations of distinct ionocyte cell types, which are specialized for absorbing sodium or chloride from ion-poor environments. In FW, ion uptake may be enhanced by an apical vacuolar-type hydrogen ATPase (VHA), whose active extrusion of protons makes absorption of cations more favorable electrochemically (Lee et al. 2011). Sodium may enter the cell via an apical sodium-hydrogen exchanger (NHE), a sodium-chloride cotransporter (NCC), or an acid-sensing ion channel (ASIC; Dymowska et al. 2012, 2014). Interestingly, NKCC has also been identified in some FW ionocyte sub-types (Hwang & Lin 2013; Hsu et al. 2014).

Research objectives.— My research goal was to characterize how euryhalinity has evolved following halohabitat transitions by examining salinity-, age-, and population-dependent differences in the euryhaline Threespine Stickleback (*Gasterosteus aculeatus*; henceforth "stickleback"). Across its circumpolar range, stickleback have a well-documented history of parallel evolution following transitions from marine to FW habitats, many of which became landlocked following post-glacial rebound. These colonization events and subsequent ecological adaptation have become a prime example of contemporary ecological speciation by giving rise to a replicated set of derived FW populations whose ages vary from the post-glacial Pleistocene (10,000-20,000 years ago) to only a few generations (Bell & Foster 1994; Bell et al. 2004; Baker et al. 2010). I am especially interested in how osmoregulatory plasticity and halotolerance breadth change in derived FW populations that no longer experience saline environments.

The core objective of my dissertation is summarized in the following question: *How does the interplay between genetics, environment, and ontogeny affect the physiology underpinning salinity*

tolerance? This principal question can be unpacked into questions that isolate four main effects expected to influence evolution of the stickleback's osmoregulatory system:

1. How does salinity treatment - be it acute change or gradual acclimation - affect osmoregulation?
2. How do temporal dynamics of the osmoregulatory response change as inexperienced fish acclimate to new salinities?
3. Does early ontogeny influence halotolerance/-preference?
4. How do marine, anadromous, and freshwater stickleback populations differ in their range of osmoregulatory capacity, and how quickly does divergence evolve?

To answer these questions, I raised the offspring of stickleback from marine, anadromous, and lake sites in common salinity environments. Juvenile fish at various life stages were then subjected to either a foreign salinity or a salinity preference chamber to evaluate halotolerance or halo-preference, respectively. I measured effects of evolution on osmoregulatory function at multiple scales, ranging from organismal performance down to cellular and molecular composition of osmoregulatory machinery. By taking this multi-level approach, I characterized some of the physiological differences that may underlie the stickleback radiation. At each level of analysis, I assessed the mark of selection on osmoregulation by comparing populations in both the ancestral and derived salinities. Differences in the slope of reaction norms revealed interplay between alternative modes of selection acting at each condition. For example, following the transition from anadromy to FW, positive selection on enhanced FW tolerance in lake stickleback resulted in rapid divergence in response variables relative to ancestral groups, whereas relaxed selection on SW tolerance led to slower emergence of differences among populations.

The stickleback as an appropriate physiological model.— The persistence of the SW-adapted lineage of ancestral marine/anadromous phenotypes has allowed evolutionary biologists to make direct experimental comparisons between ancestral and derived forms to aid our understanding of the evolutionary consequences of halohabitat transitions. The majority of this research has been focused on characterizing the rapid evolution of lateral plate and pelvic morphology, trophic specialization, and reproductive

behavior observed following FW colonization events (McKinnon & Rundle 2002; Colosimo et al. 2005; Aguirre et al. 2008; Foster et al. 2008; Arnegard et al. 2014). However, selective pressures acting on the osmoregulatory physiology of a stickleback in FW is likely stronger than those imposed on its morphology or life history, since disruption of ion homeostasis would be fatal within days if left unmitigated. Thus, intense selection on the colonizers' ability to initiate a rapid and appropriate osmoregulatory response may represent the first fitness hurdle that must be cleared for successful establishment in the new environment. Subsequently, if osmoregulatory plasticity is lost through adaptation and/or relaxed selection within a restricted FW halo-niche, then local salinity regime could also contribute to divergence between marine and lake-resident stickleback.

In one of the first direct examinations of divergence in halotolerance between these ecotypes, Heuts (1946) found population-specific differences in egg survival that correlated with approximately native salinity. Other researchers detected salinity-dependent survival in egg and larval stages (Campeau et al. 1984; Belanger et al. 1987), or measured factors influencing salinity preference (Baggerman 1957; Audet et al. 1985). But these later organismal-level studies lacked population contrasts and often did not probe any physiological mechanisms (Guderley 1994). Schaarschmidt et al. (1999) attempted to address this problem by examining osmolyte and gill enzyme activity levels following salinity challenges of marine and stream populations in northern Germany. Although the authors linked poor survival of marine fish in a cold FW treatment to a drop in the osmolyte taurine, they did not identify any other physiological differences between the populations. Recent work has shown that ancestral and derived phenotypes exhibit divergence in osmoregulatory genes (DeFaveri et al. 2011; Shimada et al. 2011; Jones et al. 2012b) as well as osmoregulatory gene expression (McCairns & Bernatchez 2010; Taugbøl et al. 2014; Wang et al. 2014).

Nonetheless, given the potential importance of salinity for shaping the stickleback radiation, the lack of physiological data on this prolifically-studied species is surprising. For example, the absence of osmoregulatory data on stickleback from the recent Fish Physiology volume *Euryhaline Fishes* (McCormick et al. 2013a) underscores the need to investigate the physiological underpinnings that

enabled migrating ancestral stickleback populations to survive their initial passage into ion-poor environments and to assess how rapidly these traits have evolved in isolated FW systems. Moreover, the diversity of FW ionocyte cell-types described in other euryhaline species suggests that osmoregulatory adaptations are phylogenetically-dependent, so the stickleback cannot be assumed to have followed the same evolutionary trajectory as other orders of fishes.

There are numerous advantages of using the stickleback as a model for investigating physiological evolution. First, the availability of the extant ancestral stock allows side-by-side comparisons of marine, anadromous, and independently-derived FW-resident populations. Because lake populations vary in age of colonization and include several recent introductions, I can test the pace of evolution of the osmoregulatory system in real time. Moreover, the relative ease of rearing stickleback in the laboratory is conducive for conducting "common garden" experiments, which control for environmental variables. Large-scale laboratory manipulations also enable high throughput sampling of integrated, multi-level (molecular/cellular, tissue, systems and organismal) targets: survival and behavioral data can be gathered on large numbers of individuals held at multiple salinity treatments, while osmoregulatory organs can be collected for examining potential mechanistic causes for observed differences in performance. For example, gill tissue can be allocated for a suite of molecular assays, such as osmoregulatory gene and protein expression or localization, enzyme activity, and scanning electron microscopy of ionocytes. And because the stickleback has a well-annotated genome (Ensembl 2016), putative osmoregulatory genes can be readily targeted for designing gene- or protein-specific probes.

Overview of research framework.— Our knowledge of evolutionary adaptation, behavioral ecology, and population genetics has been far advanced through many decades of intensive study of the Threespine Stickleback radiation. My unique contribution to this large body of research was to investigate a still-unoccupied niche of physiological divergence, which I directly linked to organismal performance. I adopted a biologically holistic approach to examining stickleback osmoregulation: I quantified divergence in osmoregulatory machinery at the molecular, cellular, and tissue levels, while also documenting impacts

of osmotic stress on whole-organism physiology and performance. In a related set of experiments, I measured salinity preference behavior by allowing juvenile stickleback to select from among several conditions. All experiments were conducted on multiple populations and larval age-classes to assess osmoregulatory evolution and plasticity as a function of early development. This broad analytical scope can be lacking in reductionist osmoregulatory studies focused on measuring a narrow set of responses in a more limited number of treatments.

Although I studied osmoregulatory evolution in the laboratory, my findings apply to wild populations. First, clutch families were generated from at least 8-10 pairs of wild-caught parents, which adequately captured population-level differences in genotypes. Second, the treatments I chose for the salinity challenge experiments are ecologically relevant and reflect environmental conditions under which selection naturally operates on the osmoregulatory system. Additional hypersaline treatments revealed potential variation in osmoregulatory capacity among divergent stickleback populations, which may only manifest when these euryhaline fish are subject to severe osmotic challenge.

My research is valuable to integrative organismal biologists in general because it unites multiple levels of physiological responses to provide functional (mechanistic) explanations, which I interpret in an evolutionary context. My work is especially relevant to researchers interested in understanding how the environment influences complex phenotypes along developmental trajectories, identifying criteria by which plasticity is maintained or lost, describing functional correlations among traits, or defining how emergent traits arise from interactions at lower levels of organization (Martin et al. 2015).

Chapter 1

Osmoregulatory divergence in Threespine Stickleback ecotypes: effects of early ontogeny and salinity acclimation on halotolerance and gill Na^+/K^+-ATPase activity

Introduction

The capacity of euryhaline organisms to rapidly and appropriately respond to changes in environmental salinity has played a key role in the evolutionary diversification of aquatic life (Lee & Bell 1999; Schultz & McCormick 2013). As halohabitat generalists, euryhaline organisms have greater potential for geographic range expansion because they can cross osmotic barriers impassable to species intolerant of certain salinity levels or large salinity fluctuations. Consequently, euryhalinity is commonly associated with aquatic invasive species (Ricciardi & MacIsaac 2000). Darwin observed that many fishes have large spatial distributions that span salinity boundaries, and he recognized that euryhalinity confers great dispersal advantage and evolutionary potential: "there is hardly a single group of fishes confined exclusively to fresh water, so that we may imagine that a marine member of a fresh-water group might travel far along the shores of the sea and subsequently become modified and adapted to the fresh waters of a distant land" (Darwin 1859). Colonization of isolated freshwater (FW) habitats by marine fishes is of great interest to evolutionary biology because it often leads to radiations (Bell & Foster 1994; Betancur-R 2010; Nakatani et al. 2011).

Following the halohabitat transition to FW residency, the impact that local salinity regime has on shaping physiological adaptation involves an interplay between positive selection on FW tolerance and relaxed selection on seawater (SW) tolerance, which bears consequences for euryhalinity. Selection on hyper-osmoregulatory processes should be strong because the derived population must survive constant, ion-poor conditions. In contrast, the strength of relaxed selection on SW tolerance is less certain because it depends on the fitness cost and genetic architecture underlying maintenance of osmoregulatory plasticity. General theory on rates of adaptation suggest that if a high degree of pleiotropy exists between co-adapted FW and SW gene complexes or if neutral processes dominate, then SW tolerance may persist even in a FW-stable environment (Lahti et al. 2009; Hohenlohe et al. 2012). Alternatively, if energetic

costs and/or modularity are high, then SW tolerance might erode rapidly in favor of a specialized FW phenotype (Lande 2009; Snell-Rood 2012). Halotolerance shifts may also be rapid if a tradeoff exists between osmoregulation in FW and SW, which has been demonstrated between salinity-segregated populations in a few teleosts (Brennan et al. 2015; Velotta et al. 2015).

The euryhaline Threespine Stickleback (*Gasterosteus aculeatus*; hereafter 'stickleback') is an ideal organism in which to study the evolution of physiological plasticity because it has repeatedly colonized FW environments across its circumpolar range, and derived populations can be studied in relation to ancestral marine and anadromous (collectively called 'oceanic') forms. The life histories of these three ecotypes differ with respect to salinity. Within the oceanic group, marine stickleback are strictly coastal/estuarine spawners and do not migrate upriver, whereas anadromous stickleback hatch and spawn in FW. The spawning migrations of anadromous stickleback have produced numerous derived, FW isolates, many of which have been landlocked since the Pleistocene deglaciation (Bell & Ortí 1994; von Hippel 2008). A century of empirical research on the stickleback radiation has revealed parallel evolution of morphology, reproductive life history, and behavior between ancestral and derived forms, as well the genetic underpinnings of many traits under selection (Bell & Foster 1994; Baker et al. 2008; DeFaveri et al. 2011; Jones et al. 2012b; Foster 2013; Bell & Aguirre 2013). In addition, physiological divergence between ancestral and derived ecotypes has been shown from halotolerance experiments measuring salinity-dependent survival (e.g., Marchinko & Schluter 2007; DeFaveri & Merilä 2014) or osmoregulatory genes or gene expression (e.g., McCairns & Bernatchez 2010; Shimada et al. 2011; Jones et al. 2012a). Nonetheless, comparative osmoregulatory physiology among salinity-divergent stickleback populations remains poorly understood, particularly at the level of ion transport and its underlying mechanisms.

Evolutionary divergence in haloplasticity should be rooted in physiological mechanisms, primarily involving osmoregulatory organs such as the gill, whose epithelium contains ion transporting cells called ionocytes. Specialized ionocyte types function to offset either diffusive ion losses (by absorbing ions from the FW environment) or ion gains (by secreting excess ions in SW). Both actions are

driven by the Na^+/K^+-ATPase pump (NKA), a basolaterally-bound enzyme that maintains an electrochemical gradient across the cell membrane necessary to power a suite of secondary ion transporters (reviewed by Edwards & Marshall 2013). The essential role that NKA plays in ion transport and its high abundance in ionocytes has made it the principal molecular target in osmoregulatory studies. During hypo-osmoregulation in SW, NKA establishes conditions favorable for sodium and chloride uptake through the apical membrane of FW-type ionocytes. In hyper-osmoregulation in FW, NKA facilitates chloride and (paracellular) sodium extrusion in SW ionocytes (Edwards & Marshall 2013). In euryhaline fishes, upregulation of gill NKA activity commonly occurs following SW transfers (e.g., Schaarschmidt et al. 1999; McCormick et al. 2009), although some species display a more complex, "U"-shaped pattern, where activity increases in FW as well as in SW (Kelly et al. 1999; Herrera et al. 2009).

We investigated how osmoregulatory capacity evolves among stickleback populations occupying different halohabitats. We further tested how osmoregulatory responses are affected by early ontogeny and salinity acclimation. Our main research objectives were to characterize divergence of halotolerance and osmoregulatory responses by (1) measuring survival among multiple stickleback populations subjected to osmotic challenge during early ontogeny, and (2) mechanistically link osmoregulatory performance of the whole organism to the biochemical level by examining gill NKA activity as an indicator of ionocyte function. We reared F_1-generation stickleback from representative marine, anadromous, and lake populations in common salinity environments and then challenged juveniles to more extreme salinities, including hypersaline treatments, with the goal of measuring the full extent of osmoregulatory plasticity and how halotolerance thresholds are influenced by salinity acclimation.

We hypothesized that the evolution of halotolerance would manifest as differences in both the stickleback's performance (i.e., survival) and ion transport (i.e., gill NKA activity) and that both of these responses would be influenced by ontogeny and acclimation. At the organismal level, we predicted that populations will demonstrate local adaptation as a result of differences in halotolerance breadth, evidenced as progressively higher mortality the further the departure from native (i.e., naturally experienced) salinities. For example, marine stickleback were predicted to survive best in SW, but poorest

in FW treatments, and *vice versa* for lake stickleback. Second, we predicted osmoregulatory capacity will increase with development, as seen in other euryhaline fishes (reviewed by Zydlewski & Wilkie 2013). The increase in halotolerance should be especially evident with anadromous stickleback, which transition from FW to SW within their first months of development. Third, we predicted that halotolerance will be affected by a stickleback's acclimation salinity. Thus, lake stickleback pre-acclimated to SW would be able to survive at more hypersaline treatments than they could otherwise, but this increase would still be less than the upper halotolerance thresholds of marine and anadromous populations. On a mechanistic level, we hypothesized that stickleback will respond to osmotic stress by increasing the number and/or function of gill ionocytes, as marked by an increase in gill NKA activity. In general, we expected gill NKA activity to increase when fish are hyper-osmotically challenged, which has been documented in many euryhaline teleosts. Finally, we predicted that members of the landlocked population would exhibit a diminished response in upregulating gill NKA activity to combat hyperosmotic stress compared to oceanic populations, indicating a loss of osmoregulatory plasticity as a consequence of relaxed selection on SW tolerance.

Materials & Methods

Source populations & fish husbandry.— Threespine Stickleback used in this study were sourced from three populations in south-central Alaska, representing marine, anadromous, and lake ecotypes. Marine adults were captured on their spawning grounds at the head of Resurrection Bay off the shoreline of Seward, AK on the Kenai Peninsula (60.124°N, 149.418°W). The other two populations are located in the Matanuska-Susitna Borough, near the Cook Inlet: anadromous adults were captured in Rabbit Slough, at a culvert running under the Parks Highway near Palmer (61.534°N, 149.268°W), and derived, landlocked stickleback were taken from Frog Lake (61.614°N, 149.717°W), a population presumed to have been colonized by anadromous ancestors 10,000-12,000 years ago.

In May-June 2010 and 2011, breeding stickleback from all three locales were trapped using unbaited, steel minnow traps (0.32 cm mesh) set overnight by John Baker and his team from Clark

University (Worchester, MA, USA). Adults were brought to the University of Alaska Anchorage, where they produced an F_1 generation via *in vitro* fertilization between the gametes of male-female pairs. Between four and eight full-sibling clutches for each population were initially used in the experiments (Table 1). However, as cohort size decreased, some of smaller families within populations were combined, which ensured adequate sample sizes (Table 1).

In 2010, the fertilized embryos were disinfected by bathing them in a 1% iodine solution for 3 min. They were then rinsed and incubated in aerated 0.5 ppt water before being shipped on ice overnight to the University of Connecticut's Aquatic Facility, where they developed in a common environment of 3 ppt. In 2011, each clutch was split into 0.5 ppt and 15 ppt media prior to shipment. Upon arrival, we transitioned half of the 15 ppt embryos into 30 ppt. All fish were raised in reverse osmosis (RO) water in which Instant Ocean aquarium salt (Spectrum Brands, Blacksburg, VA, USA) was dissolved to the desired rearing salinity. All salinity treatments were measured to the nearest 0.1 ppt using a Yellow Springs Instruments 85 digital salinometer (Yellow Springs, OH, USA). Conductivity measurements were also recorded for each treatment. We incubated embryos in glass Petri dishes, and after successful feedings were observed, the fry were briefly kept in quart jars before being transferred into replicate 38-L aquaria, each equipped with a Penguin 100 power filter with bio-wheel (Marineland Aquarium Products, Cincinnati, OH, USA), and a segment of plastic pipe fitted with plastic plants provided habitat enrichment. Colonies were maintained at 19 ± 1°C with a 14-h light: 10-h dark photoperiod. Larval stickleback were fed live brine shrimp nauplii daily *ad libitum*, which we hatched from *Artemia* cysts (Argentemia, Argent Chemical Laboratories, Redmond, WA, USA or Brine Shrimp Direct, Ogden, UT, USA brands). Nauplii were strained from the culture medium, washed in RO, and resuspended in batches at salinities appropriate for given acclimation conditions. More details about our fish husbandry practices can be found in Divino and Schultz (2014). All experimentation on animals was approved by the University of Connecticut's IACUC (Protocol A10-013).

Two-week salinity challenges.— In 2010, we reared all stickleback at a common 3 ppt (approx. conductivity = 4.6 mS/cm). We haphazardly selected individuals from each family for acute salinity challenge trials when the fish were 3, 7, and 10-weeks post-hatch. Fish were fasted for at least 12 h and then directly transferred from the intermediate rearing salinity into wide-mouth mason jars (Ball brand, Hearthmark, LLC, Daleville, IN, USA) containing either a low (FW ≤0.4 ppt; ≤677 µS/cm) or high (SW = 35 ppt; 50.7 mS/cm) salinity treatment. Treatments were set up for each family in duplicate with 10 fish per jar. To reduce handling stress, groups of 10 fish were first dip-netted into a hexagonal, polystyrene weighing dish (13-cm diameter) containing ~100 mL of treatment water, which was then gently poured into the jar. This step also allowed us to photograph each batch of fish before transfer to obtain standard length data from ruler-calibrated, digital measurements. Three-week and 7-week-old stickleback were placed in quart-sized jars (0.86 L) and 10-week olds in half-gallon jars (1.5 L; Table 1). Because mortality had been nonexistent for stickleback juveniles held in jars at the rearing salinity in numerous other salinity trials (J. Divino, unpubl. data), parallel control jars were not set up. However, fish were sampled from the rearing tanks to obtain baseline physiological data in Week 10.

For each age trial, salinity-challenged fish were monitored at least twice per day for 13-15 d; at each inspection, we immediately removed and recorded mortalities. We periodically checked ammonium, nitrite, nitrate, and pH levels (Aquarium Pharmaceuticals, Inc., Chalfont, PA, USA) and maintained water quality and constant salinity throughout the experiment through a combination of debris removal and water changes. Fish were fed salinity-appropriate suspensions of brine shrimp nauplii beginning on Day 2 of the trials.

Only 1/450 3-week-old stickleback survived the 0 ppt (~6 µS/cm) FW treatment. Thus, we excluded this treatment from the Week 3 analysis and used 0.2 ppt (353 µS/cm) as the FW treatment for the Week 7 trial. However, when this treatment was used on the larger, 10-week-old stickleback, another die-off occurred, and the Week 10 FW trial was re-performed at 0.4 ppt (677 µS/cm; Table 1).

Mean standard length of stickleback entering the Week 3 and Week 7 trials differed slightly among populations, with lake juveniles being, on average ≤1 mm shorter than oceanic counterparts

(which corresponded to a 12% and 3% decrease in body size, respectively; Table S1). Size distributions among populations were even more similar in 10-week-olds, with mean lengths differing by ≤2%. In all trials, length distributions overlapped completely in the low end of the range (Table S1).

At the end of each trial, we euthanized survivors with an overdose of MS-222 anesthetic (Tricaine-S, Western Chemical, Inc., Ferndale, WA, USA). Fish were then rinsed in deionized water, blot-dried, and standard lengths were measured using digital calipers (to the nearest 0.1 mm). Subsets of at least eight stickleback per treatment were selected for gill NKA activity and families were pooled to increase sample size. We micro-dissected branchial baskets (eight gill arches) from Week 7 and Week 10 juveniles, while the fish lay on ice-cold glass. Tissue samples were immersed in tubes containing 100 µL of sucrose-EDTA-imidazole (SEI) buffer (McCormick 1993), snap-frozen in liquid nitrogen or on dry ice, and stored at -80°C.

The gill tissue was later analyzed for NKA activity at the Conte Anadromous Fish Research Center (Turners Falls, MA, USA) via a 96-well microplate spectrophotometric assay, which measures the rate at which functioning, sample-derived ATPases can hydrolyze ATP (McCormick 1993). Preliminary tests using pooled stickleback gill homogenates confirmed that assay conditions, originally developed for salmonids, also worked optimally for this species (J. Divino, unpubl. data). Stickleback gill samples stored in the SEI buffer were thawed on ice, homogenized in 0.1% deoxycholate (which emulsifies the sample-derived ATPases), and centrifuged to pellet insoluble material. To initiate the reaction, we added an assay mixture containing salts (NaCl, KCl, $MgCl_2$), ATP, and reagents that enzymatically couple ADP production with NADH oxidation (phosphoenolpyruvate, and the enzymes lactic dehydrogenase and pyruvate kinase in an imidazole buffer). Kinetic oxidation of NADH was measured by repeated 340 nm absorbance readings taken for 10 min on a plate reader at 25°C using Gen5 software (BioTek Instruments, Winooski, VT, USA). For each sample, NKA activity was quantified as the difference between the mean NADH decay slope of the reaction in duplicate wells in the presence or absence of 0.5 m*M* ouabain, a potent NKA inhibitor. Readings were normalized to the sample's total protein concentration, as determined using a Pierce BCA Protein Assay (ThermoFisher, Waltham, MA, USA). We statistically

analyzed gill NKA activity using two-way ANOVA, testing for effects of population (pop), salinity (salt), and their interaction. Families and jars were pooled to increase sample size (minimum $N = 8$). For overall significant effects ($P < 0.05$), we performed Tukey's HSD multiple-comparison tests to elucidate group differences.

Multi-acclimation halotolerance studies.— In 2011, we performed a second set of experiments on F_1 stickleback crossed from the same populations, but we divided the clutches of embryos into FW (0.5 ppt; ~0.8 mS/cm), brackish water (BW = 15 ppt; 22.5 mS/cm), or SW (30 ppt; 43.8 mS/cm) acclimation groups for a total of nine population-salinity combinations. We distributed the embryos by family into 100-mm diameter, glass Petri dishes at densities of 25 eggs/dish ($N_{dish} = 107$). Water was replaced daily and embryos were monitored closely with the aid of microscopy. We removed and recorded mortalities. Proportion survival in each Petri dish was averaged during a comprehensive tally taken at 2 and 9 d post-hatch, which respectively corresponded to pre-feeding yolk-sac larvae (Stage 27) and feeding fry (Stage 29; Swarup 1958) just before we relocated them to quart jars. Containers of embryos and larvae were periodically photographed to document development. We transferred 2-week-old juveniles to 38-L rearing aquaria, pooling families to increase population-acclimation cohort sizes. At this time, we also established 10 and 20 ppt acclimation groups (which corresponded to approx. 15.1 and 29.7 mS/cm) from additional anadromous clutches, which had been reared in 3 ppt (Table 1), and individuals were allowed to acclimate to these salinities for >30 d prior to experimentation.

We assessed acute low and high salinity toxicity among all 11 population-acclimation groups when stickleback approached 3 months of age. We assigned fish to one of 11 challenge salinities, which spanned 0-0.5 ppt for low-salt and 30-50 ppt for high-salt treatments. Due to limitations in the number of fish available, treatments were selected with respect to the fish's acclimation salinity in an attempt to ensure that lower and upper lethal concentrations could be accurately estimated (see Results for details). Fish were fasted for at least 12 h prior to being transferred directly into glass jars containing 1.5 L of a

challenge salinity at a target density of 10 fish per jar; duplicate jars were set up if possible. The fish did not differ in body size among populations (Table S1).

We monitored fish multiple times daily and removed and recorded mortalities. Jar water was not replaced and food was not provided during this short 3-d trial. A final census was conducted on Day 3 before the survivors were euthanized. Fish were then rinsed, blot-dried, and measured as described above. Branchial tissue (four gill arches) was sampled from fish exposed to select challenge treatments for NKA activity analysis (see Results; target $N = 6$). Control gill samples were also collected from each population-acclimation group ($N = 5$), and samples were processed as described above.

Survival analyses.— We coded each subject in the two-week salinity challenges as a survivor ("0") or a mortality ("1") with time-to-event recorded for all individuals. Survival curves were plotted using the *survfit* function in the *survival* package in R (R Core Team 2016). Final (endpoint) survival was analyzed on the binary response via a binomial generalized linear mixed-effects model (bGLMM) using the *glmer* function in the *lme4* package in R, shown below:

(1) glmer(MortScore ~ Popn*fsalt + (1|FamID/JarID), family = binomial (link = logit), nAGQ = 1, *data*)

In Eq. 1, the binary survival outcome (MortScore) of each individual is determined by the fixed effects of population (Popn), salinity (coded as a factor; fsalt), and their two-way interaction, in addition to the random effects of jar (JarID) nested within clutch family (FamID). The nAGQ argument specifies Laplace's approximation of the log-likelihood of the variance components (the default setting). Because this model uses the binomial family to relate the response variable to the predictors on a logit scale, it breaks down if there is perfect separation in one or more levels of the data, yielding standard errors that greatly exceed the coefficient estimates (Abrahantes & Aerts 2012). A category having complete survival or complete mortality in one population-salinity group occurred in each trial. For these three cases, we

changed the survival score of one stickleback so that it had a non-identical response compared to the rest of the group (N = 60-160 fish), allowing the logit-linked models to run properly.

We determined that our statistical interpretation was robust to model selection after producing similar results when the response variable was adjusted to be the proportion of stickleback that survived in each jar replicate. Results were also consistent when we ran mixed-effects, Cox proportional hazards models for the Week 3 and 7 trials (*coxme* in R; see also Divino et al. 2016). The failure of the time-to-event survival model to produce estimates for some of the model terms with the Week 10 data, as well as the similar pattern of mortality among populations (see Results), contributed to our decision to analyze endpoint survival.

For the acute salinity toxicity study in 2011, we applied logistic regression on proportion survival data to estimate lower- and upper-limit lethal salinity concentrations, or LC_x (expressed as ppt, where x is percent survival). We tested lower and upper halotolerance boundaries for each FW, BW, and SW population-acclimation group (N = 18). However, only a low-salt LC_{85} and a high-salt LC_{50} could be quantified for the FW-acclimated stickleback (see Results). In all other groups, estimates could not be accurately determined because of too few challenge treatments to serve as data points for the regression and/or because survival at the most extreme salinity was too high to extrapolate a LC_x.

Results

Two-week salinity challenges.— In all three of the 2-week salinity challenges, virtually all mortality occurred within the first 2 d, after which the survival curves stabilized (Figs. S1-S3). No 3-week-old lake stickleback survived SW, whereas 63 ± 4% (mean ± SE) of anadromous and 73 ± 5% of marine juveniles did (Fig. 1; bGLMM: pop $P < 0.00001$). However, population differences in SW tolerance disappeared in later trials (P's ≥ 0.4). Survival in SW by lake stickleback increased dramatically in 7-week olds, reaching 79 ± 5% (Fig. 2). Mean SW tolerance in 7-week-old anadromous and marine stickleback also increased compared to that of 3-week-old counterparts, with no marine fish dying in SW (Fig. 2). This led to an overall effect of salinity on survival in the Week 7 trial (bGLMM: salt $P = 0.007$). The pop*salt

interaction was also significant ($P = 0.03$). Specifically, the overall salinity effect was driven by the increase in SW relative to FW survival in oceanic stickleback, whereas the lake cohort performed similarly in both treatments (Fig. 2). In Week 10, no lake stickleback died in FW, and mean FW survival was lower in marine relative to anadromous stickleback (71 ± 5% vs. 89 ± 3%; Fig. 3). However, no significant differences were detected among populations, between salinities, or their interaction according to the bGLMM (P's > 0.2). Nearly all 10-week-old stickleback survived the SW treatment (94-99%; Fig. 3).

Inclusion of a FW treatment in the Week 7 and 10 salinity challenges enabled testing of halotolerance reaction norms. The sign of the FW-SW reaction norm slopes for each family was usually the same as that representing their respective populations (Figs. 2 and 3), and there was no correlation in the relationship between the Week 7 and Week 10 reaction norm slopes for the nine families that were tested in both trials ($R^2 = 0.005$).

Gill NKA activity exhibited strong salinity and population effects in both the Week 7 and Week 10 trials (Fig. 4; 2-way ANOVA: salt P's ≤ 0.0005, pop P's < 0.0001). NKA activity was almost 19% higher in SW than in FW when averaged over both trials. Values in FW were not different from those in the 3-ppt controls in Week 10. In both trials, marine stickleback had higher NKA activity levels than the other populations, irrespective of salinity, and lake stickleback had significantly lower activity in Week 10 (Fig. 4). Two-way interactions were non-significant in both trials (pop*salt P's ≥ 0.1). Overall, NKA activity levels were almost 20% lower in Week 10 compared to Week 7 samples.

Multi-acclimation halotolerance studies.— The 2,575 stickleback larvae hatched 7-10 days post-fertilization (dpf), with hatch-out peaking at 8-9 dpf. Hatching was typically delayed 1 d in the SW-acclimation group. Overall survivorship was 65.5% ± 2.8% (mean ± SE) in 2-day-old yolk sac larvae and 62.9% ± 2.9% in 9-day-old feeding larvae. Early-stage survival differed with respect to population and salinity in both censuses, but without a significant interaction (Table 2; 2-way ANOVAs: pop P's = 0.0003-0.001, salt P's < 0.0001, pop*salt P's = 0.5-0.6). Across all acclimation groups, lake larvae had

lower survival than their marine counterparts (9 dph: 47.9% vs. 76.2%). Larval survival was similar between the FW- and BW-groups (68.1-72.1%), but lower in the SW-acclimation group (40.4%). The SW-acclimated lake stickleback had the lowest survival of any group (28.8%), and this was lower than that of SW-acclimated oceanic counterparts (45.1-46.5%; Table 2).

When the stickleback reached ~3 months of age, all acclimation groups displayed broad halotolerance when acutely exposed to low and high salinity challenge for 3 d. Nearly all fish survived transfer to ion-poor conditions of ≤0.5 ppt, regardless of acclimation salinity (Fig. 5). Low-salt LC_{85} of the FW-acclimated marine and anadromous groups was 0.04 ± 0.07 (mean ± SE) and 0.03 ± 0.06 ppt, respectively. No lake juveniles died in the three low-salt treatments tested. In contrast, hypersaline challenge revealed population differences in halotolerance, which could not be removed completely by acclimation. For each acclimation group, members of marine and anadromous populations had higher survival in ≥40 ppt than lake individuals. Among FW-acclimated individuals, 80% of oceanic stickleback survived direct transfer to 40 ppt, whereas only 15% of lake stickleback did (Fig. 5). This population-level difference was reflected in the high-salt LC_{50} thresholds (marine: 42.5 ± 0.6 ppt, anadromous: 41.1 ± 0.6 ppt, and lake: 37.0 ± 0.6 ppt; mean ± SE).

The BW- and SW-acclimated groups of the ancestral stickleback populations also exhibited higher halotolerance thresholds: all BW-acclimated oceanic stickleback survived in 40 ppt, in contrast to 55% survival in lake counterparts. Moreover, ~60% of SW-acclimated oceanic stickleback survived transfer to 50 ppt, but no members of the lake population survived this extreme hypersaline condition (Fig. 5).

Gill NKA activity differed among stickleback acclimation groups in a "J"-shaped curve: the lowest activity was detected in fish acclimated to near isosmotic conditions of BW (15 ppt), and was higher in FW and SW groups, respectively. This nonlinear pattern was most visible in the anadromous population, which had additional intermediate-salinity acclimation groups of 10 ppt and 20 ppt (Fig. 6A; 1-way ANOVA: salt $P < 0.0001$). Across all three populations, gill NKA activity ranked, in order from highest to lowest, SW, FW, and BW groups (Fig. 6B; 2-way ANOVA: salt $P < 0.0001$): in SW, NKA

levels were 26% greater than FW and 55% greater than BW. Mean NKA activity was highest in marine stickleback gills in FW and BW compared to the other populations. However, the significant population effect ($P = 0.03$) could not be statistically resolved by the *post hoc* Tukey tests. No interaction was detected (Fig. 6B; pop*salt $P = 0.07$).

In all populations, gill NKA activity increased in stickleback exposed to saline and hypersaline conditions for 3 d, relative to the baseline level of the respective acclimation group. FW-acclimated stickleback challenged in 40 ppt had more than 46% higher NKA activity compared to 0.5-ppt controls (Fig. 7A; salt $P < 0.0001$; the 35 and 40 ppt treatments were statistically similar, as were the 0.2 ppt and 0.5 ppt groups). Similarly, BW-acclimated stickleback challenged in 40 ppt had 34% higher levels than 15-ppt controls (Fig. 7B; salt $P < 0.0001$). Even though SW-acclimated fish had the highest baseline NKA activity among all acclimation groups, levels increased further when these fish were challenged in 50 ppt (Fig. 7B; only marine and anadromous stickleback survived this hypersaline treatment; salt $P = 0.01$). FW- and BW-acclimated marine stickleback had higher NKA activity than members of the two other populations (Fig. 7A,B; pop P's ≤ 0.04). However, SW-acclimated marine stickleback had lower levels than their anadromous counterparts (Fig. 7B; pop $P = 0.04$). In each within-acclimation-group analysis, the interaction between salinity and population was not significant (pop*salt P's ≥ 0.7). Finally, when challenged in 40 ppt, the anadromous stickleback groups acclimated to 10 and 20 ppt had 62% and 40% higher gill NKA activity, respectively (Fig. 7C; *T*-tests: P's ≤ 0.002).

Discussion

In this study, we performed common garden halotolerance experiments on multiple populations of F_1-generation Threespine Stickleback, with the aim of assessing how the osmoregulatory system can evolve under different salinity regimes. We tested for evidence of local adaptation by challenging juveniles in ecologically relevant salinities. We also included hypersaline treatments in our design to expose potential among-population differences in osmoregulatory performance that might not be discernable in a standard SW treatment for this euryhaline organism. We have demonstrated that a derived population of

landlocked stickleback has delayed development of SW tolerance and a reduced hypersaline threshold, relative to oceanic ancestors. Furthermore, the reduced branchial NKA activity in this derived population provides a mechanistic link to the corresponding differences in organismal performance. Taken together, our results suggest that when a euryhaline organism no longer experiences ancestral marine conditions, relaxed selection on SW tolerance can lead to a loss of hyper-osmoregulatory capacity and plasticity in the direction of FW-specialization.

In a broader evolutionary context, divergence in halotolerance can establish an osmotic barrier between derived and ancestral populations, which has important implications for speciation. Independent invasions of FW followed by adaptive evolution to ion-poor conditions has produced the postglacial radiation of stickleback (Bell & Foster 1994). Salinity is one of many ecological conditions that impose selective pressure on marine or brackish-water species colonizing isolated, FW habitats. In some cases, the inland migrants may become landlocked (Foote et al. 1994; Velotta et al. 2015). But even where the geographic separation is incomplete, FW residents may still become isolated from conspecifics that have higher salinity tolerance (McCairns & Bernatchez 2010; Whitehead et al. 2011). A similar pattern of halohabitat-induced osmoregulatory divergence is seen in other fishes, as well as several invertebrate taxa, including copepods (reviewed by Lee & Bell 1999; Lee 2016), which highlights the importance of halohabitat as a driver of physiological evolution.

Evolution of halotolerance in fishes colonizing FW.— Euryhalinity encapsulates a suite of physiological traits that enables aquatic organisms to occupy a wide osmotic niche. We predicted that differences in halotolerance that existed among stickleback populations would persist, at least to some degree, despite salinity acclimation. In general, stickleback from the three populations we tested could successfully be acclimated to and survive challenges at a wide range of salinities. Embryos representing all ecotypes hatched in 15 ppt and 30 ppt, but typically required one additional day of incubation at these higher salinities, consistent with previous observations (Belanger et al. 1987). Furthermore, the stabilization of the survival curves during the 2-week trials indicated that stickleback could rapidly acclimate to acute FW

and SW challenge. Even members of the Frog Lake population, which has been landlocked for ~10,000 years, still retained a degree of SW tolerance: a portion of each clutch could be successfully acclimated to hyperosmotic conditions, and 10-week-old juveniles (acclimated to 3 ppt) could survive direct transfer to 35 ppt at rates on par with those of marine (Resurrection Bay) and anadromous (Rabbit Slough) counterparts. Yet population differences in halotolerance supported our hypothesis: 3-week-old larval stickleback from Frog Lake could not cope at all with a direct transfer from a standard lab-rearing salinity to SW, and one month later, their survival in SW was still lower than in oceanic counterparts. In addition, members of this derived population consistently had the lowest survival in SW and markedly reduced hypersaline tolerance, which became apparent in ≥40 ppt. Our multi-acclimation trial showed that this osmoregulatory divergence in SW tolerance did not disappear after prior acclimation to high-salt conditions. Compared to the FW-acclimated lake stickleback, the BW-acclimated lake group had improved survival (55%) when challenged in 40 ppt, whereas no BW-anadromous or BW-marine individuals died in this treatment. Moreover, prior SW-acclimation of the derived fish did not enable them to withstand 50 ppt, but did confer some survival in the other populations. In sum, the reduced halotolerance breadth of derived stickleback is evidence of a loss in osmoregulatory plasticity.

A loss of SW tolerance has been seen in other derived versus anadromous stickleback population comparisons (Marchinko & Schluter 2007; McCairns & Bernatchez 2010; DeFaveri & Merilä 2014). Others have reported enhanced FW survival in derived Threespine Stickleback populations, suggesting evolution of a more specialized FW phenotype (Heuts 1947; Schaarschmidt et al. 1999; Divino et al. 2016). Taken together, the decreased SW tolerance of FW-resident stickleback in the ancestral ("foreign") habitat coupled with increased FW tolerance in the derived ("local") habitat is a classic demonstration of local adaptation (Kawecki & Ebert 2004). Such a performance tradeoff is exhibited in FW-resident populations of Alewife (*Alosa pseudoharengus*; Velotta et al. 2015), Mummichog (*Fundulus heteroclitus*; Brennan et al. 2015), as well as in a calanoid copepod (*Eurytemora affinis*; Lee et al. 2003).

We did not observe a distinct FW-SW tradeoff in this study, as Frog Lake stickleback did not have significantly higher survival in FW. However, our inability to detect enhanced FW tolerance in lake

stickleback may have been masked by some proportion of FW mortalities caused by extraneous factors indirectly linked to ion-poor conditions. Even so, despite the added stressors associated with the FW treatment in small-volume jars (which were experienced by all subjects), few 10-week-old stickleback died in the 0.4 ppt FW trial. In a similarly-designed experiment, improved FW tolerance was detected in 6-week-olds from a recently lake-introduced population that had been stocked with anadromous adults from Rabbit Slough (Divino et al. 2016). The researchers challenged fish at 0.4, 0.2, and 0 ppt and achieved higher survival rates at these conditions than we report here, likely because they fed subjects artificial pellets. If we had conducted our salinity challenges using this improved feeding technique, we would have been better able to discern whether or not FW halotolerance differences emerged between the ancestral and derived populations.

The dramatic increase in SW tolerance exhibited by lake stickleback from Week 3 to Week 10 underscores the importance of early development on hypo-osmoregulatory function. Early juvenile development is an important period for increasing osmoregulatory capacity, and body size is positively related to improved osmoregulatory function in many euryhaline fishes (reviewed by Zydlewski & Wilkie 2013). Larger juvenile fish have more developed branchial anatomy, which can better function as an osmoregulatory organ: longer filaments facilitate increased ionocyte abundance over the greater epithelial surface area (Finn & Kapoor 2008). During our study, juvenile stickleback more than tripled in body length from Week 3 to Week 10, with size discrepancies among population decreasing during that span. While the increase in body size likely contributed to the increase in osmoregulatory performance overall, lake individuals consistently underperformed oceanic counterparts in each SW challenge. Since the smallest size-classes were represented in all populations, we do not believe that the modestly smaller average size of the lake cohort can account for their complete failure to survive in SW as 3-week olds. Rather, we conclude that derived stickleback have evolved a lower absolute halotolerance threshold, as well as a delay in the developmental timing of hypo-osmoregulatory function following FW residency. Developmental changes in osmoregulatory capacity have been best studied in anadromous fishes, largely with respect to seasonality (Zydlewski & McCormick 1997; McCormick et al. 2013b). Our findings

reveal that examination of early ontogenetic effects on osmoregulation is also needed to fully understand the physiological evolution of derived populations subsequent to their FW invasion.

Patterns of gill NKA activity.— To establish mechanistic support for population differences in halotolerance following salinity challenge, we quantified the stickleback's osmoregulatory investment by measuring levels of gill NKA activity in branchial ionocytes. NKA is an important mediator of hypo-osmoregulation and upregulation of NKA activity in SW has been well-documented in the gills of phylogenetically diverse euryhaline fishes, including Atlantic Salmon (*Salmo salar*; McCormick et al. 2013b), Gilthead Sea Bream (*Sparus aurata*; Sangiao-Alvarellos et al. 2003), Japanese Medaka (*Oryzias latipes*; Kang et al. 2008), Senegalese Sole (*Solea senegalensis*; Arjona et al. 2007), as well as anadromous and FW-resident Alewife (*A. pseudoharengus*; Christensen et al. 2012; Velotta et al. 2015) and Inconnu (*Stenodus leucichthys*; Howland et al. 2001). Recently, Divino et al. (2016) found higher levels of NKA activity in gills of F_1 lab-reared juvenile Threespine Stickleback from an anadromous and a recently lake-introduced population exposed to 35 ppt compared to control (3 ppt) or FW-challenged juveniles.

Consistent with our predictions and with these previous reports, gill NKA activity increased in juvenile stickleback exposed to SW. Across all experiments in this study, we detected a salinity-induced upregulation of NKA activity by 72 h, which persisted for at least 2 weeks of high-salinity exposure. Schaarschmidt et al. (1999) acclimated wild-caught, adult stickleback to 10 ppt, transferred them to 35 ppt water, and measured gill NKA activity during a 43-d time course experiment. Gill NKA activity increased on Day 1 of SW exposure, continued to rise on Days 3 and 7, and peaked at Day 29 of the experiment. This temporal pattern indicates that SW-type ionocytes recruit to the gill epithelium quickly to expel excess ions in response to hyperosmotic conditions, and they continue to proliferate to maintain ion homeostasis during salinity acclimation. Their results also suggest that the rapid upregulation of NKA activity we observed in the 3-d hypersaline challenge would have likely continued to increase over time.

Longer-duration salinity challenges are necessary to determine when and at what rate NKA activity plateaus in juvenile stickleback.

Although halotolerance increased with age in juvenile stickleback, we did not find a corresponding increase in gill NKA activity between 7-week and 10-week-old fish. A possible explanation for the slight decrease in gill NKA activity levels we observed is that as the juveniles developed, the gill epithelium became increasingly used for non-ionoregulatory functions, such as gas exchange. Alternatively, this result may be an artifact caused by surface area: volume scaling in larger branchial baskets, such that the ionocyte-rich epithelial layer comprised a smaller fraction of the total gill tissue in the samples from older fish.

Our multi-salinity acclimation study revealed a nonlinear, convex relationship between environmental osmolality and gill NKA activity: levels were moderate in stickleback acclimated to FW, lowest in those acclimated to BW (where salinity approached isosmotic conditions), and highest in SW-acclimated counterparts. Moreover, NKA activity further increased when fish were challenged in hypersaline conditions, and did so irrespective of the fish's acclimation salinity. Collectively, the response resembled a "J"-shaped curve. A similar pattern was found in Black Seabream (*Mylio macrocephalus*; Kelly et al. 1999) and Wedge Sole (*Dicologoglossa cuneata*; Herrera et al. 2009). Although these authors often refer to "U"-shaped NKA activity response curves, they are often more accurately described as a "J" because the relationship is asymmetric about the isosmotic point, i.e., with values from fish exposed to saline or hypersaline treatments exceeding those in FW.

In response to either hypo- or hyperosmotic stress, euryhaline fishes recruit more FW or SW-type branchial ionocytes, respectively, both of which are powered by basolateral NKA (Edwards & Marshall 2013). Thus, using NKA activity as a proxy for osmoregulatory expenditure, the convex pattern we observed implies that euryhaline fishes expend the least energy maintaining ion balance at or near isosmotic conditions, and work harder to absorb or secrete ions in more extreme halohabitats. Interestingly, some populations of the euryhaline copepod *E. affinis* also displayed a similar pattern of NKA activity across a smaller range of salinities (Lee et al. 2011). A nonlinear relationship between gill

NKA activity and salinity may apply to other euryhaline organisms, and researchers should also take note whether other constituents of osmoregulatory machinery, e.g., ion transporters and transcription factors, are likewise downregulated in BW and upregulated in FW and SW.

The increase of branchial NKA activity from an isosmotic salinity to changes in environmental osmolality in either direction has important implications concerning study design and inferences made about NKA-related osmoregulatory responses to salinity transfers - especially since activity rates of NKA are presumably linked to its gene and/or protein expression. Conclusions about up- or downregulation of NKA in response to salinity may be contingent on which "FW" and "SW" treatments are chosen. For example, McCairns and Bernatchez (2010) compared gill NKAα1 (*atp1a1a.4*; splice variant transcript ID ENSGACT00000018945; Ensembl 2016) expression in larval stickleback from parapatric estuarine and stream residents of the St. Lawrence River, out of which they reared F_1 progeny in either <1 ppt or 20 ppt. They noted substantial upregulation in the FW treatment in both demes. They concluded that a FW-specific NKA isoform associated with FW adaptation was responsible for the negative relationship between salinity and NKA expression.

Differentially-expressed FW and SW NKA isoforms (e.g., NKAα1a and NKAα1b) have been found in several teleosts (Scott et al. 2005; Aykanat et al. 2011; Dalziel et al. 2014), and localize to distinct FW and SW ionocytes on the gill (McCormick et al. 2009). Across multiple continents, ancestral and derived stickleback populations exhibit ecotype-specific sequence signatures in several osmoregulatory genes, including NKAα1 (*atp1a1*), that are characteristic of directional selection (DeFaveri et al. 2011; Shimada et al. 2011). However, functionally distinct NKAα1a and α1b paralogs have not been identified in the stickleback genome.

Given that the NKA pump drives ion uptake in hyper-osmoregulation, a plausible alternative explanation for McCairns and Bernatchez's (2010) detection of relatively higher NKAα1 expression in FW follows from the increase in osmoregulatory effort expected in stickleback transferred from a near isosmotic 20 ppt to a FW condition, which corresponds to the left side of the "J"-shaped NKA activity response curve described above. It remains unclear whether the expression of the *atp1a1a.4* splice variant

they measured is upregulated exclusively in ion-poor conditions, or whether it would also be involved in a response to a more effective hyperosmotic challenge. Curiously, this locus maps to NKAα1b orthologs in salmonids and Zebrafish (*Danio rerio*; Norman et al. 2012). More work is needed to verify whether or not reciprocally salinity-responsive NKA isoforms exist in stickleback and if they evolved independently from those identified in other teleost lineages.

Local salinity regime affected the physiological evolution of stickleback ecotypes, as demonstrated by population differences in gill NKA activity. In almost all salinity challenge experiments we performed in 2010 and 2011, F_1-generation marine stickleback exhibited higher gill NKA activity than did members of an anadromous or a landlocked population. Lake stickleback, on the other hand, often had the lowest levels among the three populations, and these fish exhibited the poorest survival in SW and hyper-SW treatments. The inability of derived stickleback to upregulate gill NKA activity to the same degree as ancestral populations provides an important mechanistic link contributing to their reduction in SW tolerance during 10,000 years of lake isolation. Decreased survival in SW and a concomitant decrease in NKA activity was also found in landlocked versus anadromous Atlantic Salmon (*S. salar*; Nilsen et al. 2003; Nilsen et al. 2007) and Arctic Char (*Salvelinus alpinus*; Staurnes et al. 1992). Interestingly, multiple FW isolates of a copepod (*E. affinis*), which invaded FW ca. 70 years ago, also had lower SW tolerance and NKA activity relative to their respective coastal populations (Lee et al. 2011). These examples implicate salinity as a potent ecological factor and demonstrate how the lack of SW exposure can lead to rapid loss of hypo-osmoregulatory function in marine organisms that transition to FW.

Future investigation.— The multitude of Threespine Stickleback populations occupying different halohabitats across their circumpolar range makes it an invaluable study organism for advancing our understanding of the evolution of the plasticity of the osmoregulatory system, particularly in regard to relaxed selection on hypo-osmoregulation. Future halotolerance studies on stickleback should include older age-classes and compare additional FW-resident populations to confirm whether or not the loss of SW tolerance we observed in the landlocked Frog Lake stickleback can be more broadly generalized for

this derived ecotype. Lake populations with known colonization dates that vary on a wide temporal scale would prove especially informative for assessing rates of physiological evolution following transition to FW. Some stickleback populations have colonized FW in the past few decades (Bell & Aguirre 2013; Lescak et al. 2015). Even more recently, Alaska's Cheney Lake and Scout Lake have been stocked with anadromous stickleback, providing an excellent opportunity for examining osmoregulatory divergence in real time (Bell et al. 2016; Divino et al. 2016).

The comprehensive study of osmoregulatory evolution following halohabitat transitions requires an integrated, multi-level approach. In stickleback, most of this work has been done on osmoregulatory genes and gene expression (e.g., Shimada et al. 2011; Jones et al. 2012a; Wang et al. 2014). Less is known at the protein level, such as on the abundance and localization of membrane transporters likely involved in epithelial ion uptake or secretion (e.g., NHE, NCC, CFTR or NKCC), which have been described in other teleost models (reviewed by Edwards & Marshall 2013; Hwang & Lin 2013). Studies should also incorporate whole-body osmoregulatory performance measures, such as plasma osmolality and organic osmolyte content, and endocrine factors, which will provide deeper insights into the effects of osmotic stress at the organismal level. To conclusively demonstrate salinity-induced osmoregulatory evolution between ancestral and derived populations, we will need the corroborating evidence that comes from finding parallel divergence in a suite of physiological endpoints.

Table 1. Study designs of the salinity acclimation and challenge experiments performed on F_1-generation juvenile Threespine Stickleback, sorted chronologically by fish age. Three Alaskan populations were compared: M = marine (Resurrection Bay); A = anadromous (Rabbit Slough); L = landlocked lake (Frog Lake). For the 2-week trials, fish were fed brine shrimp nauplii (BSN) *ad libitum*, beginning on Day 2.

Year Class	**Age Post-hatch**	**Standard Length** (mm) mean ± SD	**Populations-Families**	**Total Families** (# mixed) [a]	**Acclimation Salinities** (ppt)	**Acute Challenge Salinities** (ppt) lower, upper	**Trial Duration** (d)	**Feeding**	**Container Type**	**Total Subjects**	**Total Gill Samples**
2010	3 weeks	7.8 ± 1.1	M-8, A-7, L-8	23 (0)	3	0 [b] , 35	15	BSN	quart jar	900 (450 SW)	---
	7 weeks	19.4 ± 1.3	M-3, A-4, L-4	11 (2)	3	0.2 , 35	14	BSN	quart jar	440	66
	10 weeks	25.6 ± 1.9	M-4, A-5, L-5	14 (3)	3	0.4 [c] , 35	13	BSN	½-gal jar	540	113
2011	~2 days ~9 days	6.5 ± 0.4 7.3 ± 0.6	M-4, A-4, L-4	12	0.5, 15, 30 [d]	---	---	BSN	Petri dish	2,575	---
	11 weeks	30.0 ± 2.3	M, *A*, L	pooled	0.5, *3*, *10*, 15, *20*, 30 [e]	---	---	fasted	10-gal aquarium [f]	---	62
	11.5 weeks	30.0 ± 2.1	M, *A*, L	pooled	0.5, *3*, *10*, 15, *20*, 30	0-0.5 , 30-50 [g]	3	fasted	½-gal jar	949	103

[a] Within populations, full-sibling families that were too small to achieve target experimental quotas were combined to form a "mixed" family.

[b] The reverse osmosis water (0 ppt) treatment resulted in complete fish mortality and was excluded from the analysis.

[c] After an initial trial of 0.2 ppt resulted in nearly complete mortality of 10-week olds, the FW trial was conducted again at 0.4 ppt.

[d] In 2011, the full-sibling clutches were divided among the three main acclimation salinities as embryos.

[e] Due to greater cohort abundance, the anadromous population had additional 3, 10, and 20 ppt acclimation groups (*italics*).

[f] Control samples were collected from rearing tanks 2-3 d prior to the start of the 3-d challenge.

[g] The specific lower and upper challenge salinities tested depended on the acclimation salinity (see Results).

Table 2. Percent survival of larval stickleback for each level of population (marine, anadromous, lake) and salinity acclimation. Survival was recorded on censuses taken 2 and 9 days post-hatch (dph) and averaged across Petri dish replicates containing 25 embryos each. Data are presented as the mean ± SD, with the sample size of each group given in parentheses.

Salinity	Dph	Marine	Anadromous	Lake
0.5	2	88.9 ± 7.2 (20)	74.1 ± 18.3 (20)	54.0 ± 32.2 (16)
	9	87.7 ± 7.2	71.7 ± 19.0	53.0 ± 32.5
15	2	83.4 ± 14.9 (7)	62.5 ± 28.9 (9)	63.4 ± 38.0 (7)
	9	83.4 ± 14.9	62.1 ± 28.8	60.6 ± 39.6
30	2	56.7 ± 19.3 (9)	50.3 ± 31.6 (10)	31.1 ± 30.5 (9)
	9	45.1 ± 22.4	46.5 ± 29.5	28.8 ± 30.6

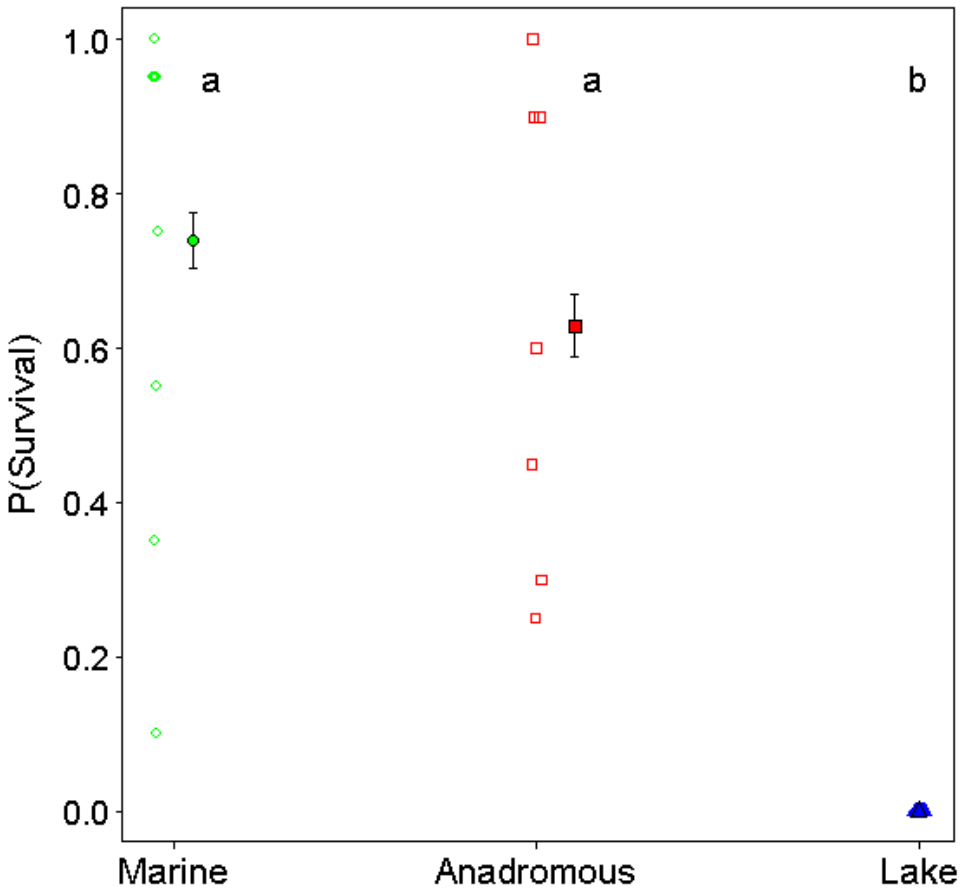

Figure 1. Proportion survival of 3-week-old Threespine Stickleback acutely exposed to SW (35 ppt). Three Alaskan populations were compared: Marine (Resurrection Bay; green circles), Anadromous (Rabbit Slough; red squares), and landlocked Frog Lake (blue triangles). Data are presented as overall population means (± SE; filled symbols) and mean survival of each family (open symbols; 20 fish per family; points offset for clarity). Letters denote population differences as determined by a mixed effects, binomial GLM.

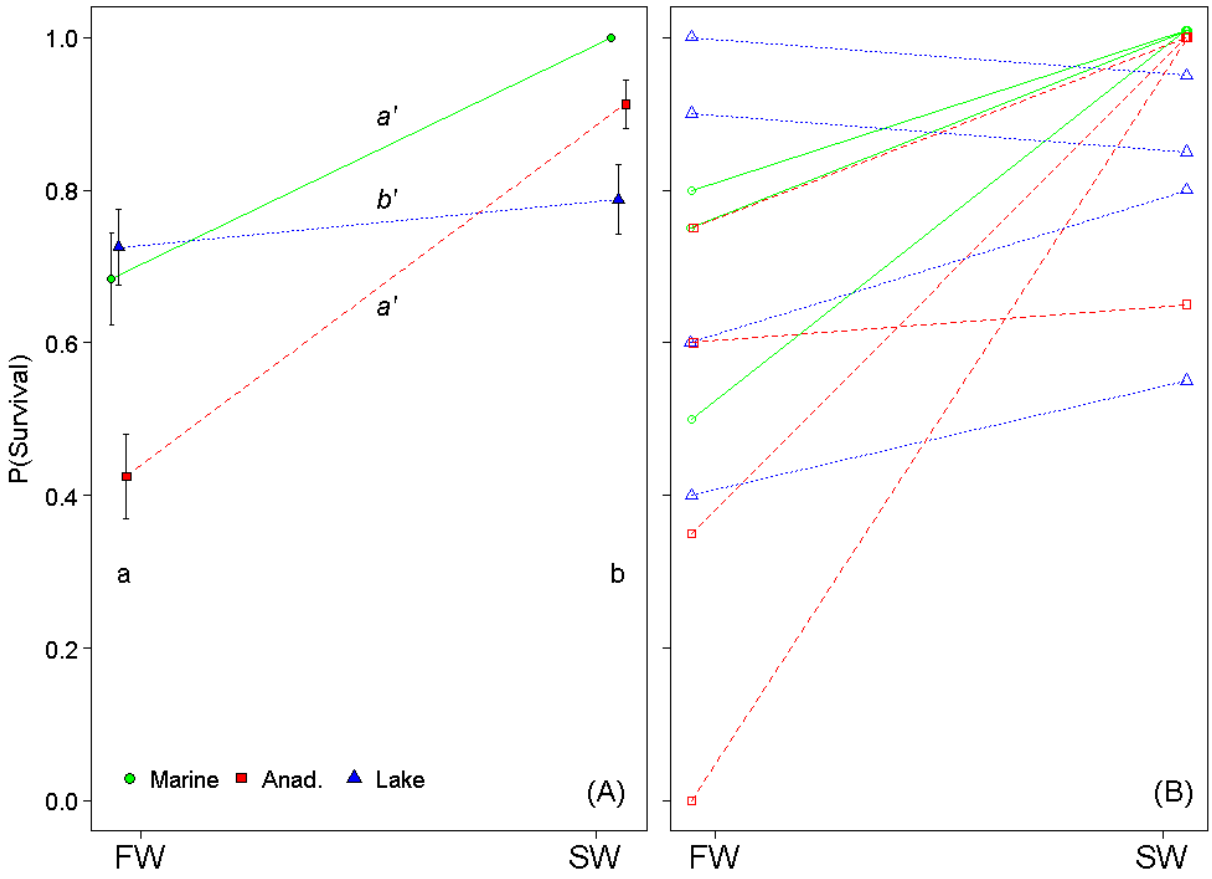

Figure 2. Reaction norms for proportion survival of 7-week-old Threespine Stickleback acutely exposed to FW (0.2 ppt) or SW (35 ppt). Three Alaskan populations were compared: Marine (Resurrection Bay; green circles, solid lines), Anad. = Anadromous (Rabbit Slough; red squares, dashed lines), and Lake = Landlocked Frog Lake (blue triangles, dotted lines). (A) Overall population means (± SE) in each environment (points offset along x-axis for clarity). A mixed effects, binomial GLM identified an overall effect of salinity (horizontally-aligned letters) and an interaction between the reaction norm for the Lake population relative to the two others (vertically-aligned, prime letters). (B) Mean survival by family (20 fish per family per treatment), which was a random effect in the model.

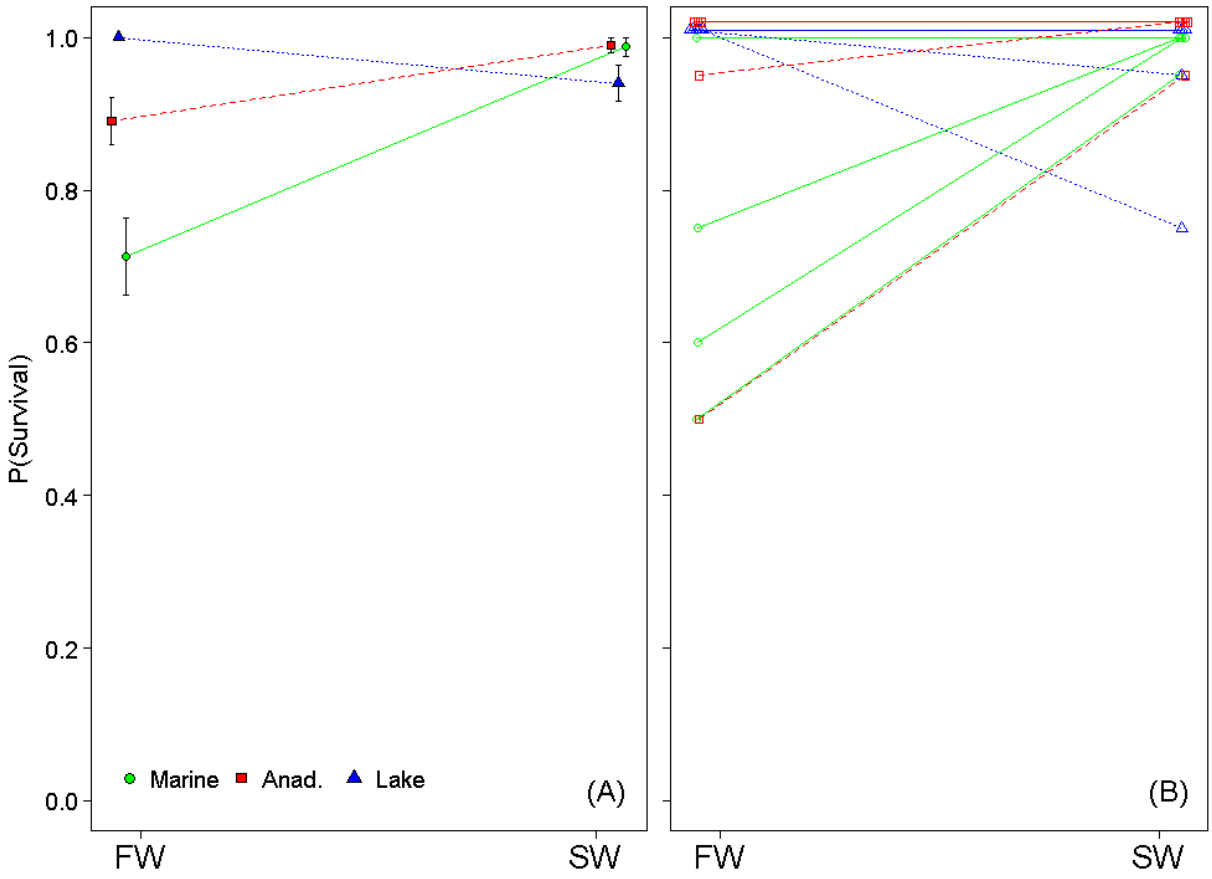

Figure 3. Reaction norms for proportion survival of 10-week-old Threespine Stickleback acutely exposed to FW (0.4 ppt) or SW (35 ppt). Three Alaskan populations were compared: Marine (Resurrection Bay; green circles, solid lines), Anad. = Anadromous (Rabbit Slough; red squares, dashed lines), and Lake = Landlocked Frog Lake (blue triangles, dotted lines). (A) Overall population means (± SE) in each environment (points offset along x-axis for clarity). A mixed effects, binomial GLM found no group differences. (B) Mean survival by family (20 fish per family per treatment), which was a random effect in the model.

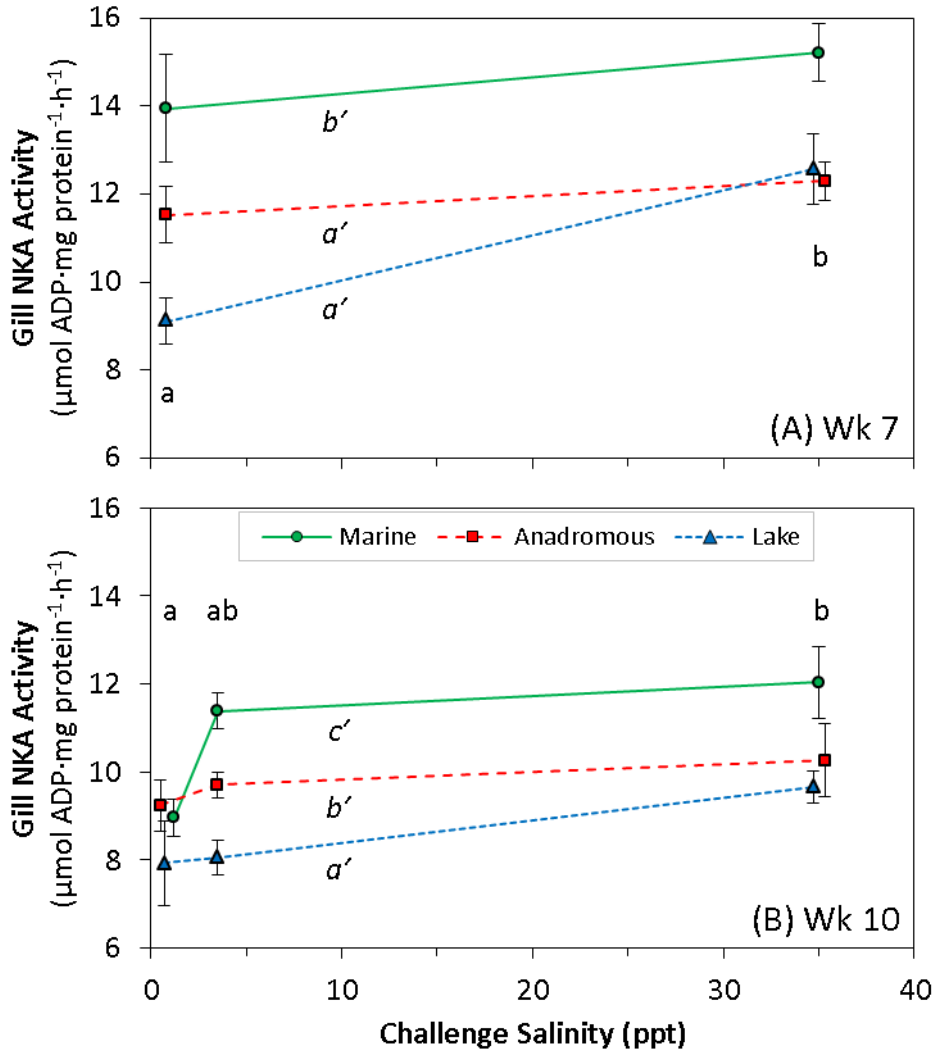

Figure 4. Gill NKA activity in juvenile marine (Resurrection Bay; green circles), anadromous (Rabbit Slough; red squares), and landlocked (Frog Lake; blue triangles) Threespine Stickleback, following two weeks exposure to FW (0.2-0.4 ppt) or SW (35 ppt) beginning when fish were (A) 7-weeks or (B) 10-weeks old. Unchallenged fish from the common rearing salinity (3 ppt) were also analyzed in the latter trial. Data are presented as the mean ± SE of a minimum of eight samples (average $N = 11$; points offset along x-axis for clarity). Horizontally-aligned letters identify salinities that differed significantly, whereas vertically-aligned, prime letters denote population differences, as determined by Tukey *post hoc* tests. The interaction between these two main effects was non-significant for both trials.

			Population																	
			Anadromous									Marine					Lake			
Acclimation→ Salinity (ppt)			0.5		10		15		20		30	0.5		15		30		0.5		15		30
Challenge Salinity (ppt)	Low	0	.9									1	1									
		0.1	.8	.9	.1							1	.2	1								
		0.2	1	1								1	1	1	1			1	1			
		0.3	1	1	.9	1						1	1					1	1			
		0.4	1	1			1	1	1	1		1	1	1	1			1	1	1	1	
		0.5							1	1	1					1	1					1	
	High	30	1	1	1	1	1	1	1	1		1	1	1	1			1	1	1	1	
		35	1	1								1	1					1	.5			
		40	.6	.8	.9	1	1	1	1	1		.8	1	1	1			.2	.1	.7	.4	
		45	.1	0								.2	0	.1				0				
		50									.9	.3	0			.7	.5					0	

Figure 5. Halotolerance matrix in juvenile Threespine Stickleback. Clutches from three populations were split and acclimated to various salinities as embryos and subjected to salinity challenge when fish were 3-months old. Color-coded cell values are the proportion of 10 fish that survived 3-d exposure in a 1.5 L jar containing one of 11 challenge salinities, with a target of two jars per treatment (N_{jar} = 96). Limitations in the number of fish available in each population-acclimation group prevented some combinations from being tested (shaded cells); treatments were selected with respect to the fish's acclimation salinity in an attempt to ensure that lower and upper lethal concentrations could be accurately estimated. Underlining marks the treatments from which gill samples were collected for NKA activity analysis. Control samples were also taken for each acclimation group (not shown).

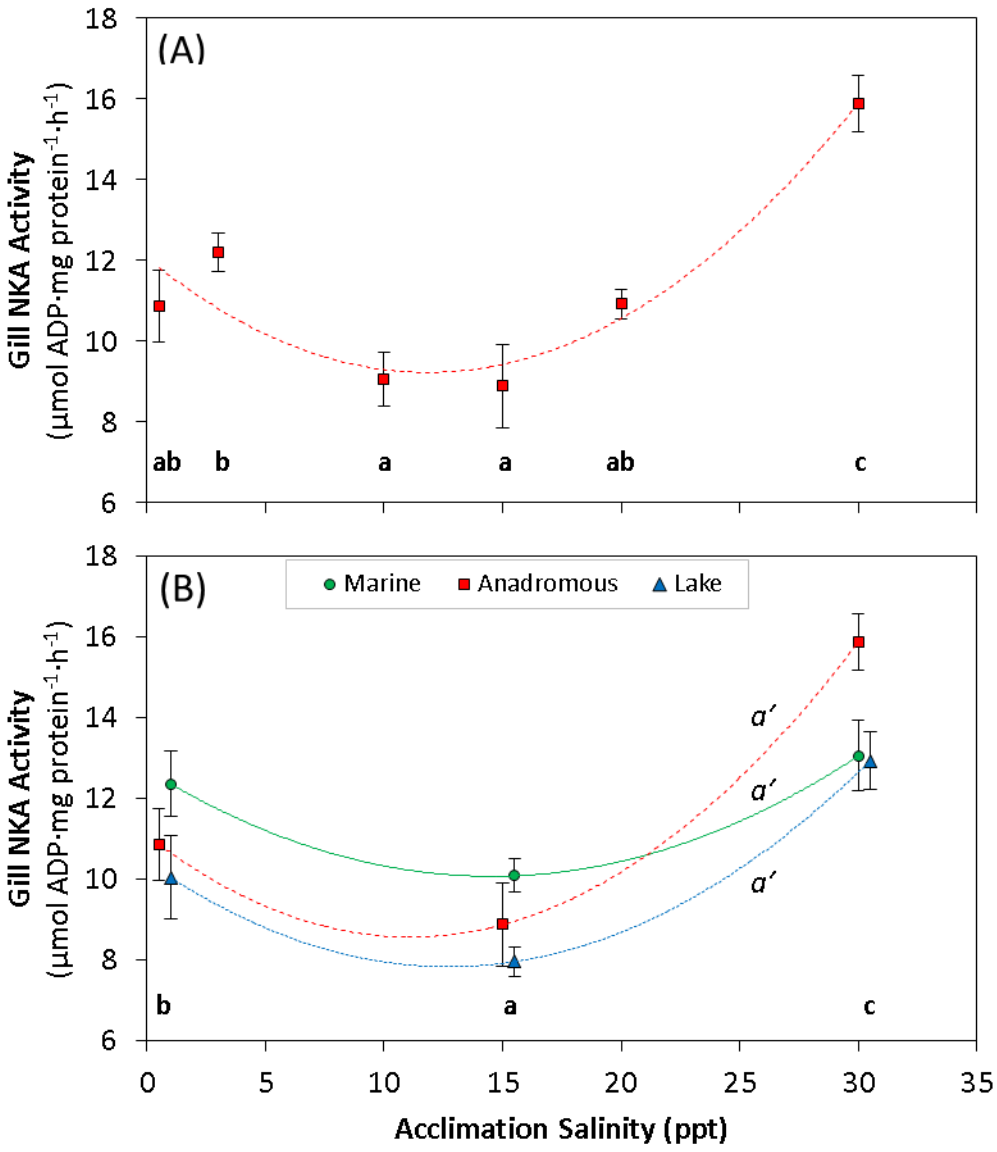
(A)
Gill NKA Activity
(µmol ADP·mg protein-1·h-1)
ab
b
a
a
ab
c
(B)
Marine
Anadromous
Lake
a′
a′
a′
b
a
c
Acclimation Salinity (ppt)

Figure 6.

Figure 6. Gill NKA activity in juvenile Threespine Stickleback, which were acclimated to different salinities as embryos. Data are presented as the mean ± SE of five samples (points offset along x-axis for clarity). Horizontally-aligned letters identify salinities that differed significantly in the response variable, as determined by Tukey *post hoc* tests. (A) Members from an anadromous population (Rabbit Slough; red squares) were raised in 0.5 (FW), 3, 10, 15 (BW), 20, or 30 ppt (SW). (B) Gill NKA activity from the FW, BW, and SW-acclimated groups were compared to that of a marine (Resurrection Bay; green circles) and landlocked (Frog Lake; blue triangles) population. Although a two-way ANOVA indicated a significant, overall population effect in (B), no population pairs significantly differed according to Tukey *post hoc* tests (vertically-aligned prime letters).

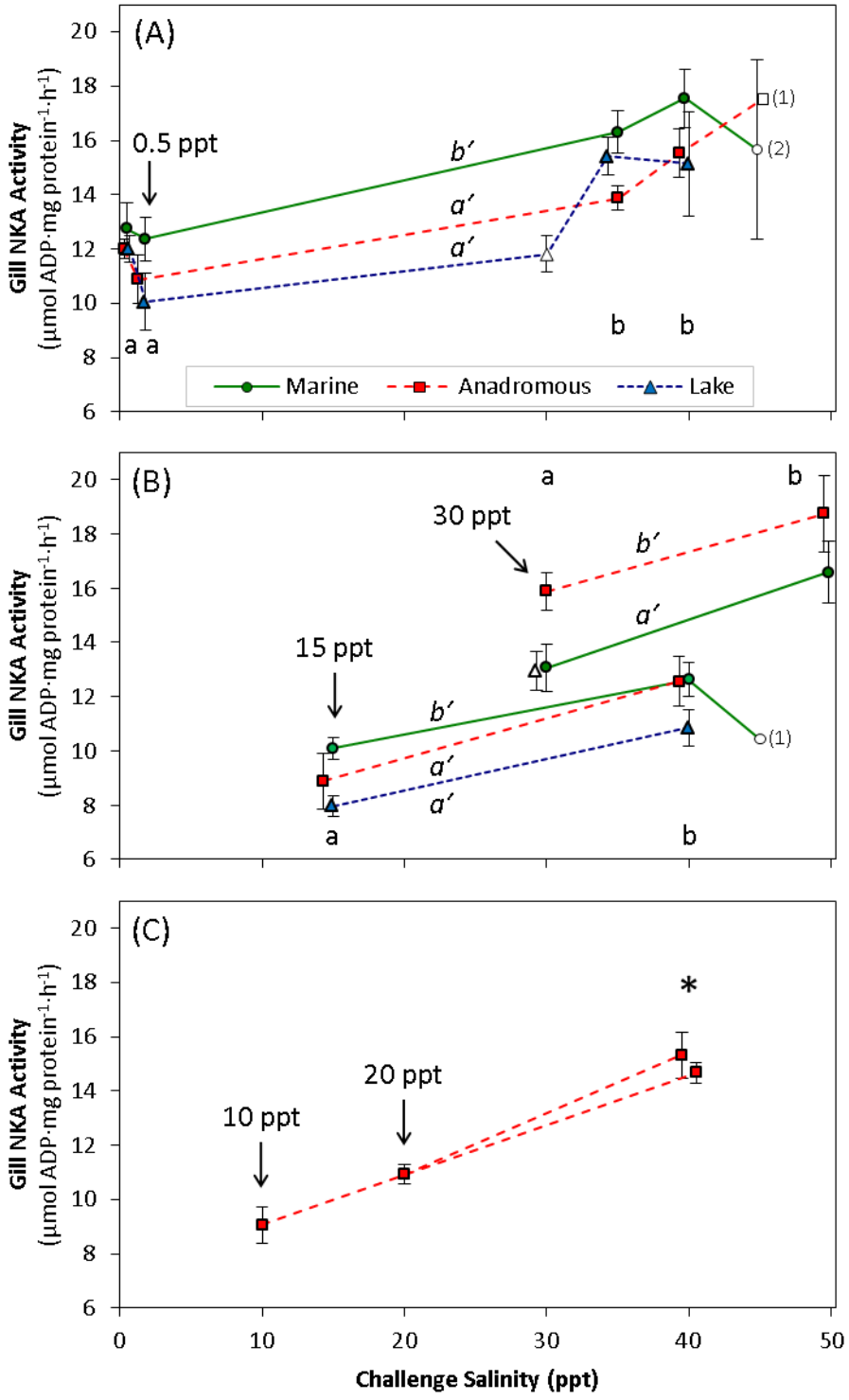
(A)
0.5 ppt
b′
a′
a′
a a
b b
(1)
(2)
Marine
Anadromous
Lake
(B)
30 ppt
15 ppt
a
b
b′
a′
a′
b′
a′
a′
a
b
(1)
(C)
10 ppt
20 ppt
*
Gill NKA Activity
(µmol ADP·mg protein-1·h-1)
Challenge Salinity (ppt)
0
10
20
30
40
50
6
8
10
12
14
16
18
20

Figure 7.

Figure 7. Gill NKA activity in juvenile marine (Resurrection Bay; green circles), anadromous (Rabbit Slough; red squares), and landlocked (Frog Lake; blue triangles) Threespine Stickleback, which had been acclimated to various salinities as embryos and then transferred to a foreign salinity for 3 d. In each panel, groups of control fish are designated by arrows (see Fig. 6). Data are presented as the mean ± SE of 5-6 samples, unless otherwise noted in parentheses (points offset along x-axis for clarity). Within acclimation groups, horizontally-aligned letters denote salinities that differed significantly in the response, whereas vertically-aligned, prime letters denote population differences, as determined by Tukey *post hoc* tests. The interaction between these two main effects was non-significant in all cases. Open symbols were excluded from statistical analysis due to missing levels or low sample size. (A) Fish acclimated to FW (0.5 ppt) were challenged at either 0.2, 35, or 40 ppt. (B) Fish acclimated to BW (15 ppt) were challenged at 40 ppt, while fish acclimated to SW (30 ppt) were challenged at 50 ppt (no Lake stickleback survived this hypersaline treatment). (C) Additional anadromous stickleback acclimated to 10 or 20 ppt were compared to counterparts challenged at 40 ppt, and the asterisk denotes significant salinity-induced upregulation in both cases.

Table S1. Summary statistics of stickleback standard lengths by population and age (post-hatch) at the start of each experiment. Length distributions are described in percentiles (P).

Trial	Starting Age	Population	Mean ± SD (N)	P1	P10	P25	P50	P75	P90	P99
2-week acute Challenge (2010)	3 weeks	Marine	8.4 ± 1.3 (260)	5.8	6.7	7.4	8.3	9.5	10.1	11.1
		Anadromous	7.8 ± 0.8 (258)	6.1	6.7	7.2	7.8	8.3	8.8	9.4
		Lake	7.3 ± 0.7 (280)	6.0	6.4	6.8	7.3	7.8	8.3	9.2
	7 weeks	Marine	19.7 ± 1.3 (120)	16.3	18.1	18.9	19.8	20.5	21.3	22.3
		Anadromous	19.4 ± 1.5 (160)	14.0	17.4	18.7	19.6	20.2	21.0	22.9
		Lake	19.1 ± 1.1 (160)	15.6	17.9	18.5	19.1	19.8	20.3	21.7
	10 weeks	Marine	25.4 ± 1.9 (238)	19.0	23.0	24.2	25.5	26.6	27.6	29.2
		Anadromous	26.0 ± 1.7 (308)	22.2	23.8	24.8	25.9	27.2	28.0	30.5
		Lake	25.5 ± 2.2 (239)	20.1	23.2	24.2	25.4	27.0	28.5	30.3
Larval Survival (2011)	2 days	Marine	6.6 ± 0.4 (30)	5.9	6.0	6.4	6.7	6.9	7.0	7.2
		Anadromous	6.4 ± 0.4 (23)	5.1	6.0	6.1	6.4	6.6	6.8	7.2
		Lake	6.4 ± 0.5 (25)	5.7	5.8	6.0	6.4	6.6	7.0	7.5
	9 days	Marine	7.2 ± 0.7 (50)	6.0	6.5	6.7	7.1	7.7	8.2	8.8
		Anadromous	7.4 ± 0.6 (63)	6.1	6.6	6.9	7.4	7.9	8.0	8.7
		Lake	7.2 ± 0.5 (63)	5.2	6.5	6.9	7.2	7.5	7.7	8.3
3-d acute challenge (2011)	11.5 weeks	Marine	29.9 ± 2.5 (85)	24.0	26.4	28.3	30.1	31.8	33.0	35.5
		Anadromous	30.0 ± 1.7 (136)	26.6	27.5	29.0	30.0	31.1	32.2	33.8
		Lake	30.0 ± 2.6 (67)	24.4	26.6	28.1	29.4	32.3	33.7	36.2

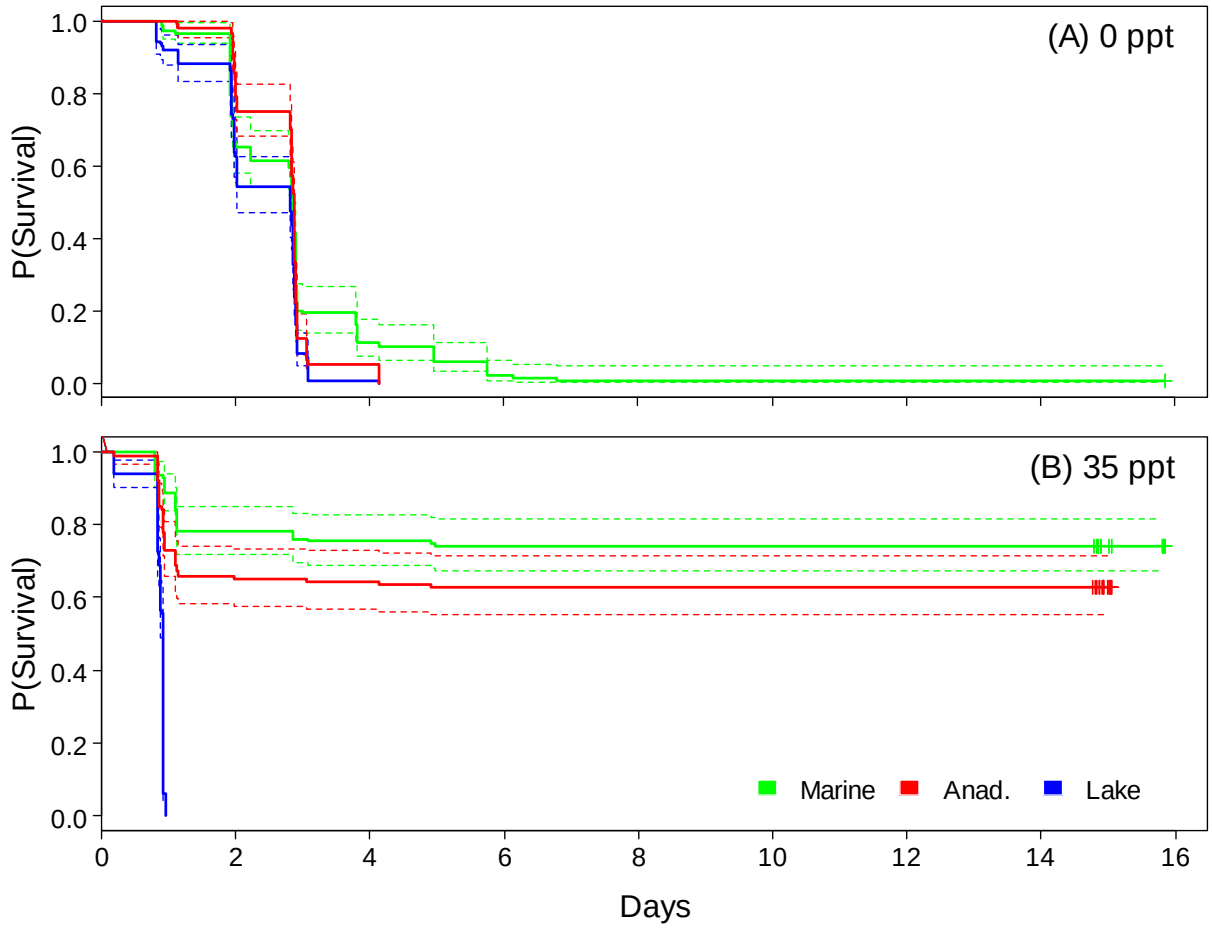

Figure S1. Proportion survival over time (Days) of 3-week-old Threespine Stickleback acutely exposed to (A) 0 ppt (FW; not analyzed) or (B) 35 ppt (SW). Three Alaskan populations were compared: Marine (Resurrection Bay; green lines), Anad. = Anadromous (Rabbit Slough; red lines), and Lake (Landlocked Frog Lake; blue lines). Families and replicate jars were pooled to depict overall population means with 95% confidence intervals in dashed lines. Vertical tick marks in (B) indicate when survivors were censored at the end of the trial.

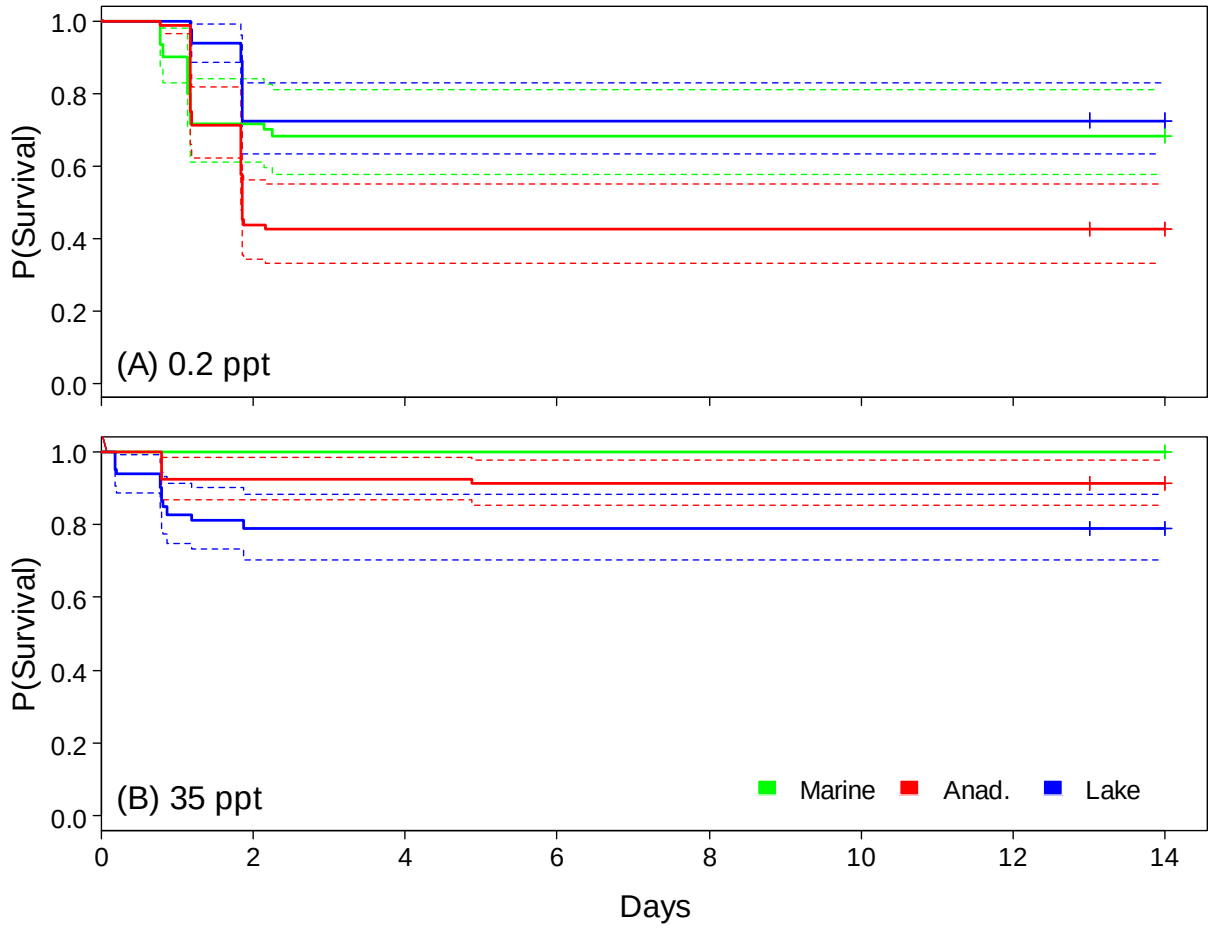

Figure S2. Proportion survival over time (Days) of 7-week-old Threespine Stickleback acutely exposed to (A) 0.2 ppt (FW) or (B) 35 ppt (SW). Three Alaskan populations were compared: Marine (Resurrection Bay; green lines), Anad. = Anadromous (Rabbit Slough; red lines), and Lake (Landlocked Frog Lake; blue lines). Families and replicate jars were pooled to depict overall population means with 95% confidence intervals in dashed lines. Vertical tick marks indicate when gill tissue samples were collected from a subset of the survivors at the end of the trial.

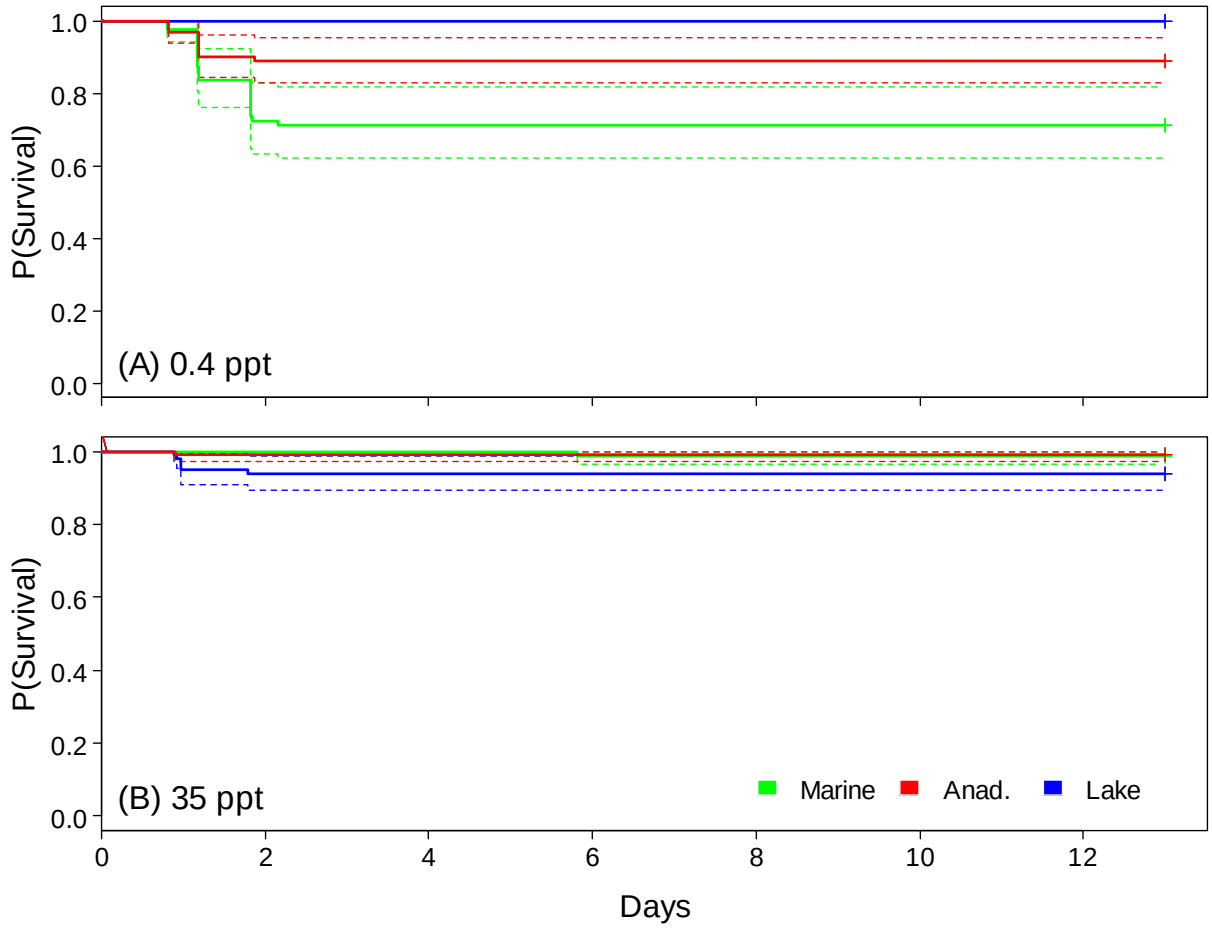

Figure S3. Proportion survival over time (Days) of 10-week-old Threespine Stickleback acutely exposed to (A) 0.4 ppt (FW) or (B) 35 ppt (SW). Three Alaskan populations were compared: Marine (Resurrection Bay; green lines), Anad. = Anadromous (Rabbit Slough; red lines), and Lake (Landlocked Frog Lake; blue lines). Families and replicate jars were pooled to depict overall population means with 95% confidence intervals in dashed lines. Vertical tick marks indicate when gill tissue samples were collected from a subset of the survivors at the end of the trial.

Chapter 2

Characterizing population- and salinity-dependent divergence in gill ionocyte composition among Threespine Stickleback ecotypes using scanning electron microscopy

Introduction

Aquatic organisms that osmoregulate – i.e., maintain ion homeostasis in disequilibrium with the environment – devote a great amount of energetic resources to expel excess ions in seawater (SW) or take up ions in fresh water (FW). However, relatively few species possess the physiological plasticity to survive in both environments, which require opposite functional responses that integrate cellular processes across multiple organ and endocrine systems. For example, <3% of fishes are euryhaline (Betancur-R et al. 2015), even though this trait confers the advantages of greater habitat availability and resource exploitation. Indeed, euryhaline fishes have high evolutionary potential because they can expand their range, crossing osmotic barriers to colonize FW environments that are isolated from each other and possess diverse ecological conditions and niche space (Schultz & McCormick 2013). Given the complex interplay between selective forces that can act on SW and FW tolerance, euryhaline fishes are especially important to investigate because they can inform us about how the osmoregulatory system evolves following halohabitat transitions. For instance, experiments comparing derived, FW-resident populations, which no longer need to hypo-osmoregulate, with marine ancestors will help us learn how osmoregulatory plasticity evolves in response to changing salinity regime.

Besides its role as a respiratory organ, the fish's highly vascularized gill epithelium is also a key osmoregulatory organ, serving as a large surface area for the exchange of electrolytes with the environment. Specialized ionoregulatory cells, called ionocytes, line the gill epithelium and actively transport ions against their electrochemical gradients to counteract ion imbalances with the environment. Transepithelial ion transport involves the coordinated action of a distinct configuration of membrane-bound transporters, which are localized in ionocyte types specialized for ion secretion in SW or absorption in FW. These salinity-specific ionocytes are taxonomically widespread among euryhaline organisms and have distinct cellular morphologies, including the apical surface, which is in contact with

the water (Lee et al. 1996; Kaneko & Hiroi 2008; Edwards & Marshall 2013). The apical opening of FW-type ionocytes is relatively large, flat or convex, in relation to surrounding epithelial pavement cells, and are ridged or studded with microvilli to increase absorptive surface area. In contrast, the apical opening of SW-type ionocytes is deeply recessed, forming a pit or 'crypt', which is often shared in a multicellular complex of ionocytes and accessory cells (Christensen et al. 2012). The narrow apical opening, formed by a ring of pavement cells, serves the purpose of concentrating the chloride ions secreted from the ionocytes in the crypt, which create an electrical gradient favorable for drawing out sodium ions through paracellular channels that lie between the ionocyte and the accessory cells (Kaneko & Hiroi 2008).

In response to salinity change, euryhaline fishes can rapidly remodel their gill epithelium through a combination of recruitment of new ionocytes as well as the functional transformation of pre-existing ionocytes via morphological alteration and translocation of ion transporters (Hiroi et al. 2005). Salinity-induced remodeling of branchial epithelia has been well described in the developmental process of smoltification in out-migrating Atlantic Salmon (*Salmo salar*; Lubin et al. 1989; McCormick 2013), as well as in Mummichog (*Fundulus heteroclitus*; Whitehead et al. 2012), Mozambique Tilapia (*Oreochromis mossambicus*; Lee et al. 1996; Inokuchi et al. 2009; Choi et al. 2011), and Nile Tilapia (*O. niloticus*; Fridman et al. 2011). In these species, researchers characterized the distribution of branchial ionocytes using scanning electron microscopy (SEM) and/or immunocytochemistry, used to fluorescently label ion transporters that generally distinguish ionocytes from other epithelial cells (Na^+/K^+-ATPase; NKA), as well as to identify specific ionocyte types recruited for ion uptake in FW (e.g., Na^+/H^+ exchanger; NHE3 and Na^+/Cl^- cotransporter; NCC) or for ion secretion in SW (e.g., $Na^+/K^+/2Cl^-$ cotransporter; NKCC). Similarly, FW-type ionocytes have been identified in the swimming legs of a euryhaline copepod (*Eurytemora affinis*) via immunostaining of ion transporters (Johnson et al. 2014).

Topological analysis of the gill epithelia is valuable because it consolidates the many molecular changes that may result from ion perturbation into a quantifiable, integrated osmoregulatory response at the tissue level. Dual-imaging of branchial ionocytes, which pair scanning electron microscopy (SEM) of the gill filament with immunolocalization of transporters, have confirmed that superficial differences in

apical morphology distinguishable by SEM are directly linked to FW- and SW-cell types (Inokuchi et al. 2009; Choi et al. 2011). This means that quantification of gill ionocyte types based on their morphology under SEM also characterizes functional differences associated with osmoregulation in FW or SW.

Unfortunately, *in situ* examinations of how branchial ionocyte composition changes in response to osmotic stress or across populations are rarely quantified, including tests for divergence among ecotypes that occupy different salinities. Data are lacking for many euryhaline teleosts, such as the Threespine Stickleback (*Gasterosteus aculeatus*; hereafter 'stickleback'). Across their Holarctic range, ancestral marine stickleback populations have independently colonized isolated FW lakes and streams, where they have subsequently undergone evolutionary changes in morphology, life history, and physiology (Barrett et al. 2011; DeFaveri et al. 2011; Bell & Aguirre 2013). The parallel nature of this evolution implies local adaptation to local ecological conditions, including environmental osmolality. Differences in halotolerance have been well-characterized between marine and FW stickleback ecotypes (e.g., Heuts 1947; DeFaveri & Merilä 2014; Divino et al. 2016; Chapter 1), and this divergence has a basis in osmoregulatory genes and gene transcripts (e.g., Shimada et al. 2011; Wang et al. 2014). Little is known, however, about the ultrastructure of the osmoregulatory epithelia of the stickleback gill, morphological changes in branchial ionocytes in response to osmotic stress, or about how gill osmoregulatory tissue has evolved among salinity-divergent ecotypes. Branchial ionocytes were identified in stickleback using transmission electron microscopy, but only generally assessed for degeneration resulting from exposure to toxicants (Matthiessen & Brafield 1973; Holm et al. 1991).

We used SEM techniques to formally describe effects of salinity on branchial ionocytes in stickleback. Our objective was to assess how osmoregulatory plasticity of gill tissue has evolved among representative marine, anadromous, and FW-resident populations. We selected the same Alaskan populations shown previously to differ in SW tolerance and degree of osmoregulatory investment, as measured by differences in gill NKA activity (Chapter 1). We tested whether corresponding, population-level changes in the osmoregulatory response to salinity challenge would be detectable in the composition of ionocytes on gill epithelia. We hypothesized that mean densities of SW-type ionocytes would increase

in fish held in SW, whereas FW-type ionocytes would proliferate following the fish's exposure to hypoosmotic conditions. We further predicted that derived stickleback from a landlocked lake would exhibit divergence with respect to salinity-dependent ionocyte densities on the gill filament in a manner consistent with local adaption to salinity. Specifically, we expected gill filaments of lake stickleback exposed to SW to contain relatively less SW-type ionocytes than marine and anadromous counterparts as a result of relaxed selection on SW tolerance in the derived group. Conversely, the gills of lake stickleback exposed to FW should have the highest abundance of FW-type ionocytes due to positive selection on FW tolerance. Finally, given their migratory life history, anadromous stickleback might exhibit the greatest plasticity among the populations with respect to salinity-specific regulation of ionocyte types.

Materials & Methods

Fish populations, husbandry, & salinity challenge.— The Threespine Stickleback used in this experiment were collected from three populations in south-central Alaska, representing marine (Resurrection Bay), anadromous (Rabbit Slough), and lake (Frog Lake, presumably colonized by anadromous ancestors 10,000-12,000 years ago) ecotypes. Between four and eight full-sibling clutches for each population were generated via *in vitro* fertilization of the gametes of male-female pairs to produce an F_1 generation, which we raised in a common environment of 3 ppt. More details about field collection and our fish husbandry practices can be found in Chapter 1 and in Divino and Schultz (2014).

We performed an acute salinity challenge when the stickleback reached 10-weeks post-hatch, in which fish from each family were directly transferred from the intermediate rearing salinity into either a low (FW = 0.4 ppt) or high (SW = 35 ppt) salinity. Treatments were run in duplicate jars with 10 fish per jar (Fig. 1). We monitored the stickleback at least twice per day for 14 d and removed and recorded mortalities at each inspection. We maintained water quality and constant salinity throughout the experiment and fed fish salinity-appropriate suspensions of brine shrimp nauplii beginning on Day 2 of the trial. This salinity challenge was conducted as part of a larger study and is described in more detail in

Chapter 1. All experimentation on animals was approved by the University of Connecticut's IACUC (Protocols A10-013 and A13-019).

Gill processing.— At the end of the 2-week trial, we euthanized the stickleback with an overdose of MS-222 anesthetic (Tricaine-S, Western Chemical, Inc., Ferndale, WA, USA). We then rinsed, blot-dried, and measured (standard length) the fish as part of a larger sampling effort (see Chapter 1 for details). Subsets of four stickleback per treatment-population were selected for SEM imaging. We stratified this sampling by selecting two fish per family and one per jar. We also sampled two stickleback from each population from the rearing tanks (3 ppt) as controls.

As described in Paolino (2011), we micro-dissected 2-4 branchial arches while the fish lay on ice-cold glass. Individual gill arches were rinsed with distilled water and immediately submerged in an ice-cold fixative solution (2% glutaraldehyde and 2% paraformaldehyde in a 0.1 *M* phosphate buffer; pH 7.4) in glass vials. The volume of fixative was adjusted to always exceed that of the sample by a factor of 20. We stored the tissue samples at 4°C until use. To prepare samples for SEM imaging, we washed the branchial arches in ice-cold 0.1 *M* phosphate buffer (pH 7.4; 3 x 10 min). After the second rinse, we selected a single gill arch from the set that appeared in the best condition for imaging. This arch was incubated in 2% osmium tetroxide in 0.1 *M* phosphate buffer for 16 h at 4°C, followed by washing with 4°C distilled water (3 x 10 min). We then dried the samples via an ethanol series, incubating them for 15 min in increasing concentrations of ethanol (first in 30%, 50%, and 70% at 4°C and then at room temperature, once in 95% and finally four times in 100%). Samples were stored in 100% ethanol for 24 h and then critical point dried using a Polaron E3000 Series Critical Point Drying Apparatus (Polaron Equipment Ltd., Line Lexington, PA, USA), in which samples were incubated in liquid CO_2 for 90 min. Immediately following critical point drying, the arches were mounted sagittally to aluminum stubs using double-sided carbon tape, painted with silver, and then sputter-coated using a Polaron Series II Sputtering System (Type E5100). We imaged specimens at the UConn Bioscience Electron Microscopy Laboratory (Storrs, CT, USA) using a Zeiss DSM982 Field Emission Scanning Electron Microscope (FESEM; Zeiss

Microscopy, Peabody, MA, USA), with an accelerating voltage of 2 kV and a working distance of 7 mm. For each specimen (N = 30), we imaged the afferent (or trailing) edge of a filament centrally-located on the gill arch, which was where branchial ionocytes were prevalent (Fig. 2). Specifically, we digitally captured non-overlapping images of the focal filament at 2000x magnification at approximately evenly-spaced intervals along the length of the proximal-distal axis (i.e., from the base to the tip; mode = 12 images/filament). Each image included a metric scale bar.

Ionocyte analysis.— Stickleback branchial ionocytes were quantitatively analyzed in the collection of digital SEM micrographs (N = 341) by three independent observers (JND, DAP, and ZRS). To remove the possibility of scoring bias, the file names of the images did not reveal information about the specimen to the analyst. Images were analyzed using ImageJ software (v. 1.51d; Wayne Rasband, National Institutes of Health; https://imagej.nih.gov/ij/). First, we defined criteria for classifying ionocytes in our specimens by the morphology of their apical opening, which was based on similarly-described cell types in Mozambique Tilapia (Table 1; Lee et al. 1996). We then enumerated and categorized ionocytes using the Cell Counter plugin, scoring them as Type 1 (Wavy Convex), Type 2 (Shallow Basin), Type 3 (Deep Hole), or a fourth category for ionocytes that could not be equivocally assigned to a morphotype (Table 1). The sum of the cell counts in these four categories yielded total ionocytes.

We calculated the density of each ionocyte type in each image by dividing the cell tally by epithelial surface area, which we delineated by digitally outlining the filament with a calibrated polygon (Fig. S1). The filament was carefully traced to only include the portion censused; we excluded areas that were obstructed, damaged, or out of focus. Overall ionocyte densities were also calculated for the entire filament (i.e., per fish) by dividing the total counts from the image set for each specimen by the cumulative surface area censused. To examine ionocyte distribution across gill filament length, we measured linear distance along the approximate midline of the focal filament in each image. These segments were summed to yield a total length for each filament, from which we apportioned ionocyte

densities and proportional composition of cell types into 10 standardized percentiles (deciles). Due to differences in absolute filament length among fish, sample sizes varied among deciles (*N*'s = 31-39).

The density of ionocytes per fish was statistically analyzed using two-way ANOVA, testing for effects of population, salinity, and their interaction. Fish family and jars were pooled to increase sample size. To analyze patterns of ionocyte distribution along the proximal-distal axis of the gill filament, we constructed a linear mixed-effects model using the 'lmer' function in the *lme4* package in R (R Core Team 2016). Here the abundance of total ionocytes in each SEM image was examined across the standardized deciles of filament length, with the individual fish included as a random effect. We ran similar models with the proportion of each ionocyte type as the response variable. We performed Tukey's HSD *post hoc* multiple-comparison tests on overall significant effects ($P < 0.05$) to elucidate group differences.

In 2012, we performed a similar salinity challenge experiment on 3-month-old, F_1-generation stickleback from the same anadromous population (Rabbit Slough). However, a large proportion of the mounted gill preparations were of poor quality (Fig. S2), so only qualitative results are presented here.

Results

Density estimates of total branchial ionocytes ranged from 0.406 ± 0.022 to 0.464 ± 0.027 cells/100 μm^2 (mean ± SE) among the three observers. The total number of ionocytes counted per image was strongly positively correlated between combinations of observer pairs (Pearson's r = 0.87-0.89). Following this among-observer validation for precision in the image analysis, we report here the results from the most comprehensive census performed by JND.

All three ionocyte morphotypes were clearly identifiable in both 10-week and 22-week-old stickleback (Figs. 3 and 4). In the former image set, we counted a total of 1,962 branchial ionocytes, of which ~53% could be unambiguously categorized. Ionocytes were detected in approximately 94% of the images (319/341). At least one of the specific ionocyte types was absent in 54-66% of the images. All 30 specimens contained unidentifiable (Type 4) ionocytes, as well as the transitional Type 2 category. Type

1 ionocytes were absent in two stickleback held in SW; Type 3 ionocytes absent in eight fish, seven of which were from the FW treatment.

We found no differences in ionocyte density among populations or in the population*salinity interaction for any category (P's ≥ 0.2). Salinity did not affect Type 1 or Type 2 ionocyte densities (Fig. 5A,B; P's ≥ 0.1). However, an overall salinity effect was detected for Type 3 ionocyte density, which increased 6.6-fold in SW compared to the other treatments (Fig. 5C; 0.153 vs. 0.023 cells/100 μm^2; P = 0.001). An overall salinity effect was also present in the total ionocyte density (which includes the unidentifiable group): abundance was more than 50% higher in the fish held in FW or SW compared to the control group (Fig. 5D; 0.501 vs. 0.319 cells/100 μm^2; P = 0.02).

Ionocytes of all types were present along the entire proximal-distal axis of the gill filament, but their abundance differed among deciles (Fig. 6; P's ≤ 0.008). In general, the distribution of ionocytes across filament length was concave, with lower densities typically at the base and/or the tip, i.e., the 10^{th} and 90^{th} deciles. The relative proportions of Type 2 and 3 cells did not vary across filament length (P's $\geq$ 0.1), but this effect was significant for Type 1 ionocytes (P = 0.04), with fewer found at the distal end than in the 20^{th} percentile (Fig. 7). Unidentifiable ionocyte types composed the greatest proportion of cells in each decile.

Discussion

Invasion of FW environments by marine organisms produces derived populations that experience new selective pressures on the osmoregulatory system. Specifically, there is positive selection on the capacity to hyper-osmoregulate in the ion-poor environment and relaxed selection on hypo-osmoregulation. We examined the effects of the interplay of these evolutionary forces on the ion-exchanging surface of the gill in marine versus landlocked Threespine Stickleback. We quantified osmoregulatory responses to salinity challenge in juveniles of each ecotype, using SEM to identify and count ionocytes, and found no interpopulation differences. Across all populations, juvenile stickleback upregulated ionocytes in response to both hyper- and hypo-osmotic stress. In SW, this was most markedly demonstrated by the induction of

ion-secretory cells, as identified by the increase in abundance of apical crypts on the gill epithelium. Ionocytes were present along the length of the entire length of the gill filament, but were less abundant near the base and the tip. This distribution pattern was similar for all ionocyte types.

Our 2-week salinity challenge was well within the timeframe required for ionocyte changeover in fishes. Evidence of replacement/transition of branchial ionocytes can appear in as little as 3 h following salinity transfer (Lee et al. 1996), with full epithelial remodeling evidenced by 24 h and persisting through 7-14 d (Whitehead et al. 2011, 2012). Therefore, we are confident that we censused mixed populations of ionocyte types that had recruited to the epithelial surface and had sufficient time to mature prior to sampling. The three distinct apical morphologies we observed (Wavy Convex, Shallow Basin, Deep Hole) mirror types found in the gills of other euryhaline fishes, such as Mozambique Tilapia (Lee et al. 1996; Inokuchi et al. 2009), Mummichog (Whitehead et al. 2011, 2012), and Atlantic Salmon (Lubin et al. 1989). Each of these studies detected salinity-dependent changes in ionocyte prevalence.

In our experiment, salinity did not impact proliferation of Wavy Convex (Type 1) or transitional Shallow Basin (Type 2) cell types in stickleback gills. However, there was a strong relationship between salinity and Deep Hole (Type 3) densities. Type 3 ionocytes were mostly absent in the fish exposed to FW, but were the most common cell type in the SW treatment. In light of the functional differentiation among the ionocyte types, the large increase in Type 3 cells following SW transfer suggests that this specialized cell type is critical for ion secretion in hyperosmotic conditions in stickleback.

Contrary to predictions, we did not find a reciprocal increase of Type 1 ionocytes in FW. It is possible that our inclusion of a category for ionocytes that could not be unambiguously typified lowered our sensitivity to detect salinity-responsive differences among specific cell types, which would explain why *total* ionocytes increased in FW without a corresponding increase in Type 1 cells. Alternatively, testing stickleback at more extreme FW treatments may help resolve the unclear pattern of Type 1 upregulation. In the gills of Mummichog subjected to multiple hypoosmotic salinities, Type 1 ionocytes were present as part of a mixture of cell types in a 0.4 ppt treatment, but only predominated at 0.1 ppt (Whitehead et al. 2011).

More generally, the density of total ionocytes increased in FW and in SW, relative to control conditions. The proliferation of branchial ionocytes in response to both hypo- and hyperosmotic challenge may indicate an increase in energetic expenditure on osmoregulation. Since both FW and SW-type ionocytes are powered by ATP-consuming NKA pumps (Edwards & Marshall 2013; Hwang & Lin 2013), higher ionocyte densities likely translates into higher energetic costs. In contrast, fewer ionocytes in the unchallenged controls suggest that stickleback in a less hypotonic rearing salinity (3 ppt) did not need to invest as much in maintaining ion balance. Interestingly, our whole-tissue findings corroborate results at the molecular level: the convex, or "U"-shaped, relationship between ionocyte abundance and salinity is similar to the pattern recorded for gill NKA activity levels in these populations (Chapter 1). Gill filaments from stickleback exposed to additional salinities nearer isosmotic conditions should be analyzed to examine the relationship between salinity and branchial ionocyte abundance more fully.

Our positional analysis along the proximal-distal axis revealed that most of the length of the afferent (trailing) edge of the stickleback gill is used in osmoregulation, with the possible exception of the innermost and outermost ends, which had less than half as many ionocytes. We did not find proportional differences among the cell types by filament length, except in a pair of deciles for Type 1 cells.

We did not find differences in branchial ionocyte composition among stickleback populations, which would indicate evolution of the osmoregulation system at the tissue level. This result was somewhat unexpected, since juveniles from these populations displayed some differences in SW tolerance in a series of salinity challenges (see Chapter 1). However, the decreased SW tolerance in Frog Lake juveniles was restricted to earlier ontogeny: although no 3-week-old lake fry survived 35 ppt, our SEM samples originated from the survivors of the Week 10 trial, when survival at this treatment was similar among populations (older lake juveniles only had poorer survival in hypersaline conditions). Alternative explanations for the lack of population differences in ionocyte density include small sample size and survivor bias. We only quantified ionocyte density in the fish that successfully acclimated to the transfer salinity; it is possible that ionocyte densities were lower in the individuals that died, assuming mortality was linked with osmoregulatory failure.

In conclusion, our SEM image analysis of the stickleback gill demonstrates a valuable, quantitative technique for assessing osmoregulatory responses to osmotic stress and for identifying how this plasticity might differ among populations. *In situ* examination of branchial ionocytes should be included as part of an integrative biological approach to understanding the evolution of osmoregulation, which links whole-organism performance with underlying molecular mechanisms. Our knowledge of comparative physiology in stickleback, especially at the tissue and organ-level, is lacking. The numerous marine and FW-resident populations of Threespine Stickleback offer a unique natural experiment for assessing the evolution of physiological plasticity under different salinity regimes. Future investigations should include additional derived populations, especially ones with known dates of colonization, to test for robustness and parallelism in osmoregulatory divergence subsequent to FW establishment. Different age-classes should also be tested, including earlier life stages, which may have less developed osmoregulatory capability. Physiological examination of the stickleback radiation will reveal general mechanistic patterns applicable to other aquatic organisms and lead to new predictions about osmoregulatory evolution following FW invasion.

Table 1. Classification of branchial ionocytes in juvenile Threespine Stickleback, as viewed under scanning electron microscopy. Ionocytes were identified as one of three major types, *sensu* Lee et al. (1996), based on their apical morphologies visible at junctions of plate-like pavement cells on the gill filament epithelium. We also enumerated ionocytes that could not be firmly categorized.

Category	Ionocyte Type (Example)	Morphological Description	Proposed Function [a]
1	**Wavy Convex** (Figs. 3B, 4B)	Apical surface is flush with adjacent pavement cell membranes on the gill filament and is studded with "wavy" ridges of microvilli that appear white (and may show signs of flaking on the specimen). When fully developed, this cell has the largest surface area of the three types.	The ridged surface of microvilli maximizes the area of the apical membrane exposed for ion uptake in FW.
2	**Shallow Basin** (Figs. 3C, 4C)	At least a portion of the apical surface is partially recessed beneath the adjacent pavement cells, but it is visible and may be smooth or ridged. This is a transitional cell type between Types '1' and '3' and its surface area varies accordingly.	The partially-recessed apical crypt facilitates ion secretion in SW; considered a transitional ionocyte form that is often visible during gill remodeling.
3	**Deep Hole** (Figs. 3D, 4D)	Dark apical pit, conspicuously outlined by a ring of pavement cell membrane. The apical surface is so far recessed that it is usually not visible. When fully developed, the diameter of the opening shrinks to form a so called 'apical crypt'.	The deeply-recessed apical crypt is part of a multi-cellular complex adapted for ion secretion, involving one or several ionocytes, accessory cells, and their paracellular junctions.
4	*Unidentifiable* (Fig. S1A)	An ionocyte is present, but the specific type cannot be conclusively determined, either because it possesses a characteristic of each of the three major cell types, or it is partially hidden from view, damaged, obscured by debris, or not in focus.	NA

[a] *References*: Evans et al. 2005; Hiroi et al. 2005; Kaneko & Hiroi 2008; Christensen et al. 2012.

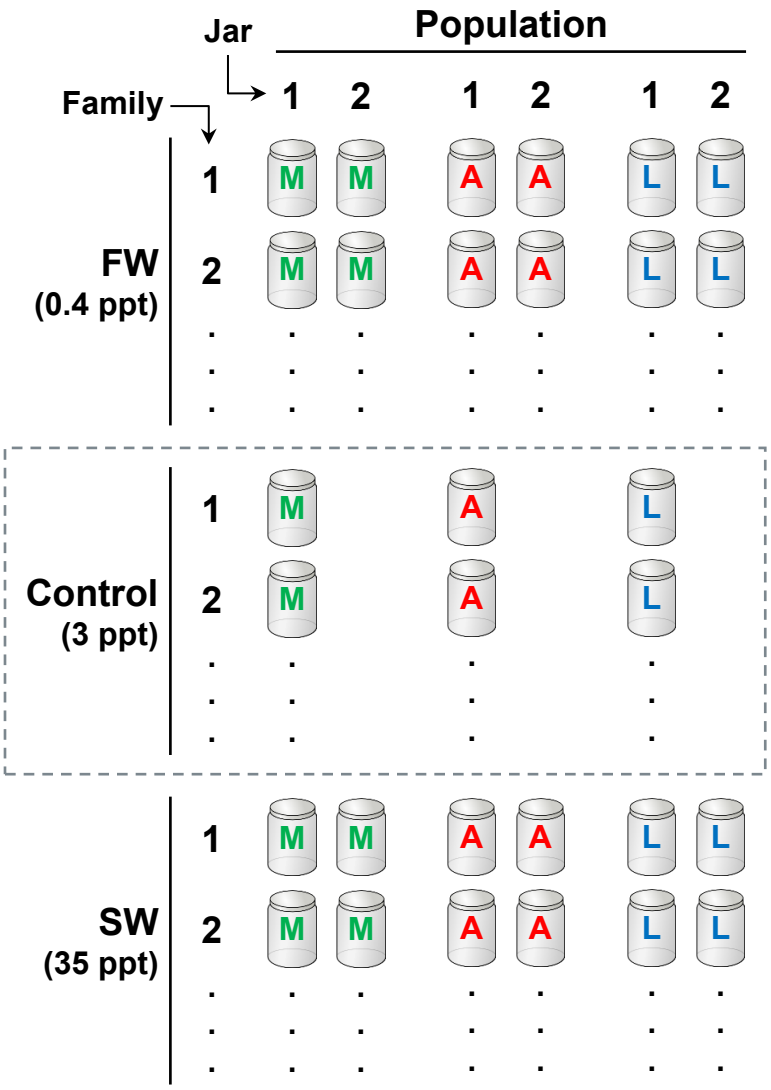

Figure 1. Schematic of the 14-d, multi-population salinity challenge performed on 10-week-old Threespine Stickleback. Full-sibling families belonging to representative marine (M; Resurrection Bay), anadromous (A; Rabbit Slough), and landlocked (L; Frog Lake) populations were transferred into duplicate jars containing 1.5 L of either FW (0.4 ppt) or SW (35 ppt) at a density of 10 individuals per jar. Additional fish held in the common rearing salinity (3 ppt) served as controls. At the end of the trial, gill arches were sampled from a subset of survivors for scanning electron microscopy image analysis.

Figure captions for the micrographs

Figure 2. Morphology of the juvenile stickleback gill, as viewed using a scanning electron microscope (SEM). (A) Dorsal view of a branchial arch, with blue lines overlaid to show the direction of water flow over the gill filaments. (The dorsal-most filaments in this specimen are missing/damaged.) Scale bar = 200 μm (100x magnification). The white box inset is enlarged in panel (B), on which arrows indicate ionocytes ('Deep Hole' type) on the afferent (trailing) edge of the filament (Af), which is the side we analyzed. Ef = Efferent (leading) edge of the filament; L = lamellae. Scale bar = 50 μm (500x mag.). (C) Lateral view of a branchial arch (BA), illustrating how the afferent and efferent edges of the filaments (F) interdigitate. R = raker. Anatomical orientation: A = anterior, P = posterior, D = dorsal, V = ventral. Scale bar = 250 μm.

Figure 3. Representative SEM images from 10-week-old Threespine Stickleback. (A) The entire branchial arch from which the entire length of the trailing edge of one centrally located filament was imaged and analyzed. Anatomical compass as detailed in Fig. 2. Scale bar = 500 μm (50x magnification). (B-D) Micrographs of the surface of the trailing edge of the gill filament, highlighting apical morphologies of the three major ionocyte types. Pavement cells are marked with asterisks. Scale bars = 10 μm (2,000x mag.). Arrows point to (B) 'Wavy Convex' (FW - Type 1), (C) 'Shallow Basin' (transitioning - Type 2), or (D) 'Deep Hole' (SW - Type 3) ionocytes, as described by Lee et al. (1996).

Figure 4. Representative SEM images from 22-week-old Threespine Stickleback. (A) The entire branchial arch from which the entire length of the trailing edge of one centrally located filament was imaged and analyzed. Anatomical compass as in Fig. 2. Scale bar = 1 mm (45x magnification). (B-D) Micrographs of the surface of the trailing edge of the gill filament, highlighting apical morphologies of the three major ionocyte types. Pavement cells are marked with asterisks. Scale bars = 10 μm (2,350x

mag.). Arrows point to (B) ‘Wavy Convex’ (FW - Type 1), (C) ‘Shallow Basin’ (transitioning - Type 2), or (D) ‘Deep Hole’ (SW - Type 3) ionocytes, as described by Lee et al. (1996).

Figure S1. Example of a SEM image of a stickleback gill filament processed for quantitative analysis using ImageJ. Ionocytes were flagged with a color-coded, numeric label (see Table 1). A polygon (red) was then traced to measure the surface area within the boundaries of the census. A linear distance (yellow) was also measured along the proximal-distal axis at the mid-line of the filament. All measurements were calibrated to the scale bar.

Figure S2. Examples of the most common issues encountered during SEM image analysis of branchial ionocytes in stickleback. (A) Granular debris obscuring the apical surfaces of ionocytes (arrows). Ionocytes that prolapsed or ruptured during sample preparation had a similar appearance. (B) Wrinkled or folded epithelial surface. (C) Portions of the afferent edge of the gill filament (Af) obscured from view, in this case by lamellae (L) from adjacent filaments. (D) Fissures in the epithelial layer or broken filaments. Scale bars = 10 μm.

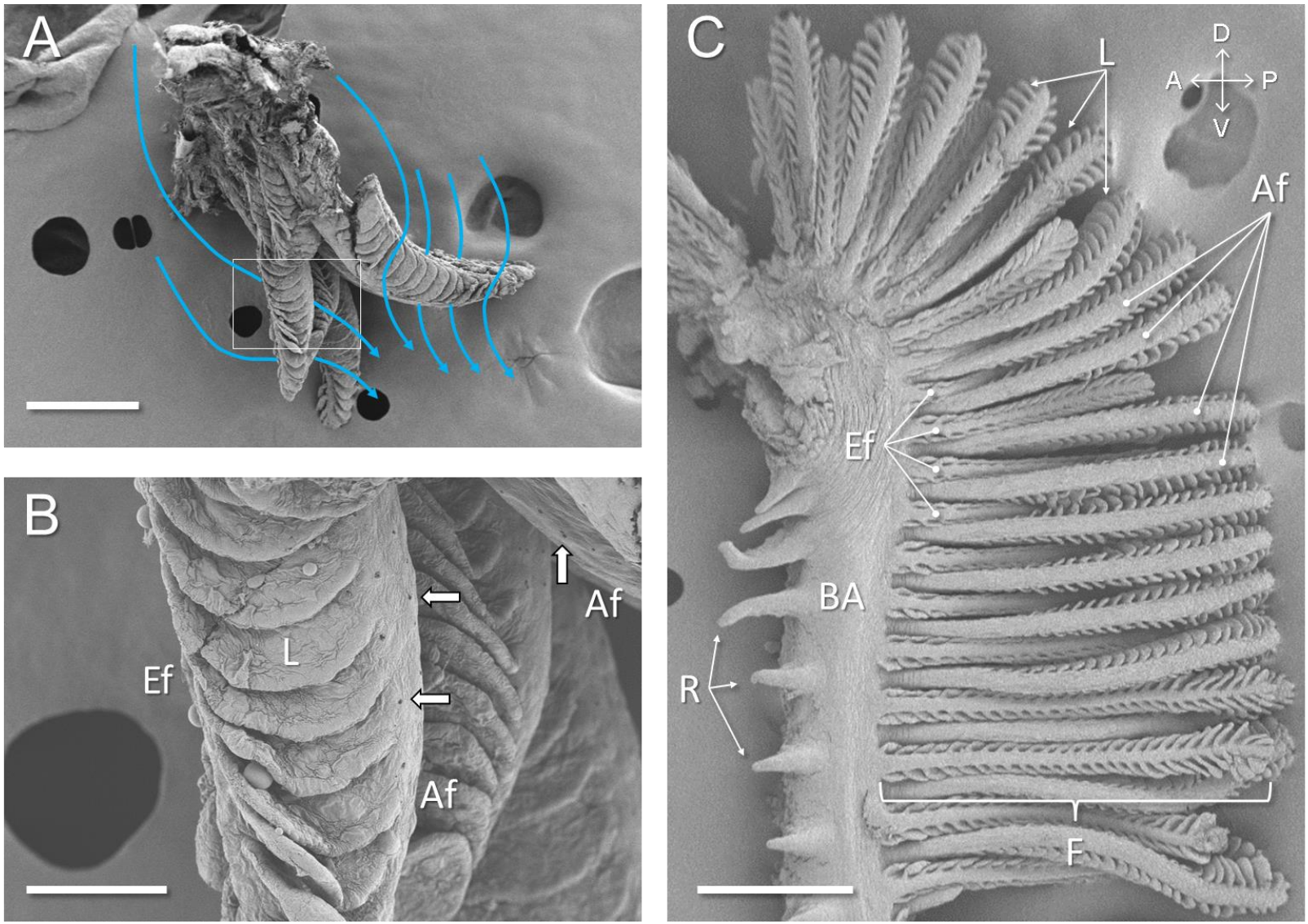

Figure 2.

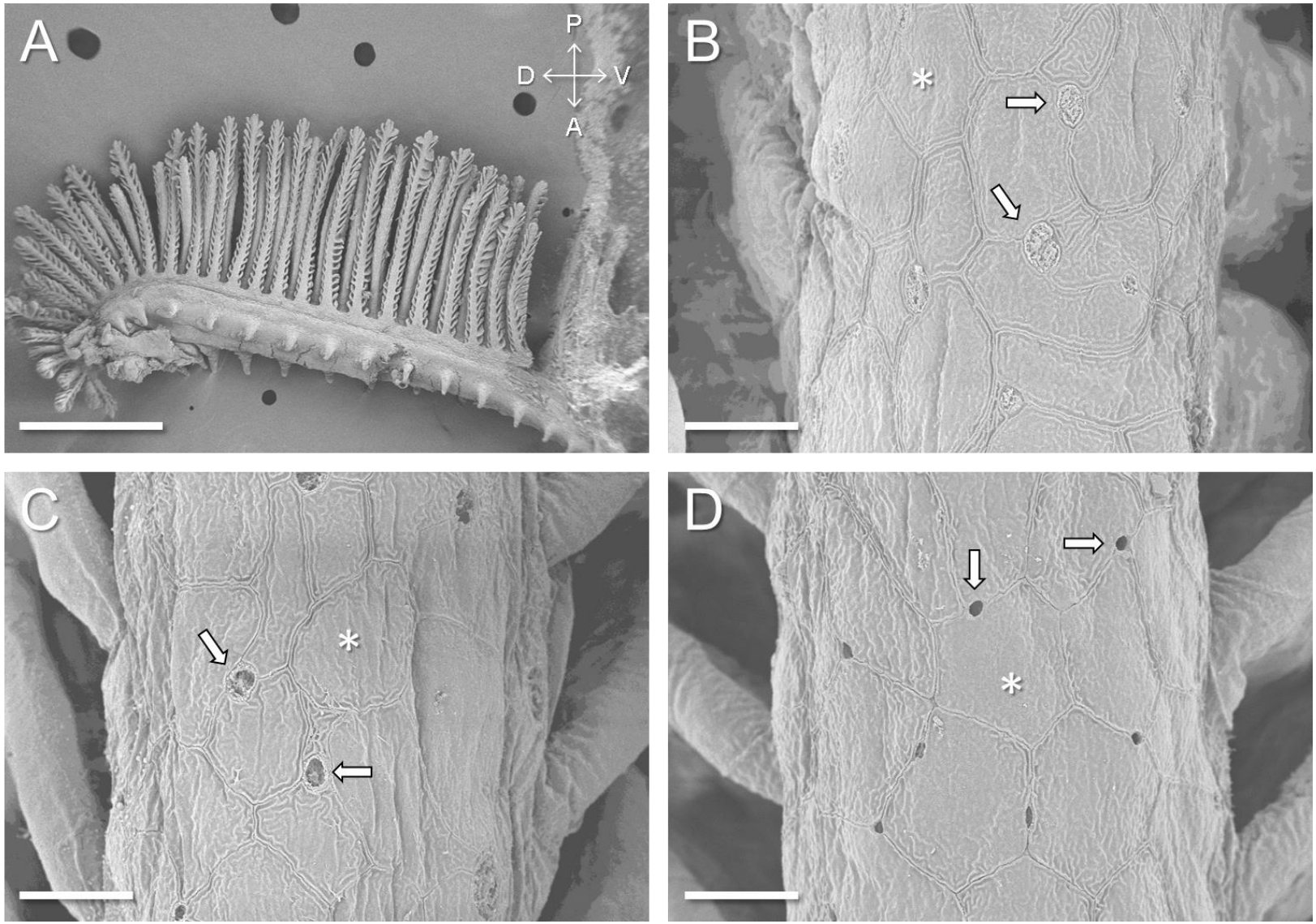

Figure 3.

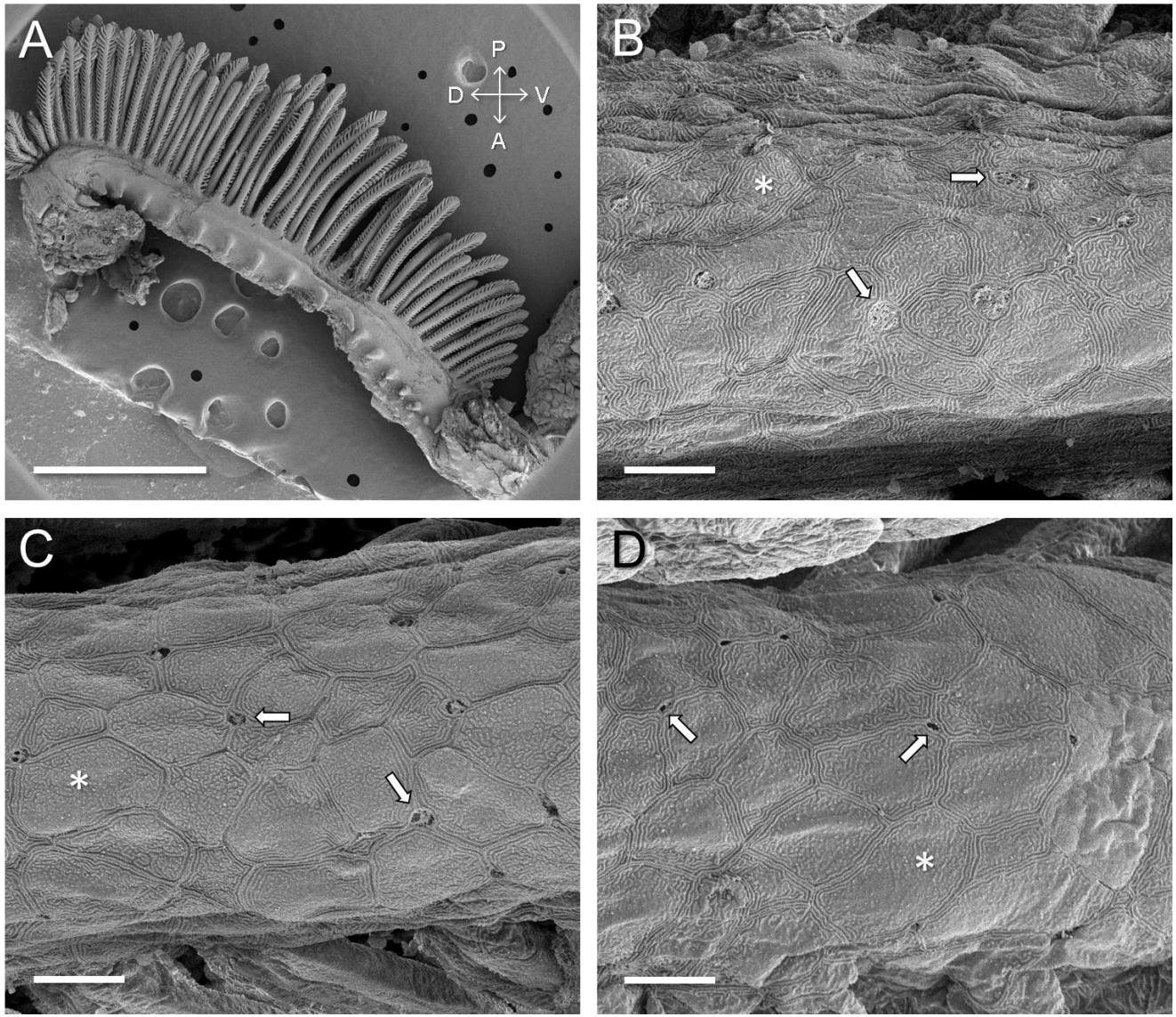

Figure 4.

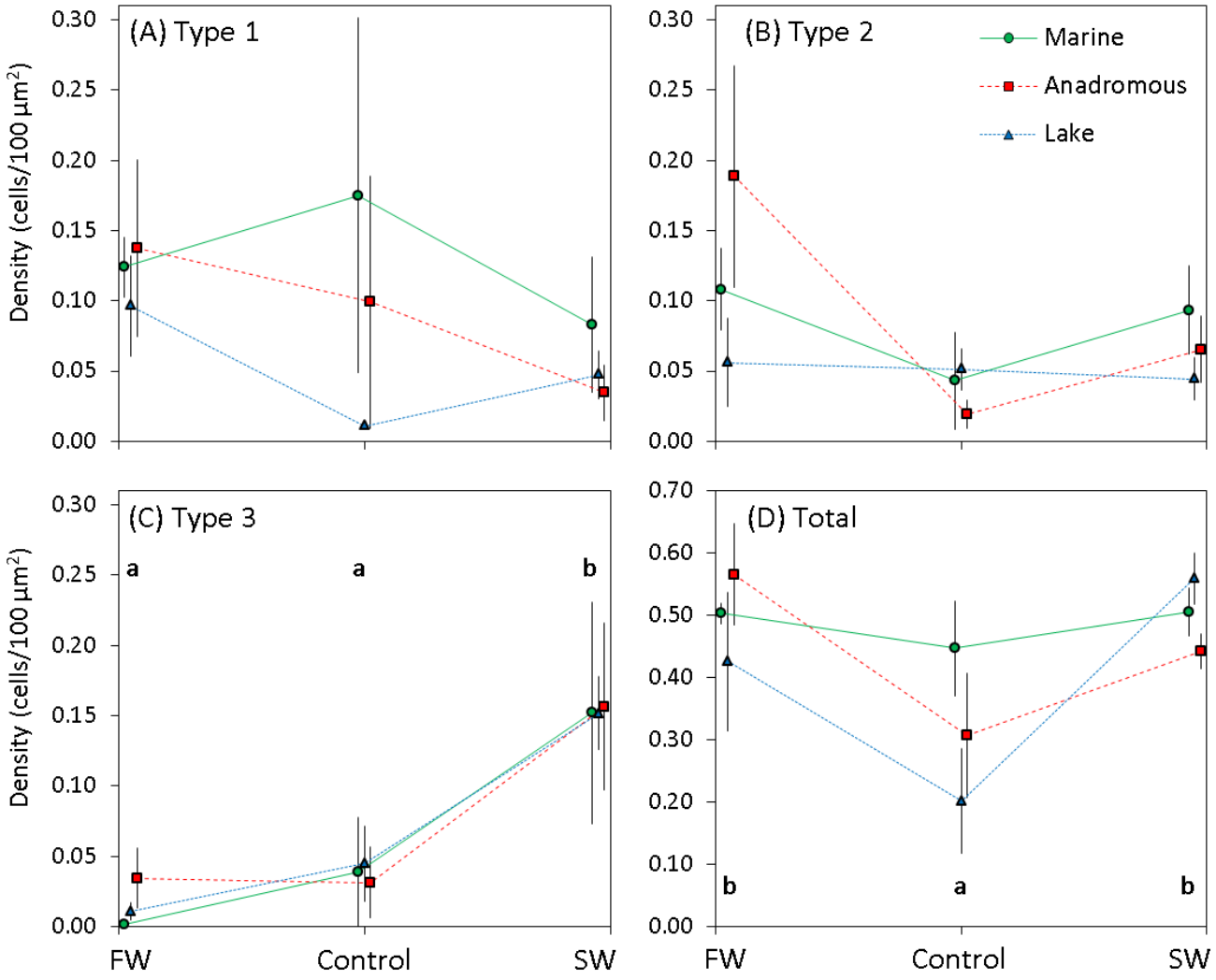

Figure 5. Branchial ionocyte densities in 10-week-old marine (Resurrection Bay; green circles), anadromous (Rabbit Slough; red squares), and landlocked (Frog Lake; blue triangles) Threespine Stickleback, as observed by scanning electron microscopy. Gills were sampled from survivors held in FW (0.4 ppt) or SW (35 ppt) for two weeks (N = 4), as well as unchallenged controls in the rearing salinity (3 ppt; N = 2). Ionocytes were enumerated on the afferent edge of a centrally-located gill filament and categorized by their apical morphology (see Table 1 for details). Mean abundance (± SE) of (A) Type 1-Wavy Convex, (B) Type 2-Shallow Basin, or (C) Type 3-Deep Hole ionocytes is presented for each population. (D) Total ionocyte density (including unidentifiable types) was also quantified. Letters identify salinities that differed significantly, according to Tukey *post hoc* tests.

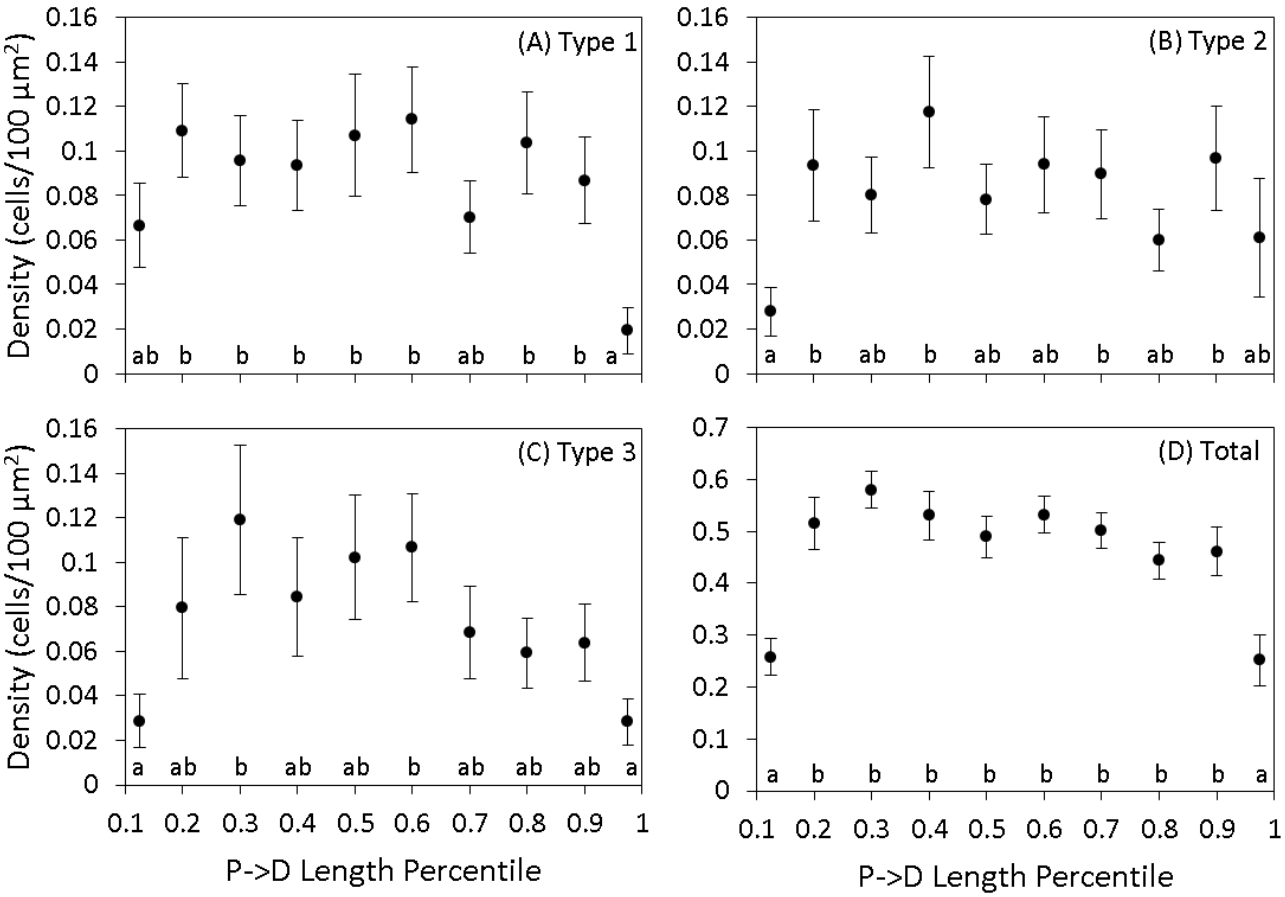

Figure 6. Distribution of branchial ionocytes along the proximal-distal axis of the stickleback gill filament. Mean (± SE) abundance of (A) Type 1-Wavy Convex, (B) Type 2-Shallow Basin, (C) Type 3-Deep Hole, and (D) total ionocytes (including unidentifiable types) are presented for each standardized percentile of filament length along the proximal-distal (P→D) axis. Due to differences in absolute filament length among fish, sample sizes varied among deciles (*N*'s = 31-39). Letters denote percentiles that differed significantly, according to Tukey *post hoc* tests.

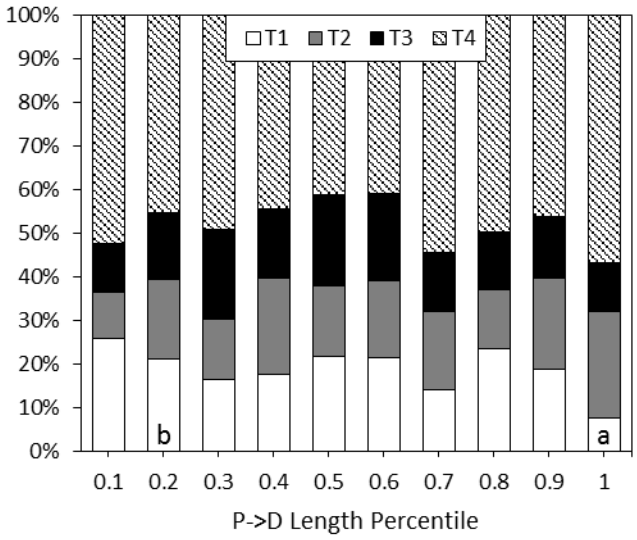

Figure 7. Stacked bar chart of proportions of each ionocyte type by percentile of filament length along the proximal-distal (P→D) axis. T1=Type 1 (Wavy Convex), T2=Type 2 (Shallow Basin), T3=Type 3 (Deep Hole), and T4=Type 4 (Unidentifiable types). Due to differences in filament length among fish, sample sizes varied among standardized deciles (*N*'s = 31-39). The letters mark the only significantly different pair of proportions, according to Tukey *post hoc* tests.

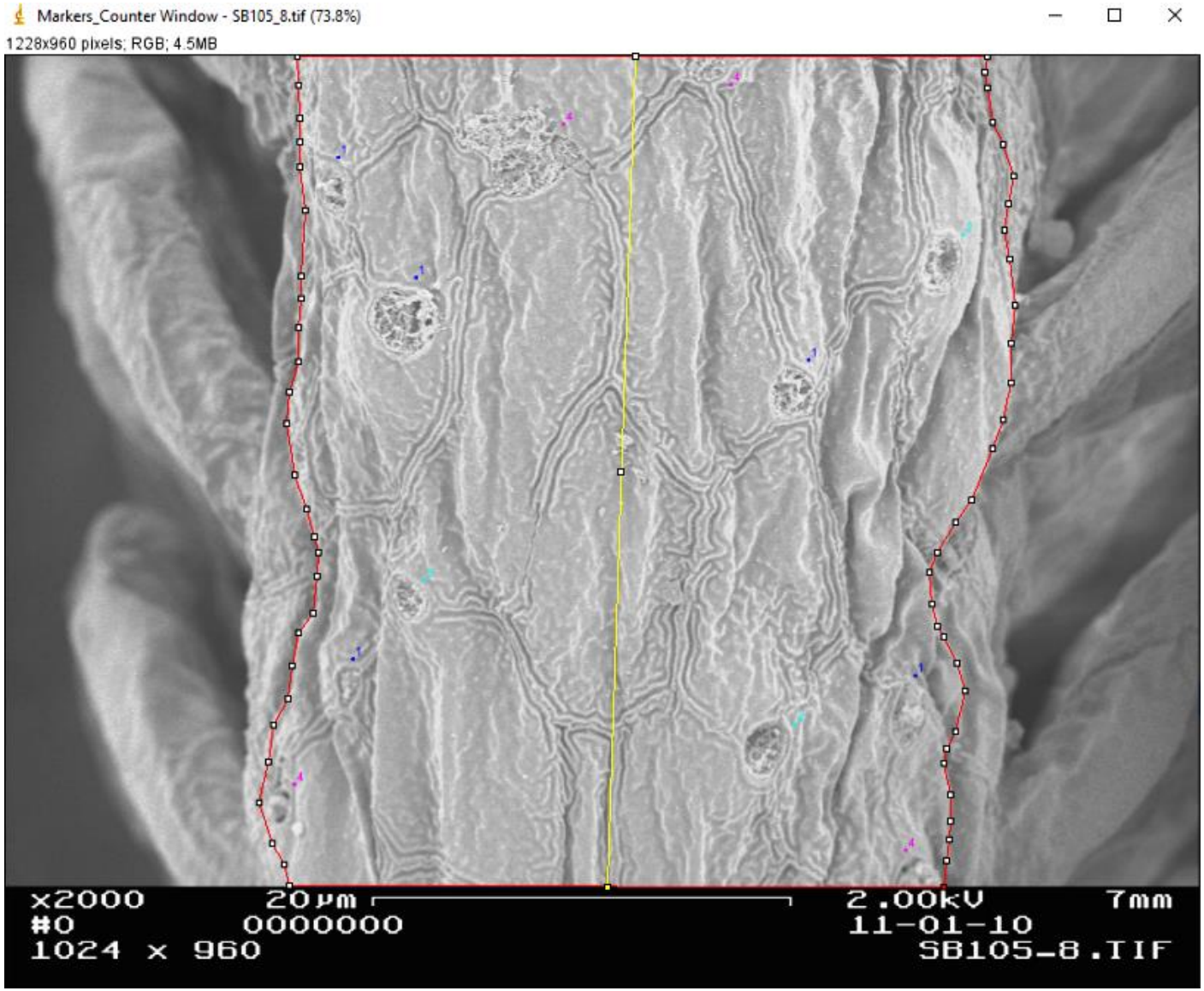
Markers_Counter Window - SB105_8.tif (73.8%)
1228x960 pixels; RGB; 4.5MB
x2000 20µm 2.00kV 7mm
#0 0000000 11-01-10
1024 x 960 SB105-8.TIF

Figure S1.

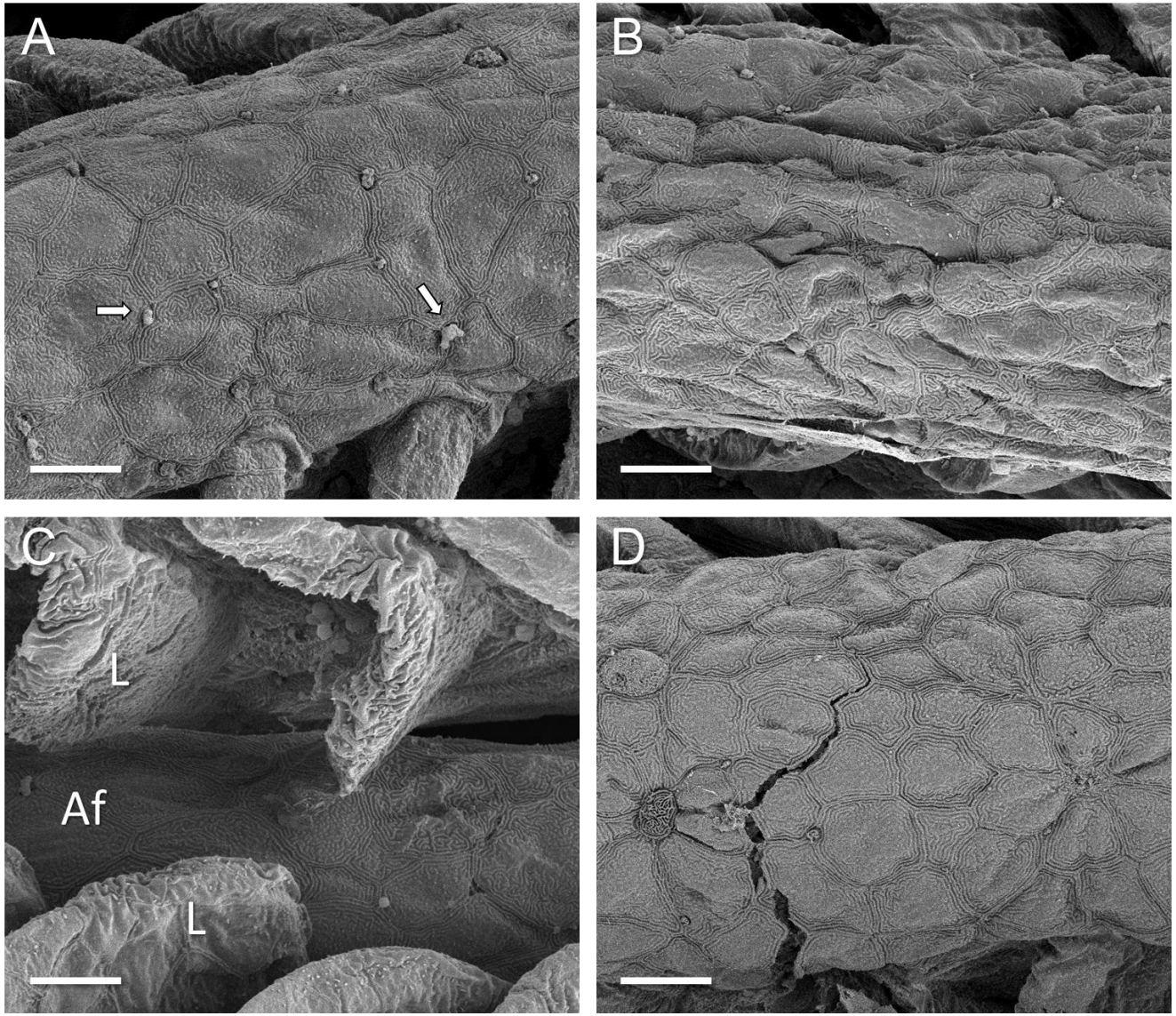

Figure S2.

Chapter 3

Osmoregulatory physiology and rapid evolution of salinity tolerance in Threespine Stickleback recently introduced to fresh water

Introduction

The degree to which an organism can physiologically adjust to counter abrupt environmental change has important implications for adaptation. Physiological plasticity, i.e., wide tolerance ranges for factors such as temperature, and nutrient, oxygen and osmotic concentrations, offers the fitness advantages of higher survival in a broader range of conditions and the ability to traverse patches of unsuitable habitat. However, there are constraints on the direction and magnitude of plasticity (Snell-Rood 2012) and it does not always evolve adaptively (Ghalambor et al. 2015). Plasticity may also be lost in canalized phenotypes that are locally-adapted to the new environment (Lande 2009; Snell-Rood 2012). These complexities compel us to ask: how rapidly can tolerance thresholds evolve in populations, and under what ecological circumstances will specialization be favored?

The potential evolutionary outcomes of plasticity can be examined in aquatic organisms that have undergone halohabitat transitions (Schultz & McCormick 2013; Lee 2016). Euryhalinity, the ability to survive across a wide salinity spectrum, is an important evolutionary innovation that facilitated range expansion and rapid adaptation of marine or estuarine taxa to freshwater (FW) halohabitats (Lee & Bell 1999; Schultz & McCormick 2013). Colonization of geographically isolated and heterogeneous FW habitats by founding euryhaline fishes that are capable of crossing osmotic barriers has often yielded prolific radiations in FW lakes and streams (Bell & Foster 1994; Betancur-R 2010; Nakatani et al. 2011). When a marine population invades FW, positive selection for enhanced performance in ion-poor conditions is initially intense because survival is contingent on maintaining ion homeostasis. Consequently, FW tolerance is expected to improve rapidly as FW descendants adapt to local conditions, possibly through a selective sweep of co-adapted FW-osmoregulatory gene complexes (DeFaveri et al. 2011; Hohenlohe et al. 2012; Jones et al. 2012b). In contrast, because selection for seawater (SW) tolerance is no longer imposed on the derived population, euryhalinity might erode through mutation

accumulation in the gene networks underlying hypo-osmoregulation (Snell-Rood et al. 2010). The evolutionary effects of relaxed selection are less clear because they may depend on maintenance costs and pleiotropy of the genes essential for hypo-osmoregulation (Lahti et al. 2009; Brennan et al. 2015). If energetic costs to maintain a functional osmoregulatory response to high salinity are high or the genes involved largely reside in a distinct regulatory module, then loss of these traits should be more rapid than if costs are small or genes are highly integrated within networks necessary for the fish to function in FW.

Evidence of local evolution of halotolerance among fish populations from contrasting salinity regimes is extensive (e.g., Whitehead 2010; Brennan et al. 2015; Velotta et al. 2015). In the majority of halotolerance studies, however, the populations or species pairs tested diverged thousands of years ago, which precludes characterization of the incipient effects of selection on the osmoregulatory system in real time. The euryhaline Threespine Stickleback (*Gasterosteus aculeatus*) is an ideal model to capture the pace of physiological evolution because it has a well-documented history of parallel divergence following transitions from marine to FW habitats across its circumpolar range. Lab-based manipulations of stickleback have also demonstrated rapid evolution of traits such as trophic morphology and cold tolerance after only a few generations (Wund et al. 2008; Barrett et al. 2011). FW colonization, and subsequent adaptation, have become a prime example of ecological speciation by giving rise to a replicated set of derived FW populations whose ages vary from the post-glacial Pleistocene (10,000-20,000 years ago; Bell & Foster 1994) to only a few generations (von Hippel & Weigner 2004; Gelmond et al. 2009; Bell & Aguirre 2013). The persistence of the SW-adapted lineage of ancestral marine/anadromous (collectively called oceanic) phenotypes has allowed evolutionary biologists to make direct experimental comparisons between ancestral and derived forms to aid our understanding of the evolutionary consequences of halohabitat transitions. Salinity transfer experiments between oceanic and lake-resident ecotypes have demonstrated salinity-dependent differences in survival that correlate with approximate native salinity, with enhanced FW tolerance and/or lower SW tolerance in derived populations (Heuts 1947; Marchinko & Schluter 2007; McCairns & Bernatchez 2010; DeFaveri & Merilä 2014). Recent work has shown that ancestral and derived phenotypes exhibit divergence in

osmoregulatory genes (DeFaveri et al. 2011; Shimada et al. 2011; Jones et al. 2012a; DeFaveri & Merilä 2013) as well as osmoregulatory gene transcription (McCairns & Bernatchez 2010; Taugbøl et al. 2014).

A major site of osmoregulation is the vascularized gill epithelium, where specialized ion transporting cells called ionocytes buffer against osmotic perturbations by taking up ions from the environment (hyper-osmoregulation) or secreting excess ions from circulating plasma (hypo-osmoregulation) to compensate for diffusive ion losses in FW or gains in SW (Edwards & Marshall 2013). Detailed models of teleost branchial ionocyte function in FW and SW have mapped suites of membrane-bound transporters that control the intake or expulsion of ions. The basolateral sodium-potassium ATPase pump (NKA) is required for both functions because it produces electrochemical gradients across the cell membrane that drive the coordinated work of secondary co-transporters and exchangers (Edwards & Marshall 2013). However, NKA is often upregulated in SW exposure because it facilitates paracellular extrusion of sodium and also powers the sodium-potassium-chloride cotransporter (NKCC), which is involved in chloride secretion (reviewed by McCormick 2001; Kaneko & Hiroi 2008).

In addition to actively pumping ions to maintain homeostasis of the extracellular fluid, fishes also regulate cell volume by adjusting intracellular concentrations of organic osmolytes, which are uncharged solutes that increase osmolality without interfering with cellular biochemistry and can also have other cytoprotectant roles (Yancey et al. 1982; Kültz 2012). Compatible osmolytes, such as taurine and other free amino acids, are upregulated in response to a rise in the osmolality of extracellular fluid during hyperosmotic stress in at least some bony fishes (Fiess et al. 2007). Conversely, osmolytes are downregulated when plasma osmolality drops (Edwards & Marshall 2013). Therefore, in at least some species, measurements of tissue osmolyte levels can serve as an indicator of plasma osmolality in the extracellular fluid, for instance, where blood samples cannot be acquired.

The precise physiological mechanisms by which euryhaline fishes adjust their osmoregulatory systems have been intensively studied in several diverse groups of teleosts, including eels, clupeids, salmonids, killifish, and tilapia (reviewed by Evans et al. 2005; McCormick et al. 2013a). Considering the potential importance of environmental salinity for shaping the stickleback radiation, the lack of

mechanistic, physiological data on this intensively-studied, evolutionary model species is surprising. Moreover, given the diverse mechanisms of ion uptake in FW described in other euryhaline models (Hwang & Lin 2013; Hsu et al. 2014), we cannot assume that osmoregulatory adaptations in Gasterosteiformes have followed the same evolutionary trajectory.

The goals of this study were to measure how rapidly osmoregulatory responses evolve after oceanic stickleback initiate FW residency and to characterize the physiological mechanisms underpinning such divergence. In a common lab environment, we reared F_1-generation stickleback from both an anadromous population and its descendants, which had been introduced approximately two generations earlier to nearby, landlocked lakes (Bell et al. 2016). We then compared halotolerance thresholds in members of the ancestral and derived populations by conducting "direct" and "gradual" salinity challenge experiments, which measure osmoregulatory capacity in complementary ways (Schultz & McCormick 2013). Direct salinity transfers assess acute osmoregulatory responses to abrupt osmotic shock. In the gradual design, salinity is changed incrementally, which reveals physiological effects of chronic exposure and also measures absolute halotolerance limits by allowing fish time to acclimate.

Our main objectives were to compare survival between ancestral and derived stickleback subjected to osmotic challenge and to mechanistically link divergence in performance to osmoregulatory machinery at the molecular and tissue levels. We adopted an integrated organismal approach, uniting multiple levels of physiological responses to provide functional explanations for halotolerance differences. We hypothesized that, compared to juveniles from an anadromous population, lake-introduced stickleback would exhibit a halotolerance shift towards FW and away from SW, and that their diminished hypo-osmoregulatory response would be evidenced by lower gill NKA activity and NKCC abundance in SW. Furthermore, the signs of osmotic stress would be detectable in organic osmolyte content, with departures from baseline levels indicating osmotic perturbation. Specifically, we predicted the lake-introduced stickleback would have a greater increase in organic osmolytes in SW to mitigate the effects of higher plasma osmolality. Conversely, anadromous stickleback would downregulate organic osmolytes to offset their relatively lower plasma osmolality when held in ion-poor conditions.

Materials & Methods

Source populations & fish husbandry.— Threespine Stickleback used in this study were sampled from an anadromous population in Rabbit Slough (RS) of the Matanuska-Susitna Borough, Alaska, and two Southcentral Alaskan lake populations derived from it (Bell et al. 2016). In 2009 and 2011, respectively, ~3,000 anadromous RS adults were captured at a culvert running under the Parks Highway near Palmer (61.534°N, 149.268°W) and released into Cheney Lake (CL; 61.200°N, 149.762°W; conductivity = ~168 µS/cm), located in the Anchorage Municipality, and Scout Lake (SL; 60.535°N, 150.832°W; conductivity = ~35 µS/cm), located to the south on the Kenai Peninsula. Both lakes lack outlet streams and had been treated with rotenone by the Alaska Department of Fish and Game to exterminate Northern Pike (*Esox lucius*); this treatment also eradicated the native Threespine Stickleback populations.

In May-June 2012, breeding stickleback from all three locales were trapped using unbaited, steel minnow traps (0.32 cm mesh) set overnight. Adults were brought to the University of Alaska Anchorage, where we produced an F_1 generation of more than 1,700 embryos from each population through "mass cross" *in vitro* fertilization. Gametes from multiple males and females were mixed prior to fertilization to increase genetic diversity. The number of parents used in the mass cross depended on the size of the female and trapping success: RS = 10 males and 7 females; SL = 15 males and 15 females; CL = 1 male and 10 females. Beginning with the initial cohort that hatched in each of the lakes during the summer of introduction, the experimental progeny from SL had persisted in FW for 2 generations, and the progeny from CL had persisted in FW for 3-4 generations, depending on whether they bred after 1 or 2 years post-introduction (Bell et al. 2016).

Fertilized embryos were disinfected with methylene blue and furan (Aquarium Pharmaceuticals, Inc., Chalfont, PA, USA), placed in aerated, 3 ppt water, and shipped to the University of Connecticut's Aquatic Facility, where they developed in a common environment. The fish were raised in reverse osmosis water in which Instant Ocean aquarium salt was dissolved to a salinity of 3 ppt, as measured by a digital salinometer (Yellow Springs Instruments 85, Yellow Springs, OH, USA). Fish were held in

replicate 38-L aquaria, equipped with filters and maintained at 19 ± 1°C with a 14-h light: 10-h dark photoperiod. Larval stickleback were fed brine shrimp nauplii, which had been gut-enriched with Self-Emulsifying Lipid Concentrate (SELCO, Brine Shrimp Direct, Ogden, UT, USA). We transitioned one month-old juveniles to a pelleted feed (Golden Pearls, Brine Shrimp Direct; Divino & Schultz 2014).

The direct salinity transfer.— When the F_1 cohort reached 6-weeks post-hatch (mean standard length = 16.7 mm ± 1.9 SD), 410 of the lab-reared individuals from each source population were randomly selected for an abrupt salinity challenge in which they were directly transferred from the rearing salinity into wide-mouth mason jars (Ball brand) containing 1.5 L of water at one of seven salinity treatments at a density of 10 fish per jar (50-60 individuals per salinity per population; Fig. 1). Three hypoosmotic (0, 0.2, 0.4 ppt) and four hyperosmotic salinity treatments (35, 40, 45, 50 ppt) were chosen to encompass anticipated lower and upper tolerance limits. Approximate conductivities for these seven treatments were: 6, 353, and 677 µS/cm for the low salinity treatments and 50.7, 57.2, 63.7, and 70.3 mS/cm for the high salinity treatments. To obtain baseline physiological data, fish were sampled from a control jar (3 ppt; conductivity = 4.9 mS/cm) on Day 0 of the time course. Because mortality had been nonexistent for stickleback juveniles held in jars at the rearing salinity in numerous salinity trials (J. Divino, unpubl. data), we did not collect additional controls at each time point.

Salinity-challenged fish were monitored at least twice per day for 10 d; at each inspection, mortalities were recorded and immediately removed. To capture potential temporal dynamics in physiological responses to salinity stress, acutely-challenged stickleback were sampled during the time course on Days 0, 0.25, 1, 3, 7, and 10 (Fig. 1). To increase sample size necessary for obtaining additional gill samples for molecular analyses after salinity acclimation, additional jars of fish were set up for sampling on Day 7 of the trial. We periodically checked ammonium, nitrite, nitrate, and pH levels in jars (Aquarium Pharmaceuticals, Inc.) and maintained water quality throughout the experiment through a combination of debris removal and water changes. Fish were fed pelleted feed beginning on Day 2 of the trial.

Owing to differences in hatch date, this experiment was performed separately on 6-week-old CL juveniles. During this period, however, maintenance work was performed on the reverse osmosis water supply, which we believe caused high mortality across the three hypoosmotic treatments, including complete loss of the 0.2 ppt group. Therefore, we have excluded direct transfer results on CL fish.

Each RS and SL fish in the direct transfer experiment was coded as either a mortality or a right-censored event (i.e., sampled fish or final survivors), with time-to-event recorded in either case. A mixed-effects, Cox proportional hazard model (*coxme* package in R; R Core Team 2016) was used to analyze the effects of population, salinity, and their interaction on survival in the lower and upper halotolerance thresholds (which we determined from the trial to be 0 and 40 ppt, see Results), with experimental jar as a random effect. To further characterize the relationship between population and salinity, we performed log-rank tests on Kaplan-Meier survival curves between each population at each threshold salinity (*survdiff* function in the *survival* package in R), with jar included as a factor. Excluding jar as a factor did not change the statistical outcomes of either the Cox or log-rank tests (data not shown).

For each population-salinity combination, mean proportion survival was calculated at each inspection out of a declining number of fish "at risk" due to censoring. Just prior to the Day 3 sampling, when most of the mortality had ceased (see Results), we estimated lower- and upper-limit lethal salinity concentrations, LC_x (expressed in ppt, where x is percent survival), using logistic regression. For each population, proportion of stickleback alive per jar (at 67 h) was plotted across the three FW treatments (0, 0.2, and 0.4 ppt) and the four high salinity treatments (35, 40, 45, and 50 ppt), and LC_x was calculated from fitted curves. It is conventional to report LC_{50}, but because of high survival of SL juveniles in 0 ppt (see Results), LC_{85} was the lowest common salinity calculable for quantifying FW halotolerance across populations.

The gradual seawater challenge.— We also performed a gradual salinity challenge experiment on 100 3-week-old, F_1 juveniles from RS, SL, and CL. Fifty fish were transferred into duplicate, 19-L aquaria initially containing the common rearing salinity (3 ppt water), which we increased by 2 ppt·d^{-1}. Each tank

was equipped with a Penguin 100 power filter with bio-wheel (Marineland Aquarium Products, Cincinnati, OH, USA), and a segment of plastic pipe fitted with plastic plants provided habitat enrichment. Fish were fed gut-enriched nauplii and/or pellets daily. The experiment ended at the salinity in which at least 50% of the current cohort died (the cohort LC_{50}). At the end of the trial, all survivors were sampled either for gill tissue or whole-body water content and osmolyte analysis, as described below.

Molecular assays.— At the designated time points of the direct salinity trial, fish were euthanized with an overdose of MS-222 anesthetic in a salinity approximating that of the challenge treatment. Eight samples were collected per jar, except in a few cases where this target could not be reached due to mortality. Fish were first rinsed in deionized water, blot-dried, and then measured (standard length) using digital calipers. Gill tissue or body samples were collected in pairs of low and high salinity treatments (Fig. 1). Branchial baskets from individuals in the 0.2 ppt and 35 ppt treatments were micro-dissected on ice-cold glass and snap frozen on dry ice, either in empty microcentrifuge tubes for NKCC protein abundance, or in tubes containing 100 µL of sucrose-EDTA-imidazole (SEI) buffer for NKA activity (McCormick 1993). For body water and osmolyte analysis, we chose stickleback from the 0 and 40 ppt treatments because inclusion of the branchial basket in the sample was necessary for measurement accuracy. These stickleback were eviscerated (to remove potentially confounding influence of the gut lumen), weighed to 0.01 mg, dried to a constant mass (48 h at 60°C), and reweighed. Percent water content was calculated as the proportional difference between the sample's wet and dry masses multiplied by 100.

Gill NKCC protein abundance was quantified by SDS polyacrylamide gel electrophoresis (SDS-PAGE) followed by Western immunoblotting with infrared (IR) detection. Gill tissue was thawed and homogenized using a Kontes motorized pellet pestle (Kimble-Chase, Vineland, NJ, USA) in a buffer containing 1% Triton X-100 and protease inhibitors (Roche Diagnostics Corp., Indianapolis, IN, USA). Homogenates were then centrifuged at 13,000 rpm for 10 min at 4°C to remove insoluble material. Total protein concentration of the supernatant was determined using a Pierce BCA Protein Assay kit

(ThermoFisher, Waltham, MA, USA). Samples were mixed with a 4x-concentrated Laemmli buffer containing 8% SDS. Ten µg of protein was loaded into each of 11 sample lanes in 12-well pre-cast, 7.5% acrylamide TGX gels (Bio-Rad, Hercules, CA, USA). A molecular weight ladder was loaded into the first lane of each gel, and to control for potential blot-to-blot variation in signal intensity, a common calibrator sample was also added into this lane, which we prepared by pooling gill homogenates from several 19-week-old juveniles that had been exposed to 35 ppt for 7 d. Proteins separated through the gel at 250 V for 45 min and were then wet-transferred onto nitrocellulose membranes by submerging both in ice-cold Tris-glycine sample buffer and applying 400 mA current for 90 min. We probed blots for NKCC with the monoclonal T4 antibody (mouse IgG1; Developmental Studies Hybridoma Bank, University of Iowa, Iowa City, USA), which binds to the conserved carboxy-terminus region of the protein (MET902-SER1212). This antibody detects both NKCC1 and NKCC2 isoforms, but only the former isoform is present in gill tissue (Hiroi et al. 2008). Immunoblots were blocked in 0.05% Tween in phosphate-buffered saline (PBS-T) containing 1% bovine serum albumin (BSA) for 1 h at room temperature and then incubated in T4 (1:1,000) overnight at 4°C. Following three washes in PBS-T, blots were incubated with a conjugated secondary antibody (1:10,000; goat anti-mouse IgG; IR-Dye 800CW, LI-COR Biosciences, Lincoln, NE, USA) for 1 h at room temperature. Blots were washed again and wet-pressed with protein side down onto a dual-channel IR laser scanner (LI-COR Odyssey Classic). Blots were scanned at 169 µm resolution at two wavelengths: the secondary antibody (800 channel, green) and the molecular weight ladder (700 channel, red). Pixel intensity of the NKCC bands was quantified from digital images using Image Studio Lite (v4.0, LI-COR). NKCC was visualized as multiple bands on the Western blots, presumably due to the presence of glycosylated and multimeric forms of the cotransporter (Fig. S1). NKCC multimers resisted cleavage even when dosed with high concentrations of reducing agents, therefore we quantified all bands to yield total NKCC abundance. Potential blot-to-blot variation in signal strength was accounted for by normalizing the signal from the sample to that of the calibrator.

Additional gill tissue in 0.2 and 35 ppt treatments was examined on Day 7 of the abrupt challenge to compare NKA activity relative to controls, following a 96-well microplate spectrophotometric assay

that enzymatically couples ADP production with NADH oxidation (McCormick 1993). Briefly, gills stored in the SEI buffer were thawed on ice, homogenized, and centrifuged to pellet insoluble material. Supernatants were then loaded into duplicate wells containing the assay mixture in the presence or absence of 0.5 m*M* ouabain, a potent NKA inhibitor. Kinetic oxidation of NADH was measured by repeated 340 nm absorbance readings taken for 10 min on a plate reader at 25°C using Gen5 software (BioTek Instruments, Winooski, VT, USA). For each sample, NKA activity was quantified as the difference between the mean NADH decay slope of the reaction with and without ouabain, normalized to the sample's total protein concentration, as determined by the Pierce BCA method.

Organic osmolyte levels were quantified in 0 and 40 ppt-treated fish using high performance liquid chromatography (HPLC; Wolff et al. 1989). The dried carcasses were first reweighed to determine appropriate dilution volumes. We dissolved the samples in ice-cold 7% perchloric acid and homogenized them using a tapered glass tissue grinder. Protein was precipitated and removed from homogenates by incubating them for 4 h at 4°C, followed by centrifugation at 15,000 rpm for 30 min (at 4°C). The supernatant was neutralized with 2 *M* KOH, passed through a C_{18} cartridge (Sep-Pak, Waters Corp., Milford, MA, USA) to remove lipids, and then a 0.22 µm filter. We separated small carbohydrates, methylamines, amino acids, and other small organic solutes by injecting the supernatant (Series 200 pump, PerkinElmer, Waltham, MA, USA) through a heated (80°C), Sugar-Pak I column (Waters Corp.). Samples were run for 60 min with peak detection by a refractive index detector (Bio-Rad #1755) and chromatogram peaks were integrated using eDAQ Powerchrom software. Sensitivity limitations of the assay necessitated within-group pooling of the smallest individuals to achieve a minimum dry mass of 10 mg per sample, which typically reduced sample size by at least half.

Pilot tests in juvenile stickleback tissue identified the following composition of organic osmolytes: taurine, myo-inositol, alanine, glycine, and creatine. Osmolyte content of each of these molecules was determined in sample homogenates in relation to 1 m*M* standards. The five values were summed to yield the total osmolyte content (OC) and normalized to the sample wet mass to more closely

approximate a physiological concentration. Removal from the osmolyte panel of creatine, which has a separate role in creatine-phosphate energy storage, did not appreciably alter patterns.

For the direct transfer experiment, we statistically analyzed physiological endpoints using three-way ANOVA, testing for effects of population (pop), salinity (salt), experimental day, and associated interactions. Two-way models were also performed on the time-course data separately for FW and SW challenge salinities, which incorporated control groups as Day 0. Models were re-evaluated with nonsignificant terms removed, but this did not affect interpretation. Multiple-comparison tests were performed on significant effects ($P < 0.05$): Tukey's HSD tests were used to examine mean differences between FW and SW treatments at each time point, whereas Dunnett's tests compared means of each FW or SW time point to pre-transfer controls. To quantify a per-generation rate of phenotypic divergence between RS and SL populations, all response variables measured in the direct salinity transfer were converted into haldanes (h_p; Table 1; Hendry & Kinnison 1999; Bell & Aguirre 2013). For the gradual SW challenge, percent water content and OC were compared across populations using nonparametric Kruskal-Wallis (K-W) tests due to small sample sizes.

Results

The direct salinity transfer.— The majority of stickleback mortality occurred within 3 d following direct transfer to extreme salinities and typically happened sooner in the SW treatments (Fig. 2). Most of the mortality in the 45 and 50 ppt hypersaline treatments, in which all fish perished, occurred within 12 h. At least 90% of stickleback survived in 0.2 ppt or 35 ppt. Survival of SL juveniles was 97% in the 0.4 ppt treatment, but for RS counterparts, two additional deaths in the Day 10 jar depressed mean survival subsequent to the Day 7 sampling, when it became the last remaining jar in the trial (Fig. 2).

At the threshold salinities, population differences in survival emerged just prior to the Day 3 sampling: compared to RS stickleback, SL fish had 89% higher survival in 0 ppt (0.85 ± 0.10 v. 0.45 ± 0.06; mean ± SD), but had 12.5% lower survival in 40 ppt (0.47 ± 0.06 v. 0.53 ± 0.06). These patterns persisted through Day 10, albeit without replication at this final time point, when the SL fish had 67%

higher survival in FW (0.67 v. 0.40), but had 20% lower survival in SW (0.40 v. 0.50; Fig. 2). At 0 ppt, total mortality was 2.4-fold higher in RS fish than in SL fish (24/60 v. 10/60), but at 40 ppt, mortality of RS fish was slightly (26%) lower (17/50 v. 23/50). The salinity-dependent change in mortality contributed to sharply different hazard function ratios for each population in the Cox proportional hazards model: risk of dying in 40 ppt, relative to 0 ppt, did not change in RS stickleback ("exp(coef)" = e^{β} = 1.01), but increased almost 5-fold in SL fish (e^{β} = 4.86). Consequently, the model yielded highly significant pop and pop*salt effects (Wald tests: pop $P = 0.0043$; salt $P = 0.97$; pop*salt $P = 0.0014$). Log-rank tests performed at the threshold salinities revealed that survival differed between the two populations only in FW (0 ppt challenge: $\chi^2 = 14.7$, df = 7, $P = 0.0401$; 40 ppt: $\chi^2 = 8.9$, df = 9, $P = 0.45$). The high survival of SL stickleback in 0 ppt relative to RS fish influenced the low-salinity LC_{85} (SL: 0.015 ppt ± 0.205; RS: 0.208 ppt ± 0.133). For two generations of development under different salinity regimes, this amounts to a population divergence rate of 0.5689 h_p (Table 1).

Although RS and SL populations did not differ statistically in the molecular physiological endpoints we measured in the direct transfer experiment, we report phenotypic haldanes for all response variables in Table 1, as recommended by Hendry and Kinnison (1999). Relative to FW and control levels (3 ppt rearing salinity), abundance of gill NKCC increased 2.6-fold in stickleback challenged with 35 ppt for one week, and was almost 3-fold higher by day 10 (Fig. 3). In FW-challenged stickleback, gill NKCC abundance remained at or slightly above control levels (Fig. 3). No population differences in NKCC protein expression were detected (3-way ANOVA: salt $P = 0.002$, day $P < 0.0001$, salt*day $P < 0.0001$, pop $P = 0.60$; salt*pop $P = 0.58$). Gill NKA activity increased by about 50% after 7 d in SW (13.8 v. 9.3 μmol ADP·mg protein^{-1}·hr^{-1}) compared to control fish (3 ppt), but it did not differ between the populations (Fig. 4; 2-way ANOVA: salt $P < 0.00001$; pop $P = 0.17$; salt*pop $P = 0.17$).

Organic osmolytes fluctuated transiently in response to acute salinity challenge in a manner consistent with the pattern of mortality in FW and SW (Fig. 5; 3-way ANOVA: salt $P < 0.0001$, day $P < 0.0001$, salt*day $P < 0.0001$). Across both populations, OC spiked more than 51% after 6 h in 40 ppt to 58.9 ± 6.8 (mean ± SD) mmol·kg^{-1} wet mass and then returned to baseline levels (38.9 ± 5.1 mmol·kg^{-1})

by Day 3 of the time course, doing so more quickly in RS fish. In contrast, the drop in OC in fish exposed to deionized water was slower, reaching minimum values in both populations by Day 3. In RS stickleback, the FW decrease in OC was significantly (31%) lower than control levels (Fig. 5). Compared to RS fish, OC in the SL group was lower overall, but all interactions involving population were non-significant (3-way ANOVA: pop $P = 0.028$, pop*salt $P = 0.62$, pop*day $P = 0.11$, pop*salt*day $P = 0.24$).

The composition of OC by osmolyte was, in descending order: taurine (47.8%), alanine (21.6%), creatine (20.0%), glycine (9.4%), and myo-inositol (1.2%). Water content of eviscerated carcasses ranged from 80 to 83% during the time course, typically increased to a maximum level at Day 3 and then returned to control levels by Day 10, irrespective of salinity. Water content in all fish held at 40 ppt was about 1% lower than those held at 0 ppt, but it did not differ between the two populations (n_{pop} = 70-72; 3-way ANOVA: salt $P = 0.0056$, day $P = 0.0006$, salt*day $P = 0.0089$, pop $P = 0.17$).

The gradual seawater challenge.— The upper threshold of salinity tolerance increased greatly when juvenile stickleback were gradually acclimated to hyperosmotic conditions, achieving an LC_{50} of 71 ppt for all three populations (RS, SL, CL), when the fish were 8 weeks old (Fig. 6). During this 35-d experiment, essentially no mortality was observed until salinity exceeded 61 ppt (Day 29), at which point feeding was reduced. At 69 ppt, fish stopped eating and the daily survival rate began to decline rapidly.

The five organic osmolytes that were observed in abruptly-challenged stickleback were also detected in gradually-challenged fish, with a proportional composition, in descending order, of taurine (38.4%), alanine (34.2%), glycine (14.3%), creatine (10.1%), and myo-inositol (3.0%). Average OC in the 71-ppt survivors was 60.5 $mmol \cdot kg^{-1}$ and did not differ among populations (K-W: $P = 0.06$). This was similar to maximal levels recorded in the 40-ppt challenge and 72% higher than levels in the Week 6 control fish. The whole-body 71 ppt samples displayed an additional HPLC peak that did not match known standards and was considerably lower in the 40 ppt samples. We did not account for the contribution of this unidentified solute in our calculation of OC, which may make our estimate of OC for

the 71-ppt group conservative. Water content in the gradual SW challenge survivors was higher in SL fish than in samples from the other two populations (n_{pop} = 4-6; RS = 76.8%, CL = 76.2%, SL = 79.1%; K-W: P = 0.01).

Discussion

After only two generations in FW, lake-introduced stickleback (SL) had enhanced FW tolerance relative to their anadromous ancestor (RS), suggesting rapid physiological evolution. Indeed, the divergence rate of 0.569 h_p we calculated for acute, low-salinity LC_{85} is much faster than evolutionary rates reported for many morphological traits in stickleback populations (Bell & Aguirre 2013). However, the FW halotolerance rate is similar to the 0.63 h_p measured for cold tolerance adaptation in an experimentally-manipulated marine population (Barrett et al. 2011), which suggests that selection on physiological traits required to survive in seasonally cold, ion-poor lakes is very strong. However, we did not detect a tradeoff in halotolerance: SL juveniles maintained a high SW tolerance, as evidenced by their similar performance in hypersaline conditions and hypo-osmoregulatory responses compared to RS fish. Nor did we identify a clear physiological mechanism for the observed population-level difference in performance under low-ion conditions: Salinity affected gill NKCC, NKA activity, and whole-body organic osmolytes, but did so similarly for each population.

Our salinity challenge experiments were designed to characterize the physiological limits and temporal dynamics of halotolerance in an evolutionary context by comparing an anadromous population with descendant populations that had only recently become FW-restricted. All F_1-generation fish used in this study had lived in a common rearing salinity since fertilization, thus we cannot rule out the potential influence of maternal or epigenetic effects. Our panel of FW and SW treatments included salinities that were ecologically relevant to anadromous Threespine Stickleback. Deionized and hypersaline treatments were also included to expose potentially hidden variation among populations in reaction norms, which may only appear at extreme salinities (Whitehead 2010). We focused our halotolerance tests on early ontogeny because juveniles in this anadromous population typically emigrate from RS to the Cook Inlet

marine environment when they are 6-10 weeks old (John Baker, Clark University, personal communication). Thus, it is possible that anadromous juveniles could lose hyper-osmoregulatory capacity as they develop, which has been shown in anadromous American Shad (*Alosa sapidissima*; Zydlewski & McCormick 1997).

To assess divergence in FW and SW halotolerance, survival was analyzed at extreme salinity thresholds. Population-level performance was similar in 40 ppt, but differences in deionized water indicate rapid evolution of the osmoregulatory system in a manner consistent with local adaptation to low-ion conditions. Enhanced FW tolerance has been documented in embryos and adults from other derived stickleback populations (Heuts 1947; Schaarschmidt et al. 1999). In contrast, others have found no ecotypic-level differences in FW survival, but reported that derived populations had lower SW tolerance compared to anadromous fish (Marchinko & Schluter 2007; McCairns & Bernatchez 2010; DeFaveri & Merilä 2014). These seemingly conflicting survival reaction norms are difficult to reconcile because the salinities selected as the "FW" and "SW" treatments are typically singular and differ widely across studies, yet patterns may reflect different colonization histories of derived populations in evolutionary time.

In other fishes that have transitioned from SW to FW halohabitats, improved FW performance can be associated with loss of SW tolerance. Compared to ancestral anadromous Alewives (*Alosa pseudoharengus*), derived landlocked populations have lower survival and higher osmotic imbalance when challenged with SW (Velotta et al. 2014, 2015). Similarly for a killifish species pair, the euryhaline Rainwater Killifish (*Lucania parva*) and the landlocked Bluefin Killifish (*L. goodei*) each display higher survival in their native salinity and the latter has a much lower halotolerance limit (Fuller et al. 2007; Whitehead 2010). Salinity-stratified populations of Mummichog (*Fundulus heteroclitus*) inhabiting the Chesapeake Bay watershed differ in their physiological and transcriptomic responses to osmotic stress (Whitehead et al. 2011; Brennan et al. 2015). These examples suggest a tradeoff between FW and SW osmoregulatory ability, which may arise from antagonistic pleiotropies between gene complexes that govern each pathway (Snell-Rood et al. 2010; Hohenlohe et al. 2012).

A FW-SW tradeoff was not detected in this study: survival in the 40 ppt hypersaline treatment was statistically comparable between RS and SL fish, which indicates that the derived stickleback have retained full hypo-osmoregulatory capability after two generations of FW residency. Similarly, in the gradual SW challenge the ancestral and both derived populations (SL and CL, landlocked for 2 and ~4 generations, respectively) had the same LC_{50}, remarkably withstanding up to 71 ppt. Future salinity challenges conducted on the lake-introduced populations may yet reveal a decline of SW tolerance after more time has elapsed in the FW environment. Gradual loss of SW tolerance in lake stickleback has been used as a "physiological clock" to estimate timing of FW colonization. For example, in British Columbia lakes containing benthic-limnetic species pairs, decreased hatching success and survival in SW of benthic, but not limnetic, stickleback was used to argue that the benthic stickleback had invaded FW before the limnetic ecotype (Kassen et al. 1995).

Application of general theory on rates of adaptation following environmental change suggests that following SW-FW transitions, the pace of evolution of osmoregulatory plasticity is expected to be slow in situations where negative pleiotropies are absent and there is little or no cost to maintain SW tolerance in the derived habitat. Specifically, relaxed selection on SW tolerance experienced by derived FW-residents, will slow the decay of hyper-osmoregulatory capacity if it is governed strictly by neutral processes (Lahti et al. 2009). Likewise, genetic assimilation of specialized FW phenotypes from euryhaline ancestors will be gradual in the predictable lake environment (Lande 2009). Such mechanisms could explain why nonanadromous Sockeye Salmon (*Oncorhynchus nerka,* called Kokanee) landlocked for ~10,000 years still exhibit an increase in SW tolerance during the seasonal period of smoltification undergone by anadromous conspecifics (Foote et al. 1992; Foote et al. 1994).

Euryhaline fishes can plastically switch from hypo- to hyper-osmoregulation by remodeling their ion-exchanging epithelia upon acclimating to new halohabitats (McCormick 2001; Kaneko & Hiroi 2008; Evans 2010; Christensen et al. 2012). Hyperosmotic challenge caused both RS and SL stickleback to increase salt-secreting branchial ionocytes, as evidenced by increases in both NKCC and NKA during the 10-d time course. Increases in these proteins during acclimation coincided with return of tissue osmolytes

to resting levels and no further mortality, suggesting that gill epithelia successfully remodeled to excrete excess ions and restore internal osmolality within one week. Upregulation of NKCC and/or NKA activity following SW transfer has been reported in many euryhaline teleosts, such as Atlantic Salmon (*Salmo salar*; Pelis et al. 2001; McCormick et al. 2009), anadromous Alewife; Christensen et al. 2012; Velotta et al. 2015), Mozambique Tilapia (*Oreochromis mossambicus*; Hiroi et al. 2008), Mummichog (Berdan & Fuller 2012), and Japanese Medaka (*Oryzias latipes*; Hsu et al. 2014).

Although there were not enough survivors of the gradual SW challenge to perform the planned molecular assays on gill tissue at desired sample sizes, gill NKCC abundance at 71 ppt appears to be strongly elevated in both RS and SL stickleback, relative to levels found at lower salinities (Socheata Lim and M. Monette, unpubl. data). This preliminary finding invites further examination of gradual osmoregulatory responses to extreme hypersaline challenge, with the aim of comparing the magnitude of salinity-dependent upregulation of SW transporters across populations.

The increase of gill NKCC over time in 0.2 ppt-challenged stickleback was unexpected and may be attributable to cross-reactivity of the T4 antibody with a structurally similar apical transporter responsible for ion uptake in FW ionocytes, sodium chloride cotransporter (NCC). Apical NCC has been detected immunohistochemically with T4 in branchial FW ionocytes in other teleosts (Hiroi et al. 2008; Hsu et al. 2014), and an apical NCC-like protein has been found in stickleback using this antibody (Makoto Kusakabe, University of Tokyo, personal communication). Upregulation of NCC would be expected during FW acclimation, which may have increased the NKCC signal in this treatment due to their shared epitope in the C-terminus. However, in SW the presence of NCC would be minimal (Hiroi et al. 2008), so it is unlikely that NKCC levels in the 35 ppt treatment were confounded by NCC-bound T4. In fact, because NKCC abundance in FW may be overestimated, true salinity-dependent differences in NKCC may be greater than we have reported. Future immunoblotting work using stickleback-specific antibodies to each transporter will be necessary to resolve changes in stickleback NCC-like proteins during acclimation to hypoosmotic conditions.

The fluctuation in whole-body organic osmolytes during the 10-d time course revealed short-term osmotic shock and later acclimation of the survivors. Furthermore, the asymmetry in the deviation from baseline osmolyte levels between the FW (0 ppt) and SW (40 ppt) treatments matched the observed pattern of mortality. The initial slopes of the survival curves dropped steeply in the SW treatments, but the decline was more gradual and delayed in FW conditions. Correspondingly, a rapid spike in OC 6 h after SW transfer indicated that internal osmolality was elevated almost immediately. In deionized water, however, diffusive loss of salts to the environment may have been slower, as suggested by the slower decline in OC (more strongly seen in the RS samples), which again matched the period of mortality in FW. Few stickleback died after Day 3, which coincided with organic osmolyte levels returning to near baseline levels. Water content in the acutely-challenged stickleback did not fluctuate widely and did not differ between populations, but compared to FW samples, the SW treatment had a slight dehydrating effect. In contrast to the transient response of OC in the direct transfer experiment, juveniles gradually SW-challenged for 35 d matched the maximum OC levels recorded in fish abruptly-challenged at 40 ppt, which suggests chronic hyperosmotic stress and ultimately osmoregulatory failure as the cause of death. Water content was lower in stickleback surviving the 71 ppt gradual challenge compared to those directly transferred to 40 ppt, in accord with expectations of greater dehydration resulting from increasingly hyperosmotic conditions. However, the pattern of population differences in water content in the gradual SW challenge was opposite the prediction that anadromous stickleback would be superior hypo-osmoregulators. SL fish were significantly less dehydrated than the other populations, albeit sample size was small.

Analysis of multiple organic osmolytes and the sensitivity of OC to transient salinity responses via HPLC is a promising alternative (or addition) to measuring osmotic stress, particularly when ion concentrations cannot be measured from blood plasma. A wider use of this technique could enrich comparative studies of osmoregulation by providing an additional metric of physiological performance. In both our direct-transfer and gradual salinity challenges, taurine was the predominant osmolyte, approaching 50% of the OC, with lesser contributions from alanine and glycine. Similar relative

proportions of these free amino acids were detected in tissues from adults from anadromous and stream populations in Germany (Schaarschmidt et al. 1999). Myo-inositol, a major osmolyte in some Mozambique Tilapia tissues (Fiess et al. 2007), composed no more than a few percent of OC in our samples. The relative proportions of osmolytes contributing to OC did not change between the direct and gradual experiments, with the exception of creatine. Creatine in the 71 ppt survivors was half the level found in abruptly-challenged fish (10% v. 20%), which might be due to cessation of feeding in the former group as the rising salinity became intolerable. These chronically, hyperosmotically-stressed stickleback may have also upregulated an additional osmolyte, which we could not identify in our HPLC analysis.

The physiological endpoints we measured did not provide mechanistic explanations for differences in survival between the anadromous and landlocked populations. Osmoregulatory divergence may be operating at other molecular levels and/or on other ion transporters. Genome scanning of oceanic and FW stickleback has identified many osmoregulatory genes under strong directional selection between these environments, including *atp1a1* (NKA), *aqp3* (aquaporin 3; a water channel), and *kir2.2* (a potassium channel) (Shimada et al. 2011; DeFaveri et al. 2011). Because performance differed in FW, researchers should consider examining the expression or abundance of transporters associated with ion uptake (e.g., NHE, VHA, NCC; Evans 2011), as well as tight junction and mucous proteins (mucins), which help reduce diffusive ion loss across the gill epithelium (Jones et al. 2012a; Bossus et al. 2015). These proteins may differ among salinity-divergent stickleback populations with respect to their gene expression, abundance, or isoform variants. Transcriptomic analysis may reveal regulatory networks and transcriptional pathways that have evolved and could account for improved FW tolerance in derived stickleback. Another possibility is that population-level differences in osmoregulatory responses may manifest further downstream in protein function via transporter localization to the cell membrane or their rapid activation. For example, an increase in the proportion of phosphorylated NKCC in response to osmotic stimuli would suggest more functionally-active protein, and hence, a higher capacity for salt secretion (Flemmer et al. 2010). Signaling pathways responsible for phospho-activation of ion transporters (e.g., cAMP-dependent protein kinase A in the case of NKCC) may therefore be targeted by

selection rather than the transporters themselves. At the tissue level, branchial ionocyte topology along gill filaments could be compared among populations, salinities, and exposure times using scanning electron microscopy (Whitehead et al. 2012).

The recent stocking of RS stickleback into CL and SL simulated colonization events that have occurred repeatedly since the last ice age (Bell & Foster 1994). Our examination of osmoregulatory performance in these ancestral and derived populations provides a baseline for future studies of physiological evolution in these lakes and other young, FW isolates (see Gelmond et al. 2009; Bell & Aguirre 2013; Lescak et al. 2015; Bell et al. 2016). The rate at which osmoregulatory plasticity evolves will be better understood by examining a time series of derived stickleback populations that have older, known dates of FW invasion. Comparisons between populations that had established FW-residency ~10,000 years ago to others less than a century old could reveal the degree, rate, and physiological basis of evolutionary change of halotolerance breadth and plasticity. It may be of value for future studies to incorporate additional developmental stages, e.g., pre- and post-outmigration juveniles, as well as adults, since osmoregulatory capacity changes with ontogeny (Zydlewski & Wilkie 2013). Complementary work examining evolution of salinity preference behavior (e.g., Baggerman 1957; Audet et al. 1986) may yield important insights into evolution of halotolerance, especially in freshwater populations of Threespine Stickleback whose migratory routes to the sea are intact.

The stickleback radiation in FW is an exemplar of salinity's role in phenotypic divergence and ecological speciation (Bell & Foster 1994; McKinnon & Rundle 2002). The availability of ancestral oceanic populations throughout coastal regions of the northern hemisphere, coupled with the adaptive radiation of derived FW populations, many having a unique history of isolation, makes this species complex ideal for characterizing the evolution of euryhalinity. Our work underscores the advantages of using this model fish to investigate divergence of osmoregulatory responses and their mechanisms following halohabitat transition.

Table 1. Per-generation rate of phenotypic divergence (haldanes; h_p) for all physiological responses measured in juvenile anadromous (Rabbit Slough; RS) and lake-introduced (Scout Lake; SL) stickleback in the 10-d direct salinity transfer experiment.

Trait	Measurement	Salinity (ppt)	Trial Day	RS Mean (SD, N)	SL Mean (SD, N)	h_p [a]
FW halotolerance	LC_{50} [b]	0, 0.2, 0.4	3	0.004 (0.123, 12)	NA[c]	NA
	LC_{85}	0, 0.2, 0.4	3	0.208 (0.133, 12)	0.015 (0.205, 12)	**0.569**
SW halotolerance	LC_{50}	35, 40, 45, 50	3	40.3 (1.5, 13)	39.7 (1.5, 13)	0.190
	LC_{85}	35, 40, 45, 50	3	38.3 (2.1, 13)	37.7 (2.3, 13)	0.121
Gill NKCC abundance	normalized fold change	0.2	10	2.99 (1.91, 8)	1.98 (1.49, 8)	0.296
		35	10	4.61 (2.45, 8)	3.58 (1.31, 8)	0.274
Gill NKA activity	µmol ADP·mg $protein^{-1}·h^{-1}$	0.2	7	10.2 (1.8, 8)	11.0 (3.1, 8)	0.159
		35	7	12.6 (2.4, 8)	15.0 (1.8, 8)	0.573
Total organic osmolyte content	mmol/kg wet mass [d]	0	3	28.5 (5.8, 2)	29.7 (3.3, 5)	0.160
		40	0.25	61.3 (5.9, 4)	54.1 (7.6, 2)	0.576
Water content	percent	0	3	84.3 (2.2, 4)	83.2 (1.8, 8)	0.298
		40	0.25	78.3 (1.4, 8)	81.1 (3.3, 6)	0.621

[a] Phenotypic haldanes were calculated using the following equation: $h_p = |(x_1 - x_2)/SD_{pooled}/g|$, where x is the mean trait value for a population, SD_{pooled} is the pooled standard deviation, and g is the generation time since divergence (= 2 in this comparison). Bold values denote significance at the population level as determined by inferential statistics.

[b] Lethal salinity concentrations were determined using logistic regression models, fitted for proportion survival (per experimental jar) by salinity.

[c] The LC_{50} was not calculable for SL due to high survival in FW.

[d] Osmolyte content was measured on pooled samples. Because salinity had a transient effect on osmolyte and water content, populations were compared at time points of maximal hypo- and hyperosmotic stress.

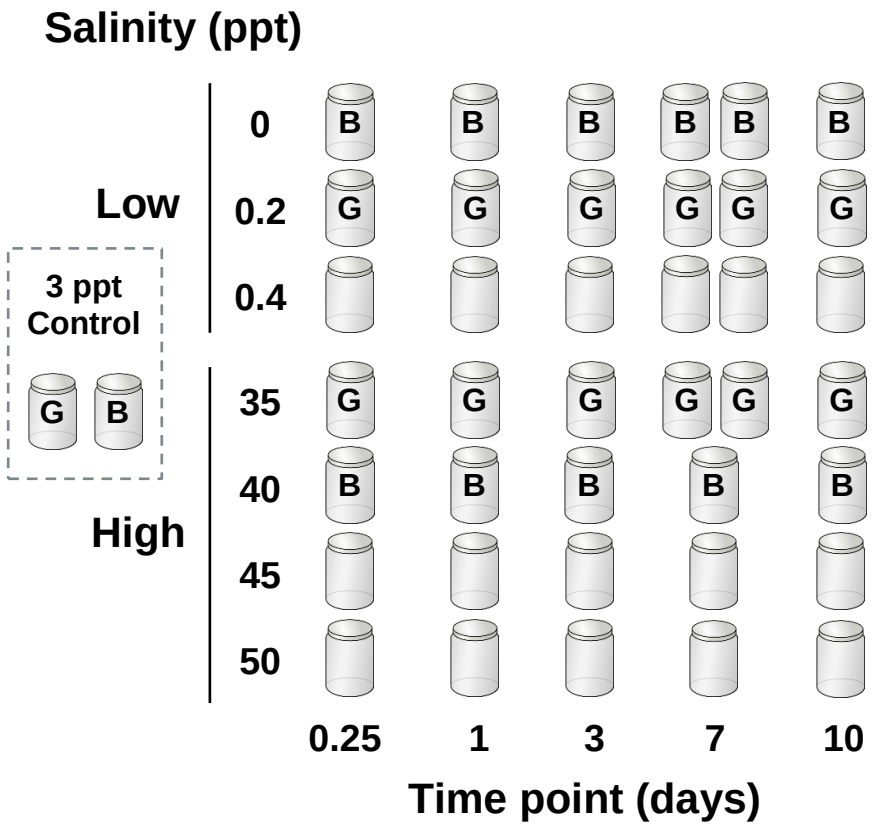

Figure 1. Experimental design of the acute salinity challenge time course, in which 6-week-old anadromous and lake-introduced stickleback were transferred from the rearing salinity (3 ppt) to one of a range of low (FW) or high (SW and hypersaline) salinity treatments at a density of 10 juveniles of each population per jar (1.5 L water). Mortality was recorded at all salinities for 10 d. During the trial, survivors were sampled from the lettered jars at control (Day 0; 3 ppt) and low and high salinity treatments for physiological endpoints: gill NKCC abundance (G), gill NKA activity (G, Day 7), and whole-body water content and organic osmolytes (B).

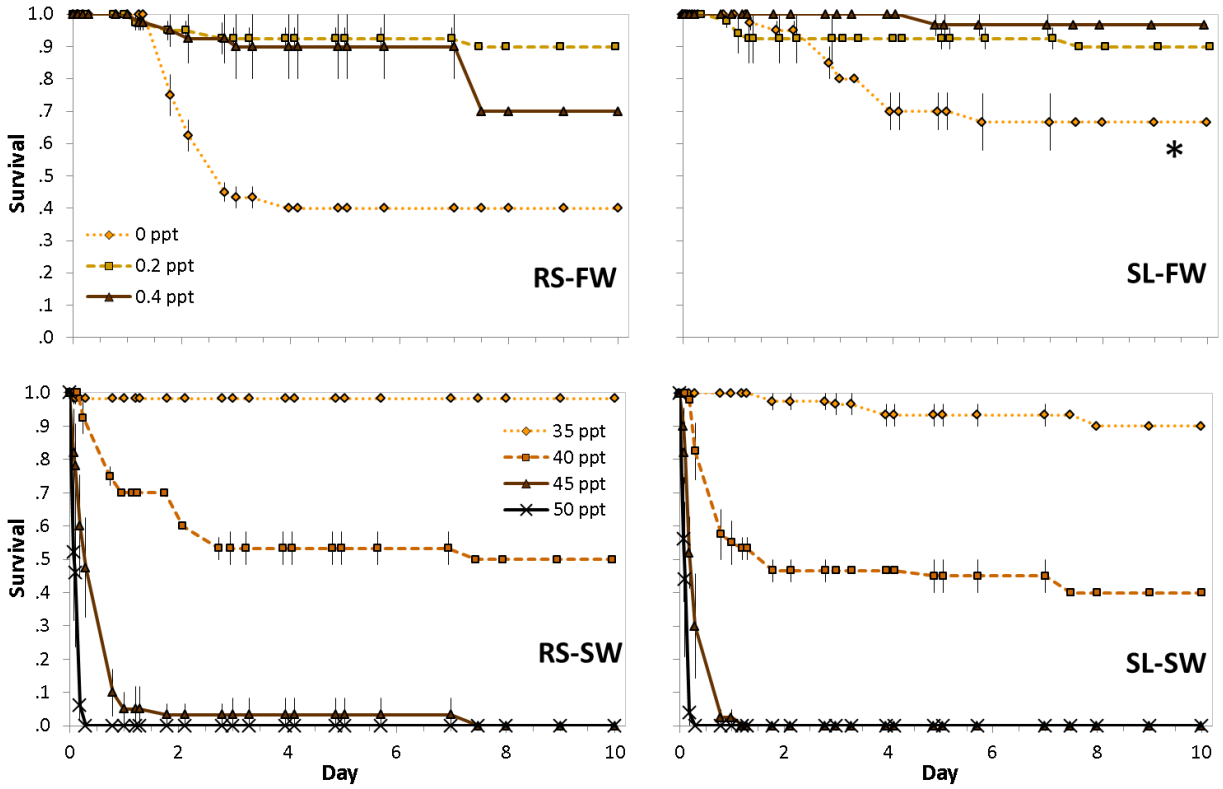

Figure 2. Survival of 6-week-old ancestral anadromous (Rabbit Slough; RS) and lake-introduced stickleback (Scout Lake; SL) held at low (FW) and high salinities (SW) for 10 days. Fish were held in replicate jars and were systematically censored from the trial at designated sampling times (Fig. 1). Each data point represents the mean proportion (± SE) of fish alive during a census. We performed a survival analysis at the threshold halotolerances, 0 ppt and 40 ppt. The asterisk denotes a significant difference in the 0 ppt survival curves between the two populations according to log-rank tests.

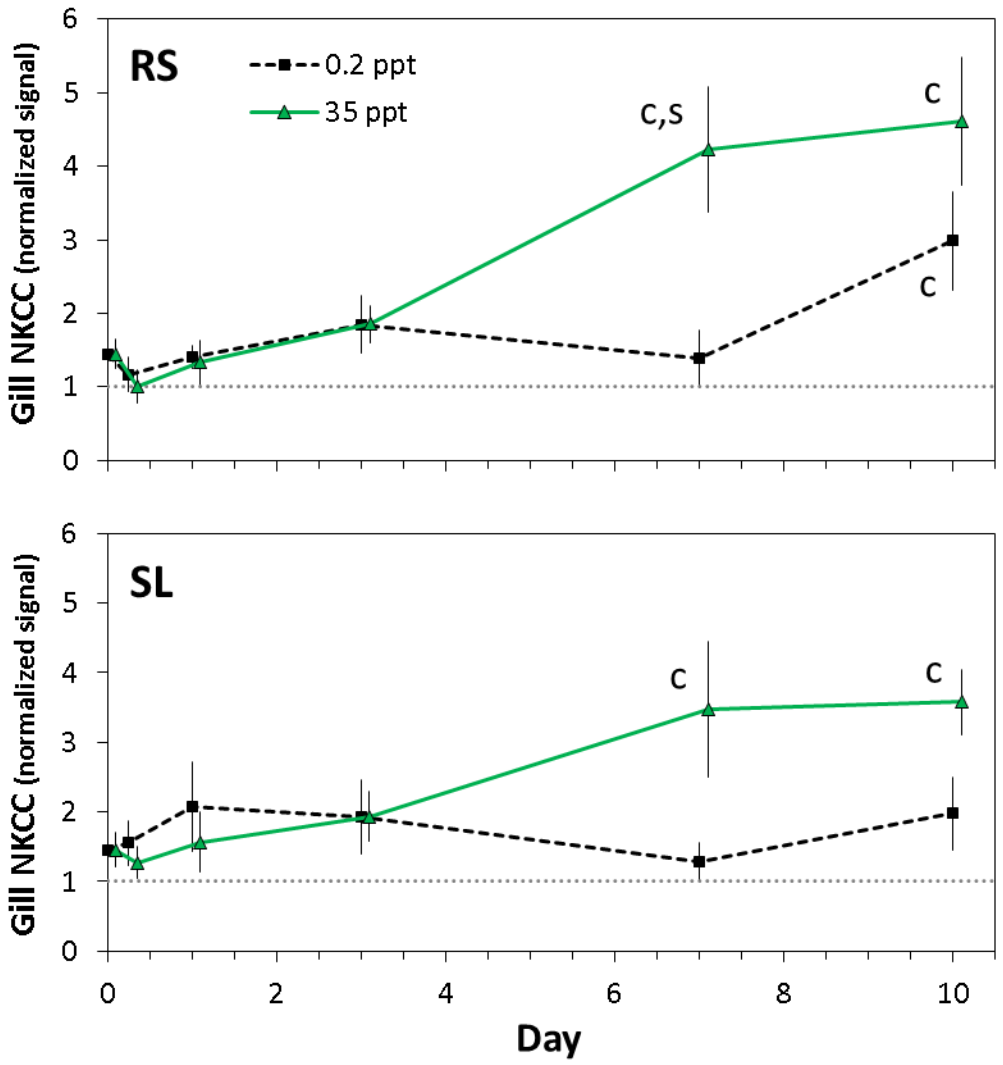

Figure 3. Protein abundance of gill NKCC in anadromous (Rabbit Slough; RS) and lake-descendant (Scout Lake; SL) stickleback challenged in 0.2 ppt or 35 ppt for 10 d. Total NKCC was determined by IR fluorescence immunoblotting using the T4 antibody. Protein expression was normalized by dividing sample signal by that of a calibrator run in each blot. The horizontal line represents the calibrator's signal, set to one. Letters denote time points when protein expression differed significantly from control levels ("C") and/or between salinities ("S"), according to Dunnett and Tukey *post hoc* tests, respectively. Each data point represents the mean (± SE) of eight individuals.

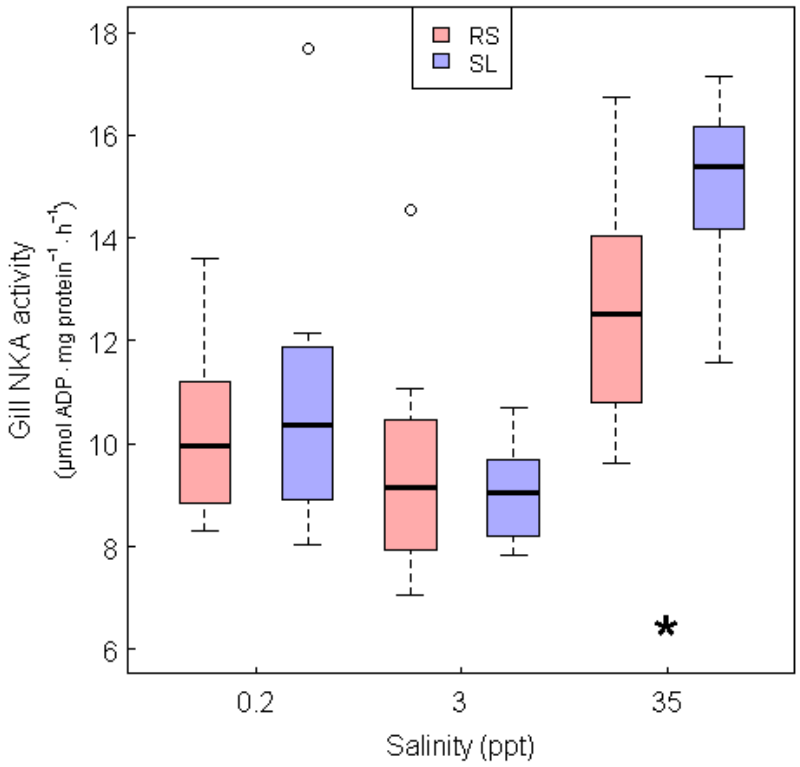

Figure 4. Gill NKA activity in anadromous (Rabbit Slough; RS; red) and lake-descendant (Scout Lake; SL; blue) stickleback held in the rearing salinity (3 ppt) or challenged for 7 days in FW (0.2 ppt) or SW (35 ppt). The asterisk denotes that NKA activity was higher in SW compared to the other salinities, as indicated by a 2-way ANOVA.

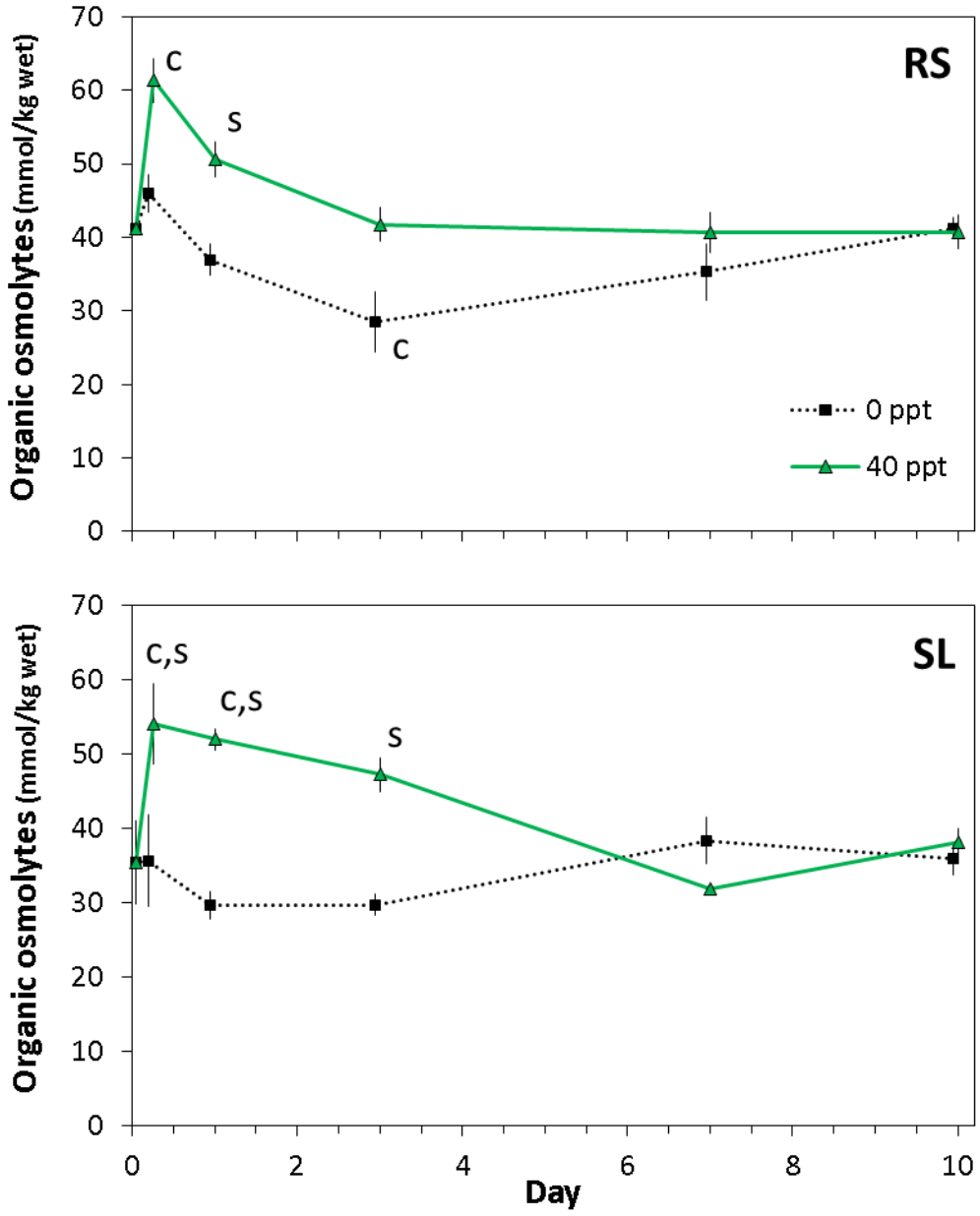

Figure 5. Total organic osmolyte content (OC) in 6-week-old anadromous (Rabbit Slough; RS) and lake-descendant (Scout Lake; SL) stickleback subjected to extreme low (0 ppt) and high (40 ppt) salinities for 10 d. Total OC for each population is expressed per unit wet mass. Letters denote time points when OC differed significantly from control levels ("C") and/or between salinities ("S"), according to Dunnett and Tukey *post hoc* tests, respectively. Each data point represents the mean (± SE) of individual and pooled samples; only one pooled Scout Lake sample was measured in the Day 7, 40 ppt group.

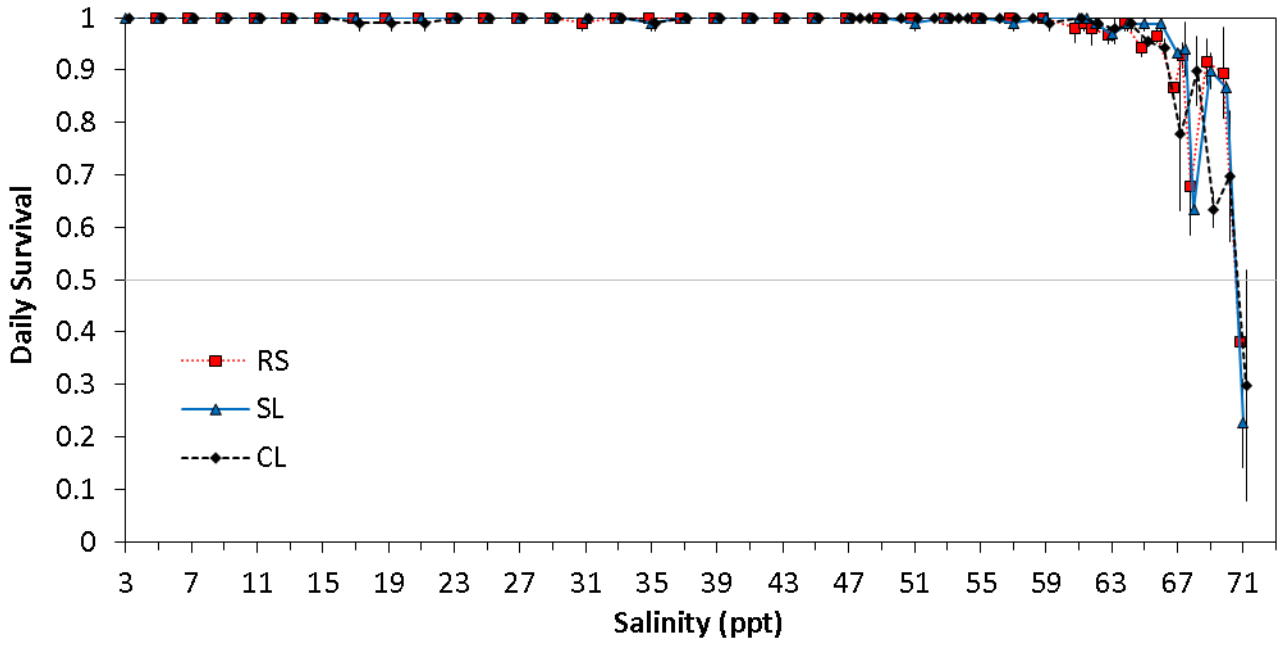

Figure 6. Salinity tolerance over time in 3-week-old threespine stickleback gradually exposed to increasingly hyperosmotic conditions at a rate of +2 ppt·d^{-1}. Juveniles from the anadromous ancestor (Rabbit Slough; RS) and two introduced-lake descendants (Scout Lake; SL and Cheney Lake; CL) were initially held at the common rearing salinity of 3 ppt. Survival is plotted as the mean daily proportion alive over time (± SD). The trial ended when half or more of the surviving cohort died (defined as the LC_{50}), which was at 71 ppt for all groups (Day 35).

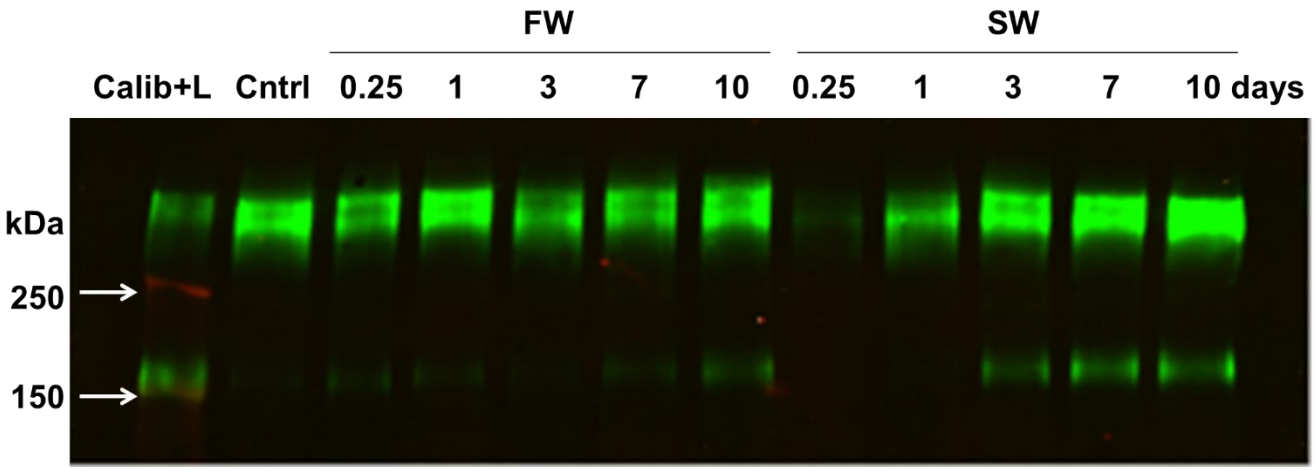

Figure S1. Representative immunoblot of NKCC protein levels in anadromous stickleback gills. NKCC was visualized by incubating blots in the T4 antibody and probing with an IR-fluorescent conjugate (green bands). Blots were digitized by high-resolution infrared scanning and fluorescence intensity of smaller (monomeric) and larger (multimeric) bands was quantified for total NKCC abundance. Each blot (n = 16) comprised a panel of homogenized gill samples selected from each time point and salinity (FW = 0.2 ppt; SW = 35 ppt). Potential blot-to-blot variation in signal strength was accounted for by normalizing to a common calibrator (Calib) consisting of gill tissue from pooled samples and run in the first lane of each blot. Molecular masses of the protein ladder (L; red bands) are labeled in kilodaltons.

Literature Cited

Abrahantes JC, Aerts M (2012) A solution to separation for clustered binary data. Stat Modelling 12:3-27

Aguirre WE, Ellis KE, Kusenda M, Bell MA (2008) Phenotypic variation and sexual dimorphism in anadromous threespine stickleback: implications for postglacial adaptive radiation. Biol J Linn Soc 95:465-478

Arjona FJ, Vargas-Chacoff L, Ruiz-Jarabo I, Martin del Rio MP, Mancera JM (2007) Osmoregulatory response of Senegalese sole (*Solea senegalensis*) to changes in environmental salinity. Comp Biochem Physiol A Mol Integr Physiol 148:413-421

Arnegard ME, McGee MD, Matthews B, Marchinko KB, Conte GL, Kabir S, Bedford N, Bergek S, Chan YF, Jones FC, Kingsley DM, Peichel CL, Schluter D (2014) Genetics of ecological divergence during speciation. Nature 511:307-311

Audet C, FitzGerald GJ, Guderley H (1986) Environmental control of salinity preferences in four sympatric species of sticklebacks *Gasterosteus aculeatus*, *Gasterosteus wheatlandi*, *Pungitius pungitius*, and *Apeltes quadracus*. J Fish Biol 28:725-740

Audet C, FitzGerald GJ, Guderley H (1985) Salinity preferences of four sympatric species of sticklebacks (Pisces: Gasterosteidae) during their reproductive season. Copeia 1985:209-213

Aykanat T, Thrower FP, Heath DD (2011) Rapid evolution of osmoregulatory function by modification of gene transcription in steelhead trout. Genetica 139:233-242

Baggerman B (1957) An experimental study on the timing of breeding and migration in the three-spined stickleback (*Gasterosteus aculeatus* L.). Arch Néerl Zool XII:105-318

Baker JA, Heins DC, Foster SA, King RW (2008) An overview of life-history variation in female threespine stickleback. Behaviour 145:579-602

Baker JA, Wund MA, Chock RY, Ackein L, Elsemore R, Foster SA (2010) Predation history and vulnerability: conservation of the stickleback adaptive radiation. Biol Conserv 143:1184-1192

Barrett RDH, Paccard A, Healy TM, Bergek S, Schulte PM, Schluter D, Rogers SM (2011) Rapid evolution of cold tolerance in stickleback. Proc R Soc Lond B 278:233-238

Belanger G, Guderley H, FitzGerald G (1987) Salinity during embryonic development influences the response to salinity of *Gasterosteus aculeatus* L. (*trachurus*). Can J Zool 65:451-454

Bell MA, Aguirre WE, Buck NJ (2004) Twelve years of contemporary armor evolution in a threespine stickleback population. Evolution 58:814-824

Bell MA, Heins DC, Wund MA, von Hippel FA, Massengill R, Dunker K, Bristow GA, Rollins JL, Aguirre WE (2016) Reintroduction of the threespine stickleback into Cheney and Scout lakes, Alaska. Evol Ecol Res 17:157-178

Bell MA, Aguirre WE (2013) Contemporary evolution, allelic recycling, and adaptive radiation of the threespine stickleback. Evol Ecol Res 15:377-411

Bell MA, Foster SA (1994) The Evolutionary Biology of the Threespine Stickleback. Oxford University Press, New York, NY, USA

Bell MA, Ortí G (1994) Pelvic reduction in threespine stickleback from Cook Inlet Lakes: Geographical distribution and intrapopulation variation. Copeia 1994:314-325

Berdan EL, Fuller RC (2012) Interspecific divergence of ionoregulatory physiology in killifish: insight into adaptation and speciation. J Zool 287:283-291

Betancur-R R (2010) Molecular phylogenetics supports multiple evolutionary transitions from marine to freshwater habitats in ariid catfishes. Mol Phylogenet Evol 55:249-258

Betancur-R R, Ortí G, Pyron RA (2015) Fossil-based comparative analyses reveal ancient marine ancestry erased by extinction in ray-finned fishes. Ecol Lett 18:441-450

Bossus MC, Madsen SS, Tipsmark CK (2015) Functional dynamics of claudin expression in Japanese medaka (*Oryzias latipes*): Response to environmental salinity. Comp Biochem Physiol A Mol Integr Physiol 187:74-85

Brennan RS, Galvez F, Whitehead A (2015) Reciprocal osmotic challenges reveal mechanisms of divergence in phenotypic plasticity in the killifish *Fundulus heteroclitus*. J Exp Biol. doi: 10.1242/jeb.110445

Campeau S, Guderley H, FitzGerald G (1984) Salinity tolerances and preferences of fry of two species of sympatric sticklebacks: possible mechanisms of habitat segregation. Can J Zool 62:1048-1051

Choi JH, Lee KM, Inokuchi M, Kaneko T (2011) Morphofunctional modifications in gill mitochondria-rich cells of Mozambique tilapia transferred from freshwater to 70% seawater, detected by dual observations of whole-mount immunocytochemistry and scanning electron microscopy. Comp Biochem Physiol A Mol Integr Physiol 158:132-142

Christensen AK, Hiroi J, Schultz ET, McCormick SD (2012) Branchial ionocyte organization and ion-transport protein expression in juvenile alewives acclimated to freshwater or seawater. J Exp Biol 215:642-652

Colosimo PF, Hosemann KE, Balabhadra S, Villarreal G, Dickson M, Grimwood J, Schmutz J, Myers RM, Schluter D, Kingsley DM (2005) Widespread parallel evolution in sticklebacks by repeated fixation of ectodysplasin alleles. Science 307:1928-1933

Dalziel AC, Bittman J, Mandic M, Ou M, Schulte PM (2014) Origins and functional diversification of salinity-responsive Na^+, K^+ ATPase α1 paralogs in salmonids. Mol Ecol 23:3483-3503

Darwin CR (1859) On the Origin of Species By Means of Natural Selection. John Murray, London, UK

DeFaveri J, Merilä J (2013) Evidence for adaptive phenotypic differentiation in Baltic Sea sticklebacks. J Evol Biol 26:1700-1715

DeFaveri J, Merilä J (2014) Local adaptation to salinity in the three-spined stickleback? J Evol Biol 27:290-302

DeFaveri J, Shikano T, Shimada Y, Goto A, Merilä J (2011) Global analysis of genes involved in freshwater adaptation in threespine sticklebacks (*Gasterosteus aculeatus*). Evolution 65:1800-1807

Divino JN, Schultz ET (2014) Juvenile Threespine Stickleback husbandry: standard operating procedures of the Schultz lab. University of Connecticut. http://fishlab.eeb.uconn.edu/wp-content/uploads/sites/116/2014/07/CompleteSTBKhandbook_31jul.pdf. Accessed 1 Aug 2014

Divino JN, Monette MY, McCormick SD, Yancey PH, Flannery KG, Bell MA, Rollins JL, von Hippel FA, Schultz ET (2016) Osmoregulatory physiology and rapid evolution of salinity tolerance in threespine stickleback recently introduced to fresh water. Evol Ecol Res 17:179-201

Dymowska AK, Schultz AG, Blair SD, Chamot D, Goss GG (2014) Acid-sensing ion channels are involved in epithelial Na+ uptake in the rainbow trout *Oncorhynchus mykiss*. Am J Physiol-Cell Physiol 307:C255-C265

Dymowska AK, Hwang PP, Goss GG (2012) Structure and function of ionocytes in the freshwater fish gill. Respir Physiol Neurobiol 184:282-292

Edwards SL, Marshall WS (2013) Principles and patterns of osmoregulation and euryhalinity in fishes. In: McCormick SD, Farrell AP, Brauner CJ (eds) Euryhaline Fishes. Academic Press, New York, pp 1-44

Ensembl (2016) Stickleback *Gasterosteus aculeatus* Genome assembly BROAD S1, Release 84. The European Bioinformatics Institute. http://useast.ensembl.org/Gasterosteus_aculeatus/Info/Index. Accessed 16 June 2016

Evans DH (2011) Freshwater fish gill ion transport: August Krogh to morpholinos and microprobes. Acta Physiol 202:349-359

Evans DH, Piermarini PM, Choe KP (2005) The multifunctional fish gill: dominant site of gas exchange, osmoregulation, acid-base regulation, and excretion of nitrogenous waste. Physiol Rev 85:97-177

Evans TG (2010) Co-ordination of osmotic stress responses through osmosensing and signal transduction events in fishes. J Fish Biol 76:1903-1925

Fiess JC, Kunkel-Patterson A, Mathias L, Riley LG, Yancey PH, Hirano T, Grau EG (2007) Effects of environmental salinity and temperature on osmoregulatory ability, organic osmolytes, and plasma hormone profiles in the Mozambique tilapia (*Oreochromis mossambicus*). Comp Biochem Physiol A Mol Integr Physiol 146:252-264

Finn RN, Kapoor BG (2008) Fish Larval Physiology:724

Flemmer AW, Monette MY, Djurisic M, Dowd B, Darman R, Gimenez I, Forbush B (2010) Phosphorylation state of the Na^+-K^+-Cl^- cotransporter (NKCC1) in the gills of Atlantic killifish (*Fundulus heteroclitus*) during acclimation to water of varying salinity. J Exp Biol 213:1558-1566

Foote CJ, Wood CC, Clarke WC, Blackburn J (1992) Circannual cycle of seawater adaptability in *Oncorhynchus nerka*: genetic differences between sympatric sockeye salmon and kokanee. Can J Fish Aquat Sci 49:99-109

Foote C, Mayer I, Wood C, Clarke W, Blackburn J (1994) On the developmental pathway to nonanadromy in sockeye salmon, *Oncorhynchus nerka*. Can J Zool 72:397-405

Foster SA (2013) Evolutionary insights from behavioural geography: Plasticity, evolution, and responses to rapid environmental change. Evol Ecol Res 15:705-731

Foster SA, Shaw KA, Robert KL, Baker JA (2008) Benthic, limnetic and oceanic threespine stickleback: profiles of reproductive behaviour. Behaviour 145:485-508

Fridman S, Bron JE, Rana KJ (2011) Ontogenetic changes in location and morphology of chloride cells during early life stages of the Nile tilapia *Oreochromis niloticus* adapted to fresh and brackish water. J Fish Biol 79:597-614

Fuller RC, Mcghee KE, Schrader M (2007) Speciation in killifish and the role of salt tolerance. J Evol Biol 20:1962-1975

Gelmond O, von Hippel FA, Christy MS (2009) Rapid ecological speciation in three-spined stickleback *Gasterosteus aculeatus* from Middleton Island, Alaska: The roles of selection and geographic isolation. J Fish Biol 75:2037-2051

Ghalambor CK, Hoke KL, Ruell EW, Fischer EK, Reznick DN, Hughes KA (2015) Non-adaptive plasticity potentiates rapid adaptive evolution of gene expression in nature. Nature 525:372-375

Guderley HE (1994) Physiological ecology and evolution of the threespine stickleback. In: Bell MA, Foster SA (eds) The Evolutionary Biology of the Threespine Stickleback. Oxford University Press, Oxford; New York, pp 85-113

Helfman GS, Collette BB, Facey DE, Bowen BW (2009) The diversity of fishes: biology, evolution, and ecology. Wiley-Blackwell, Hoboken, NJ

Hendry AP, Kinnison MT (1999) The pace of modern life: Measuring rates of contemporary microevolution. Evolution 53:1637-1653

Herrera M, Vargas-Chacoff L, Hachero I, Ruiz-Jarabo I, Rodiles A, Navas JI, Mancera JM (2009) Osmoregulatory changes in wedge sole (*Dicologoglossa cuneata* Moreau, 1881) after acclimation to different environmental salinities. Aquacult Res 40:762-771

Heuts MJ (1946) Physiological isolating mechanisms and selection within the species *Gasterosteus aculeatus* L. Nature 158:839-840

Heuts MJ (1947) Experimental studies on adaptive evolution in *Gasterosteus aculeatus* L. Evolution

Hiroi J, McCormick SD, Ohtani-Kaneko R, Kaneko T (2005) Functional classification of mitochondrion-rich cells in euryhaline Mozambique tilapia (*Oreochromis mossambicus*) embryos, by means of triple immunofluorescence staining for Na^+/K^+-ATPase, $Na^+/K^+/2Cl^-$ cotransporter and CFTR anion channel. J Exp Biol 208:2023-2036

Hiroi J, Yasumasu S, McCormick SD, Hwang P, Kaneko T (2008) Evidence for an apical Na-Cl cotransporter involved in ion uptake in a teleost fish. J Exp Biol 211:2584-2599

Hohenlohe PA, Bassham S, Currey M, Cresko WA (2012) Extensive linkage disequilibrium and parallel adaptive divergence across threespine stickleback genomes. Phil Trans R Soc B 367:395-408

Holm G, Norrgren L, Lindén O (1991) Reproductive and histopathological effects of long-term experimental exposure to bis(tributyltin)oxide (TBTO) on the three-spined stickleback, *Gasterosteus aculeatus* Linnaeus. J Fish Biol 38:373-386

Howland KL, Tonn WM, Goss G (2001) Contrasts in the hypo-osmoregulatory abilities of a freshwater and an anadromous population of inconnu. J Fish Biol 59:916-927

Hsu HH, Lin LY, Tseng YC, Horng JL, Hwang PP (2014) A new model for fish ion regulation: identification of ionocytes in freshwater- and seawater-acclimated medaka (*Oryzias latipes*). Cell Tissue Res 357:225-243

Hwang PP, Lin LY (2013) Gill ionic transport, acid–base regulation, and nitrogen excretion. In: Evans DH, Claiborne JB, Currie S (eds) The Physiology of Fishes, 4th edn. CRC Press, New York, pp 205-233

Inokuchi M, Hiroi J, Watanabe S, Hwang P, Kaneko T (2009) Morphological and functional classification of ion-absorbing mitochondria-rich cells in the gills of Mozambique tilapia. J Exp Biol 212:1003-1010

Johnson KE, Perreau L, Charmantier G, Charmantier-Daures M, Lee CE (2014) Without gills: Localization of osmoregulatory function in the copepod *Eurytemora affinis*. Physiol Biochem Zool 87:310-324

Jones F, Chan Y, Schmutz J, Grimwood J, Brady S, Southwick A, Absher D, Myers R, Reimchen T, Deagle B, Schluter D, Kingsley D (2012a) A genome-wide SNP genotyping array reveals patterns of global and repeated species-pair divergence in sticklebacks. Curr Biol 22:83-90

Jones FC, Grabherr MG, Chan YF, Russell P, Mauceli E, Johnson J, Swofford R, Pirun M, Zody MC, White S, Birney E, Searle S, Schmutz J, Grimwood J, Dickson MC, Myers RM, Miller CT, Summers BR, Knecht AK, Brady SD, Zhang H, Pollen AA, Howes T, Amemiya C, Broad Institute

Genome Sequencing Platform & Whole Genome Assembly Team, Lander ES, Di Palma F, Lindblad-Toh K, Kingsley DM (2012b) The genomic basis of adaptive evolution in threespine sticklebacks. Nature 484:55-61

Kaneko T, Hiroi J (2008) Osmo- and ionoregulation. In: Finn RN, Kapoor BG (eds) Fish Larval Physiology. Science Publishers, Enfield, NH, USA, pp 163-183

Kang C, Tsai S, Lee T, Hwang P (2008) Differential expression of branchial Na+/K+-ATPase of two medaka species, *Oryzias latipes* and *Oryzias dancena*, with different salinity tolerances acclimated to fresh water, brackish water and seawater. Comp Biochem Physiol A Molec Integ Physiol 151:566-575

Kassen R, Schluter D, McPhail JD (1995) Evolutionary history of threespine sticklebacks (*Gasterosteus* spp.) in British Columbia: insights from a physiological clock. Can J Zool 73:2154-2158

Kawecki TJ, Ebert D (2004) Conceptual issues in local adaptation. Ecol Lett 7:1225-1241

Kelly S, Chow I, Woo N (1999) Haloplasticity of black seabream (*Mylio macrocephalus*): hypersaline to freshwater acclimation. J Exp Zool 283:226-241

Kültz D (2012) The combinatorial nature of osmosensing in fishes. Physiology 27:259-275

Kültz D (2013) Osmosensing. In: McCormick SD, Farrell AP, Brauner CJ (eds) Euryhaline Fishes. Academic Press, New York, pp 45-68

Lahti DC, Johnson NA, Ajie BC, Otto SP, Hendry AP, Blumstein DT, Coss RG, Donohue K, Foster SA (2009) Relaxed selection in the wild. Trends Ecol Evol 24:487-496

Lande R (2009) Adaptation to an extraordinary environment by evolution of phenotypic plasticity and genetic assimilation. J Evol Biol 22:1435-1446

Lee CE (2016) Evolutionary mechanisms of habitat invasions, using the copepod *Eurytemora affinis* as a model system. Evol Appl 9:248-270

Lee CE, Bell MA (1999) Causes and consequences of recent freshwater invasions by saltwater animals. Trends Ecol Evol 14:284-288

Lee CE, Kiergaard M, Gelembiuk GW, Eads BD, Posavi M (2011) Pumping ions: rapid parallel evolution of ionic regulation following habitat invasions. Evolution 65:2229-2244

Lee CE, Remfert JL, Gelembiuk GW (2003) Evolution of physiological tolerance and performance during freshwater invasions. Integr Comp Biol 43:439-449

Lee TH, Hwang PP, Lin HC, Huang FL (1996) Mitochondria-rich cells in the branchial epithelium of the teleost, *Oreochromis mossambicus*, acclimated to various hypotonic environments. Fish Physiol Biochem 15:513-523

Lescak EA, Bassham SL, Catchen J, Gelmond O, Sherbick ML, von Hippel FA, Cresko WA (2015) Evolution of stickleback in 50 years on earthquake-uplifted islands. Proc Natl Acad Sci USA 112:E7204-E7212

Lubin RT, Rourke AW, Bradley TM (1989) Ultrastructural alterations in branchial chloride cells of Atlantic salmon, *Salmo salar*, during parr-smolt transformation and early development in sea water. J Fish Biol 34:259-272

Marchinko KB, Schluter D (2007) Parallel evolution by correlated response: Lateral plate reduction in threespine stickleback. Evolution 61:1084-1090

Marshall WS, Grosell M (2006) Ion transport, osmoregulation, and acid-base balance. In: Evans DH, Claiborne JB (eds) The Physiology of Fishes, 3rd edn. Taylor & Francis, New York, New York, USA, pp 177-230

Martin LB, Ghalambor CK, Woods HA (2015) Integrative Organismal Biology:344

Matthiessen P, Brafield AE (1973) The effects of dissolved zinc on the gills of the stickleback Gasterosteus aculeatus (L.). J Fish Biol 5:607-613

McCairns RJS, Bernatchez L (2010) Adaptive divergence between freshwater and marine sticklebacks: insights into the role of phenotypic plasticity from an integrated analysis of candidate gene expression. Evolution 64:1029-1047

McCormick SD, Regish AM, Christensen AK (2009) Distinct freshwater and seawater isoforms of Na^+/K^+-ATPase in gill chloride cells of Atlantic salmon. J Exp Biol 212:3994-4001

McCormick SD (1993) Methods for nonlethal gill biopsy and measurement of Na^+, K^+-ATPase activity. Can J Fish Aquat Sci 50:656-658

McCormick SD (2001) Endocrine control of osmoregulation in teleost fish. Am Zool 41:781-794

McCormick SD (2013) Smolt physiology and endocrinology. In: McCormick SD, Farrell AP, Brauner CJ (eds) Euryhaline Fishes. Academic Press, New York, pp 199-251

McCormick SD, Farrell AP, Brauner CJ (2013a) Euryhaline Fishes 32:594

McCormick SD, Regish AM, Christensen AK, Björnsson BT (2013b) Differential regulation of sodium–potassium pump isoforms during smolt development and seawater exposure of Atlantic salmon. J Exp Biol. doi: 10.1242/jeb.080440

McKinnon JS, Rundle HD (2002) Speciation in nature: the threespine stickleback model systems. Trends Ecol Evol 17:480-488

Nakatani M, Miya M, Mabuchi K, Saitoh K, Nishida M (2011) Evolutionary history of Otophysi (Teleostei), a major clade of the modern freshwater fishes: Pangaean origin and Mesozoic radiation. BMC Evol Biol 11:177

Nelson JS (2006) Fishes of the World. John Wiley and Sons, Inc., Hoboken, New Jersey

Nilsen TO, Ebbesson LOE, Stefansson SO (2003) Smolting in anadromous and landlocked strains of Atlantic salmon (*Salmo salar*). Aquaculture 222:71-82

Nilsen TO, Ebbesson LOE, Madsen SS, McCormick SD, Andersson E, Bjornsson BT, Prunet P, Stefansson SO (2007) Differential expression of gill Na^+,K^+-ATPase α- and β-subunits, Na^+,K^+,$2Cl^-$ cotransporter and CFTR anion channel in juvenile anadromous and landlocked Atlantic salmon *Salmo salar*. J Exp Biol 210:2885-2896

Norman JD, Robinson M, Glebe B, Ferguson MM, Danzmann RG (2012) Genomic arrangement of salinity tolerance QTLs in salmonids: A comparative analysis of Atlantic salmon (*Salmo salar*) with Arctic charr (*Salvelinus alpinus*) and rainbow trout (*Oncorhynchus mykiss*). BMC Genomics 13:1-15

Paolino DA (2011) Relative abundance of mitochondria rich cell types in Threespine Stickleback: interpopulation differences and salinity effects. Honors Thesis, University of Connecticut

Pelis RM, Zydlewski J, McCormick SD (2001) Gill Na+-K+-2Cl- cotransporter abundance and location in Atlantic salmon: Effects of seawater and smolting. Am J Physiol -Regul Integr Comp Physiol 280:R1844-R1852

R Core Team (2016) R: A Language and Environment for Statistical Computing. v.3.3

Ricciardi A, MacIsaac HJ (2000) Recent mass invasion of the North American Great Lakes by Ponto–Caspian species. Trends Ecol Evol 15:62-65

Sangiao-Alvarellos S, Laiz-Carrión R, Guzmán JM, Martín del Río MP, Miguez JM, Mancera JM, Soengas JL (2003) Acclimation of *S. aurata* to various salinities alters energy metabolism of osmoregulatory and nonosmoregulatory organs. Am J Physiol Integr Comp Physiol 285:R897-R907

Schaarschmidt T, Meyer E, Jurss K (1999) A comparison of transport-related gill enzyme activities and tissue-specific free amino acid concentrates of Baltic Sea (brackish water) and freshwater threespine sticklebacks, *Gasterosteus aculeatus*, after salinity and temperature acclimation. Mar Biol 135:689-697

Schultz ET, McCormick SD (2013) Euryhalinity in an evolutionary context. In: McCormick SD, Farrell AP, Brauner CJ (eds) Euryhaline Fishes. Academic Press, New York, pp 477-533

Scott GR, Claiborne JB, Edwards SL, Schulte PM, Wood CM (2005) Gene expression after freshwater transfer in gills and opercular epithelia of killifish: insight into divergent mechanisms of ion transport. J Exp Biol 208:2719-2729

Shimada Y, Shikano T, Merilä J (2011) A high incidence of selection on physiologically important genes in the three-spined stickleback, *Gasterosteus aculeatus*. Mol Biol Evol 28:181-193

Snell-Rood EC (2012) Selective processes in development: implications for the costs and benefits of phenotypic plasticity. Integ Comp Biol 52:31-42

Snell-Rood EC, Van Dyken JD, Cruickshank T, Wade MJ, Moczek AP (2010) Toward a population genetic framework of developmental evolution: The costs, limits, and consequences of phenotypic plasticity. Bioessays 32:71-81

Staurnes M, Sigholt T, Lysfjord G, Gulseth OA (1992) Difference in the seawater tolerance of anadromous and landlocked populations of Arctic Char (*Salvelinus alpinus*). Can J Fish Aquat Sci 49:443-447

Swarup H (1958) Stages in the development of the stickleback *Gasterosteus aculeatus* (L.). J Embryol Exp Morph 6:373-383

Taugbøl A, Arntsen T, Østbye K, Vøllestad LA (2014) Small changes in gene expression of targeted osmoregulatory genes when exposing marine and freshwater Threespine Stickleback (*Gasterosteus aculeatus*) to abrupt salinity transfers. PLoS ONE 9:e106894

Velotta JP, McCormick SD, O'Neill RJ, Schultz ET (2014) Relaxed selection causes microevolution of seawater osmoregulation and gene expression in landlocked Alewives. Oecologia 175:1081-1092

Velotta JP, McCormick SD, Schultz ET (2015) Trade-offs in osmoregulation and parallel shifts in molecular function follow ecological transitions to freshwater in the Alewife. Evolution 69:2676-2688

von Hippel FA, Weigner H (2004) Sympatric anadromous-resident pairs of threespine stickleback species in young lakes and streams at Bering Glacier, Alaska. Behaviour 141:1441-1464

von Hippel FA (2008) Conservation of threespine and ninespine stickleback radiations in the Cook Inlet Basin, Alaska. Behaviour 145:693-724

Wang G, Yang E, Smith KJ, Zeng Y, Ji G, Connon R, Fangue NA, Cai JJ (2014) Gene expression responses of threespine stickleback to salinity: implications for salt-sensitive hypertension. Frontiers in Genetics 5:312

Whitehead A (2010) The evolutionary radiation of diverse osmotolerant physiologies in killifish (*Fundulus* sp.). Evolution 64:2070-2085

Whitehead A, Roach JL, Zhang S, Galvez F (2011) Genomic mechanisms of evolved physiological plasticity in killifish distributed along an environmental salinity gradient. Proc Natl Acad Sci USA 108:6193-6198

Whitehead A, Roach JL, Zhang S, Galvez F (2012) Salinity- and population-dependent genome regulatory response during osmotic acclimation in the killifish (*Fundulus heteroclitus*) gill. J Exp Biol 215:1293-1305

Wolff SD, Yancey PH, Stanton TS, Balaban RS (1989) A simple HPLC method for quantitating major organic solutes of renal medulla. Am J Physiol Renal Physiol 256:F954-F956

Wund MA, Baker JA, Clancy B, Golub JL, Foster SA (2008) A test of the "Flexible stem" model of evolution: Ancestral plasticity, genetic accommodation, and morphological divergence in the threespine stickleback radiation. Am Nat 172:449-462

Yancey PH, Clark ME, Hand SC, Bowlus RD, Somero GN (1982) Living with water stress: evolution of osmolyte systems. Science 217:1214-1222

Zydlewski J, McCormick SD (1997) The loss of hyperosmoregulatory ability in migrating juvenile American shad, *Alosa sapidissima*. Can J Fish Aquat Sci 54:2377-2387

Zydlewski J, Wilkie MP (2013) Freshwater to seawater transitions in migratory fishes. In: McCormick SD, Farrell AP, Brauner CJ (eds) Euryhaline Fishes. Academic Press, New York, pp 253-326